STUDIES ON ENERGY EXCHANGE BETWEEN SEA AND ATMOSPHERE FROM THE INDIAN OCEAN WITH SPECIAL REFERENCE TO ARABIAN SEA AND BAY OF BENGAL.

PADMINI . R .

THESIS SUBMITTED TO THE UNIVERSITY OF COCHIN FOR THE AWARD OF THE DEGREE OF DOCTOR OF PHILOSOPHY.

APRIL 1981

to my parents,

This is to certify that this thesis is an authentic record of the work carried out by Miss R. Padmini, M.Sc., under my supervision and guidance in the Central Marine Fisheries Research Institute, Cochin and that no part thereof has been presented before for any other degree in any University.

(Dr.A.V.S. Murty)
Scientist
Central Marine Fisheries
Research Institute
(Supervising Teacher)

Cochin-682 018
Dated 5th April 1981.

This is to certify that this Thesis is an authentic record of the work carried out by me at the Central Marine Fisheries Research Institute and that no part thereof has been presented before for any other degree in any University.

Padmini. R

(Padmini. R)

Preface

It is more than half a century, since Helland-Hansen and Nansen (1920) carried on large-scale air-sea interactions. Beset by obstacles in obtaining adequate records of sea-surface temperature and meteorological variables, by slow and cumbersome methods of data processing, and by fragmentary heat budgets of both media, they were unable to bring to fruition many sound ideas. Since then the problem has been attacked by numerous workers, and considerable knowledge has been added to explain the intricacies of the physical processes at the air-sea boundary from general considerations. Of late, a relatively large number of investigations of direct measurements of the air-sea energy exchange parameters have been reported. It is impractical at the present time to directly measure the fluxes at more than a few stations at sea in large-scale oceanographic experiments, except possibly by the use of research aircraft. Wherever and whenever complete meteorological and sea surface temperature data are available, the bulk aerodynamic exchange and radiation equations offer an opportunity of quantification of the energy budget for the ocean surface and identification of the principal spatial and temporal features of the budget components.

There are only a few attempts in the Indian Ocean to evolve reliable climatic models of energy exchange fluxes and to study their inter-annual variations. Large space-scale and time history of the flux fields could be estimated by the bulk aerodynamic exchange and radiation equation, making use of the climatic normals of the related parameters derived from the remarkably good amount of surface marine observations compiled and made available on magnetic tape TDF II by the National climatic centre of NOAA for the period of years 1854 - early 1973. In this Thesis, the author has made an attempt to calculate the thermal energy exchange fluxes in a meaningful way, using the bulk aerodynamic coefficients which depend on the changes in the wind speed. The spatial and temporal distribution of the exchanges of energy with the atmosphere and the radiative exchange of energy between the ocean and atmosphere, are presented and their impact on the climatic variations of the Indian Ocean are discussed from the point of view of predominating air-sea interaction processes.

In chapter I, a general introduction to the studies of energy exchange fluxes is given. Along with a review of literature, geographical and climatic features of the area under study is given. The general plan of work is discussed in brief.

In chapter 2, the author has given exhaustive details regarding the data processed and the methods adopted in this regard. The quality control checks used and the accuracy of heat budget components computed are discussed in detail. Details regarding the flexible coefficients of energy exchange and its relevance in the present context are given.

The annual models of energy exchange fluxes and the related parameters are presented in chapter 3. The spatial variations of the energy fluxes and their inter-relations are examined.

Chapter 4 presents the seasonal models of the energy exchange and the related climatic parameters. The spatial variations of energy fluxes and their inter-relations in different seasons are discussed. Contributions of meteorological variables, oceanic currents, atmospheric circulation and air-sea interaction processes to fluxes over the Indian Ocean region are appraised. The part played by the seasonal variations of the energy exchange fluxes and the related parameters in the genesis and fluctuations of the southwest monsoon which is the greatest climatic event of the Indian Ocean region is discussed.

In chapter 5, a quantitative assessment of zonal differences in the heat budget is attempted. The effect of the

zonal differences of the energy budget components on the circulation pattern of the Arabian Sea affecting the distribution of rainfall along the west coast of India and the repurcussions of the feed back mechanisms are discussed in detail.

In chapter 6, the year to year variations of the heat budget components for the period 1948-72 are studied, for different areas in Arabian Sea and Bay of Bengal. These inter-annual variations are studied in the light of the related climatic parameters for the appraisal of the trend of climatic changes with respect to heat balance components.

In chapter 7 the annual and inter-annual variations of sea surface temperature at different locations in the northern Indian Ocean are studied so as to derive its relationships in triggering the changes in the atmospheric circulation leading to the formation of monsoon and its variability. The harmonic analysis of the parameters - sea surface temperature, air temperature and sea level pressure is made, so as to study their annual variations, for different areas in Arabian Sea and Bay of Bengal.

In chapter 8 the author has summarised the essential results of the present studies in various chapters.

- Padmini.R

Cochin,
April 1981.

Acknowledgements

I wish to express my indebtedness to Dr.A.V.S.Murty, Senior Scientist and Head of Division of Fishery Environment Management, Central Marine Fisheries Research Institute, at whose instance, supervision and guidance these investigations were carried out.

I wish to express my sincere gratitude to Dr.E.G.Silas, Director, Central Marine Fisheries Research Institute for his constant encouragement. The author gratefully acknowledges Dr.S.Z.Qasim, former Director, Central Marine Fisheries Research Institute for giving permission and extending facilities to start the work in the Institute.

I am grateful to Dr.Daroga Singh, Director, Indian Agricultural Statistics Research Institute, Pusa, New Delhi for extending all facilities, in the Computer Centre, for the data processing. I am specially thankful to Dr.S.S.Pillai, Joint Director, IASRI for his valuable suggestions and help in computerisation of the data. I extend my thanks to Mr.S.L. Garg, Scientist and Programmer, IASRI for his valuable help in the processing of data and writing programmes.

I wish to express my thanks to Dr.R.P.Sarkar, Director General of Observatories, India Meteorological Department, Pune

for extending library facilities and giving permission to make use of the monthly sea level pressure data. My thanks are due to Dr.Sh.V.Ramanamurty, Director, Indian Institute of Tropical Meteorology, Pune for extending library facilities in connection with this work.

I wish to express my immense gratitude to Prof.E.C.Lafond, California for the many courtesies and valuable suggestions received, whom I had the previlage to meet at the Joint Oceanographic Assembly, Edinburgh, September 1976.

My thanks are due to the Council of Scientific and Industrial Research (India) for offering me with a fellowship, which provided me scope for full-time research work during years 1974-1976.

I appreciate the help and encouragement I received from my friends in the Institute, which was a constant source of inspiration.

— Padmini R

Cochin,
April 1981

'STUDIES ON ENERGY EXCHANGE BETWEEN SEA AND ATMOSPHERE FROM THE INDIAN OCEAN WITH SPECIAL REFERENCE TO ARABIAN SEA AND BAY OF BENGAL'

CONTENTS

CHAPTER - I

INTRODUCTION

In recent years, it has become increasingly clear that the oceans play an important role in determining the earth's weather and climate. To a large extent the atmosphere and ocean interact, owing to their nature to and deriving their energy from eath other. There are few atmospheric phenomenon, that are not somehow dominated by the ocean.

The great masses of water surrounding the continents are part of an elaborate ecosystem, producing climate and rainfall, without which man could not exist. Moisture is absorbed and rele ased in the atmosphere in a continious interaction of sun and sea The sun poure more heat on the equatorial region than on the pole of the earth and the tropical oceans absorb it. Vast ocean curre nts carry heat towards the poles and make temperate regions habi-table. Water evaporates from the sea into the overlying air, and this moisture is also carried towards poles. Thus heat exchange at the surface of tropical oceans is an integral part of the general circulation of the atmosphere and the global heat budget.

Malkus (1962) who, outlining kinetic energy transfer between atmospheric and oceanic eddies of various sizes, has written of 'the coexistence in each (fluid medium) of many interacting scales of motion from tiny eddy to planetary

gyre, supplying and removing energy from one another coupled in loops within loops of stable and unstable interaction'.

Large temporal and spatial variations (on the order of years and thousand kilometres, respectively) are found in the monthly and annual indices describing the general circulation of the atmosphere. However, the natural meteorological time scales are short compared to these index fluctuations. Therefore, the ocean may play an important role in the maintenance of these variations acting to influence the atmosphere through the effect of the ocean circulation upon heat exchange between the two fluid media. This heat exchange can significantly affect the wind systems in the atmosphere. In turn, the circulation in the upper layers of the ocean is driven by the wind systems. The resulting mutual interaction can be thought as a servomechanism acting to couple the two fluid media.

According to Benton et al. (1963) the atmosphere and the oceans constitute a single mechanical and thermodynamical system of two coupled fluids and they interact in a manner which is so complex that, cause and effect can not always be distinguished.

Quantification of the energy budget for the ocean surface and identification of the principal spatial and temporal features of the budget components are, but essential preliminary steps towards complete understanding of the ocean-atmosphere system.

until the early part of the present century reliable quantification of the energy budget was precluded by lack of insight into the physical processes involved and by paucity of necessary data. As the quantity and quality of atmospheric and oceanic observations improved, knowledge and understanding of the various components advanced steadily.

Review of literature

It has to be said that eventhough intensive studies were carried out in the past on the behaviour of meteorological conditions above and exchange at the surface of the ground, reservoirs or lake, similar studies on ocean surface were meagre due to difficult experimental condition. Direct measurements of evaporation were made from pans placed on board of German expedition vessels during 1890-1900. Livingston (1908, 1909) published an annotated bibliography of evaporation year-wise starting from as early as 1670 to the first decade of the current century. Dalton (1802) was the first to state clear views on the nature and properties of vapours in general, including the law of partial pressures and the dependence of transfer on pressure differences. Angstrom (1920) proposed energy-balance methods. Cummings (1929) and Richardson (1931) used this principle earlier for determining evaporation losses. Jeffrys (1918) and Giblett (1921) were among the earliest investigators to study the problem of evaporation in terms of atmospheric turbulence. The evaporation studies based on turbulence phenomena

of the atmosphere have been advanced by the great progress in the theoretical treatment of the mechanism of turbulence achieved by various workers in aerodynamics. (Taylor, 1915; Richardson, 1931; Schmidt, 1934; Prandtl, 1932; Sutton, 1932, 1934; Vonkarman, 1935; Rossby, 1936) and others.

Schmidt and other workers proved that the evaporation from pan was not representative of sea surface. Evaporation and magnitude of pan coefficient were found uncertain.

The classical work was carried out during 1930 to 40 by Rossby and Montgomery (1935, 1936) and Montgomery (1940). Their aims were a quantitative formulation of the turbulent structures at the air-sea interface and method of deducing thereby the fluxes of heat, moisture and momentum transfer from the ocean surface through the lowest layers of air above. In the intervening years, this approach has been refined and tested critically by Priestly (1959), Sheppard (1958) and Deacon, Sheppard and Webb (1956).

Sverdrup (1937), using Rossby's (1936) publications, computed the evaporation rates assuming the sea surface as a rough surface with a roughness parameter of 0.6 cm, and also as a smooth surface. Thornthwaite and Holtzman (1939) derived a formula for evaporation under neutral conditions of stability of the atmosphere, based on two level observations in the air

which eliminate all the surface parameters. Pasquill (1949) further simplified the Thornthwaite and Holtzman formula using constants relating to surface properties under neutral conditions of the atmosphere.

The mean annual evaporation over the oceans according to latitude ranges were well established by Wüst (1936), Namias (1936) and Mc Ewen (1938). Applying the heat budget equation and using the available seasonal climatic data, Jacobs (1951) computed the amounts of evaporation and of the quantity of sensible heat and total energy exchanged between sea and atmosphere within each 5° square during several seasons for the North Pacific and the North Atlantic Oceans.

Jacob's work was updated and extended by Budyko (1956, 1963, 1974). Budyko (1956) considered the climatic data available in the early 1950s sufficient in quantity and quality to make worthwhile the preparation of charts showing isopleths of all energy-budget components, over all the oceans of the globe, they were in truth still barely adequate for the purpose in most oceanic regions. With the IGY data, Budyko et al. (1963) computed more exact and detailed maps using data from 2000 stations, which included 300 oceanic areas.

Increased effort has been directed towards a better understanding and a more accurate evaluation of the different

terms involved in calculating radiation balance. Different aspects of radiation were investigated by Anderson (1952), Berliand (1952), Black (1956), Burdicki (1958) and Budyko (1956). London (1957) has computed the radiation to and from space, the atmosphere, and the surface of the earth for the Northern Hemisphere. These computations involve the theory of radiation, the temperature of the air as a function of elevation, of the temperature of the land and sea, and the water vapour and cloud content of the atmosphere. Earlier work in this area includes that of Simpson (1928) and Baur and Phillips (1935). London used the radiation theory and charts of Elsasser (1937), Moller (1943) and Yamamoto (1950). The albedo of clouds was based on the work of Fritz (1949, 1950, 1954), Hewson (1943) and Neiburger (1949).

Budyko's work (1956, 1963) encompasses the whole of earths surface. Budyko (1963) uses a table of solar radiation received at the surface of the earth on cloudless days, and a formula to estimate the amount of solar radiation received on cloudy days, developed by Berliand (1960). Kondratyev (1969) describes and discusses the table and formula.

The classical Atlas of Heat Balance by Budyko (1956, 1963), World maps of global solar radiation prepared by Black (1956) and Ashbel (1961), the review of surface measurement of solar and terrestrial radiation during the IGY and IGC by Robinson (1964), World maps of climatology edited by Landsberg (1963) and earlier studies

of the Indian Ocean by Albrecht (1950), the work by Sauberer and Dirmhirn (1954) on the heat budget of the oceans of the Northern hemisphere are some of the important works on this aspect.

Based on the presently available satellite data, radiation balance and the long-term mean heat balance of the earth and its normal seasonal variations are investigated. (Winston, 1969; Vonder Haar and Soumi, 1969, 1971; Vonder Haar and Ellis 1974 Vonder Haar and Oort, 1973, 1976).

Investigations on heat balance components over Indian ocean are very limited. The charts of heat balance parameters for February and August were prepared by Albrecht (1949). In his Atlas of Heat Balance for the Oceans, Budyko (1955) gave charts of heat balances parameters for all the twelve months using climatic data for areas of size 5° lat and 10° Long. Later on, with the accumulation of data during I.I.O.E. heat budget components for all the months of 1963 and 1964 for Indian Ocean North of 40° S were computed and presented Ramage et al. (1972). Most of the work carried out over the Indian Ocean deal with different energy-budget terms, either exchange values or radiation budget components. Venkateswaran (1956) studied seasonal variation of evaporation and annual sensible heat transfer by interpolating 5 degree-square values for the wet bulb depression from the atlas of climatic chart of the ocean and similar values for the air and sea surface temperatures from monthly meteorological charts of the Indian ocean. In his

study of evaporation from North Indian ocean including the Red sea and Persian Gulf. Privett (1959) published monthly charts of evaporation for each 5-degree-square by using a modified form of Jacob's formula and climatic data supplied by the Meteorological office, London. Computations of mean monthly sea surface temperatures and air-sea exchange parameters based on actual data for individual years were first carried out under the Meteorology Programme of the International Indian Ocean Expedition (1963-64) (Miller et al. 1963). Results of computation of evaporation flux for year 1963 have been presented by Suryanarayana and Sikka (1965). Colon (1964) discusses the south west monsoon interaction over the Arabian sea. Pishamoty (1965) discussed the evaporation from the Arabian sea and its relation to the Indian south-west Monsoon. Ramanadham et al. (1968) gives the seasonal variations of heat flux over the Bay of Bengal. Mean monthly fluxes of sensible and latent heat for year 1964 have been discussed by Saha (1970a). Saha and Suryanarayana (1972) given the results of further computations of mean monthly sea surface heat exchanges during summer monsoon months of subsequent years, 1965-67, using ship's weather data collected after the IIO E period.

As for the radiation balance components, Mani et al. (1965) have presented annual and monthly maps showing the distribution of global solar radiation and net radiation over the Indian

Ocean area, prepared from the available observations, supplemented by calculations based on other meteorological measurements. Another work in this direction is by Portman and Rymar (1971) who describes a series of stations established to measure the amount of radiant heat received from the sun and atmosphere and discusses the results of an analysis of data obtained from them for 1963 and 1964. Information on cloudiness and water surface temperature was used in the analysis for computing the remaining components of the net exchange of thermal radiation to arrive at monthly averages of net radiative exchange for the two years.

Dropsonde data by research air craft along with the temperature soundings from the vessels participating in the International Indian ocean Expedition is made use of, in the studies of interactions of Southwest monsoon current and sea surface and summer circulation by Colon (1964), Bunker (1965) and Ramage (1966). Bunker computed the heat budget of the monsoon air using the C-540 air-craft meteorological observations. Combining the dropsonde data by research aircraft and marine meteorological observations, Shumralkar (1978) has studied the relation between evaporation over the Arabian sea and the rainfall at the west coast of India during summer monsoon.

With the implementation of experiments like INDEX and MONEX, informations regarding the monsoonal heat budget components

were published. (Pant, 1977; Rao, et al., 1978).

Little work is done on the year to year variations of the heat exchange parameters and the related climatic variables of the Indian Ocean. Ramasastry and Jambunathan (1969) has studied the decade to decade climatic changes of Arabian sea and Bay of Bengal. The work of Verploegh (1960) is an extensive study of annual variations of climatic parameters.

The impact of heat exchange parameters and the related variables on the general circulation and the changes in the climatic picture are studied by few workers. Saha's papers on the zonal differences in the distribution of marine meteorological parameters their influence on the heat exchange process and its impact on the general circulation has to be mentioned in this context (Saha, 1970a,b; 1971 a; 1971 b; 1972a,b; 1973). Modal studies were carried out by Shukla (1975) and Washington (1977) on the influence of sea surface temperature anomalies, which directly influence the energy budget components and consequently have a bearing on the fluctuations of the general circulation particularly monsoon circulation.

The area under investigations

The Indian Ocean is the smallest of the three great oceans and geologically much of it is also rather youthful.

Following the International Hydrographic Bureau (Sp. Publ. 23, 1953) its boundaries are as follows. Western limits: The meridian of Cape Aghulhas (20° E) to Antartica (Queen Maud Land, the boundary of the Princess Ragnhild Coast on the east and Princess Astrid coast on the west). Eastern limits: south of Australia. The western boundary of Bass strait from Cape of Tasmania, along Meridian 147° E to the Antartic continent near Fisher Bay, George V coast. Eastern limits, north of Australia. The north eastern boundary runs from island to island through the lesser Sunda islands to Java and Sumatra and thence to Singapore. Red sea, Gulf of Aden, Persian Gulf, Gulf of Oman, Arabian sea, Laccadive sea, Bay of Bengal, Andaman Sea, Malaca Straits and Singapore Straits are marginal seas that belong unequivocably to the Indian ocean are situated along the northern sector of the Indian ocean, is sometimes taken as that part south of a line from Cape Aghulhas to Cape Leeuwin (Western Australia) recommended by the I.H.B. in 1928. The total area covered by the Indian Ocean is 75, 940,000 Km^2.

Though the climatic models are made for whole of Indian Ocean (20-120° E and 30° N-40° S) the detailed studies are concentrated on Arabian Sea and Bay of Bengal which cover most of Northern Indian Ocean.

Arabian sea extends towards the west from the west coast of India to East African Coast. From the northern boundary of

land mass, it extends up to equator. The total area covered exclusive of the Gulf of Aden and Oman, is 7, 456,000 Km^2. Bay of Bengal is the north eastern arm of the Indian ocean lying between peninsular India and Burma. It occupies about 22 x 10^6 m^2. It is bordered in the north by deltaic regions of Ganges and Brahmaputra Rivers. The southern boundary extends from the south end of Ceylon to the north tip of Sumatra and is open to the central Indian Ocean.

The northern Indian Ocean is the only ocean which is land locked in the northern side.

The Climatic peculiarities

Because of the proximity of a vast continent in the northern side, annual reversal of the wind system is experienced in the Northern Indian Ocean, which makes it different from the southern Indian Ocean or any other ocean in the world. A seasonal low-pressure area developed in the sub-continent during the summer causes these wind systems to blow persistently from the south west. In winter the monsoons, issuing from a high-pressure source forming over the Tibetan Plateau, come from the north east. The semi-annually reversing monsoon winds determine the patterns of the surface circulation over the waters between the African continent and the Malaysian archipelago. No other ocean undergoes such drastic changes in its circulation.

The annual reversal of the wind causes a corresponding change in the surface water. The Currents in the northern part are strongly influenced by the monsoons and change with seasons. Therefore, they are called the south-west and north-east monsoon drift in summer and winter, respectively. In the southern hemisphere, there are the south equatorial Current and the west wind drift. Besides these currents closely related to the wind system, there are Currents of a local nature, due mainly to the density structure of the water, such as the Mozambique Current, the Agulhas Current, the Equatorial Counter Current, the Somali Current and the West Australian Current. The southern Indian Ocean anticyclonic gyre is similar to gyres in the South Pacific and Atlantic Oceans, but it is subject to greater annual variations.

Two distinct atmospheric circulation patterns were recognised :(a) Winter (December, January and February), when a Hadley-type circulation operates over the North Indian Ocean, with north-easterly trade-winds at the surface, and(b) summer (May to September inclusive), when the troposphere is reorganised and south-westerlies replace the north-easterlies. Spring and autumn, the transition periods, were considered to be March-April and October-November respectively.

Influences of dry airmass of land origin is felt over

the North Indian Ocean during winter. During summer the moist and cold air mass from southern Indian Ocean and the dry and warm air mass of the continent origin are found. The summer monsoon gives copious rains. Somali current off the east coast of Africa is an outcome of summer monsoonal winds. Pronounced upwelling is resulted due to this strong seasonal current. This combined with the, arid continental mass in the northern part of the Indian ocean, creats the World's highest rainfall.

General Plan of work

The processing and the computation of the heat budget components from the climatic data (obtained from National Climatic centre, Carolina, NOAA) were done in computer-Burroughs 4500 of Indian Agricultural Statistical Research Institute, Pusa, Delhi. The climatic models (annual and seasonal) were made, using the results. Plotting and contouring the maps were done by hand. Time series and other graphs were also made manually.

CHAPTER 2

MATERIAL AND METHODS

A better understanding of a more accurate evaluation of the different terms involved in calculating the heat balance is needed in studying the circulations of atmosphere and ocean and the associated problems. Excellent measurements have been made recently in selected sites with sophisticated instruments. Since only a minute fraction of the oceans can be studied in this manner, it is necessary to parameterise these measurements to develop a system, which can be applied over all the oceans. The bulk aerodynamic exchange and radiation equations offer an opportunity of calculating fluxes, wherever and whenever complete weather and sea surface temperature observations have been made. With the accumulation of a huge amount of data in the past decades, with improved equatic reasonably accurate fluxes can be obtained in nearly all regions of the oceans.

The present analysis is based on nearly 120 years of data (1854-early 1973), made available by the National Climatic Centre. A huge body of surface marine observations has been collected, edited and made available on magnetic tapes by the National Climatic Centre of NOAA. The analysis is done from surface meteorological observations made by ships in the Indian Ocean and surrounding tropical seas (20°E to 120°E and 40°S to 30°N), during the above mentioned period of time.

Tape deck TDF-11 is the primary source of data, for the investigations. The TDF-11 was compiled from ship logs, ship weather reporting forms, published ship observations, automatic observing buoys, teletype reports and punch cards purchased from several national meteorological services. Tape data family 11 (TDF-11) Reference manual (National Climatic Centre, 1968) informs that the data were subjected to complex quality control procedures before processing. First, duplicate observations (which entered the data base from different sources) were eliminated. The remaining observations were then checked for internal consistency. Elements which failed to meet internal consistency checks, were either adjusted or eliminated. The data were subjected to an extreme value check, in which the highest and the lowest values of appropriate elements were listed and checked.

Regardless of the amount of quality control to which marine observations are subjected, there are many inherent problems, which can be corrected only in a general way. Among these are the difficulty in taking observations of meteorological elements from an unstable platform, different levels of observer experience, recording errors, variations in observing and coding practices, punching errors, the scarcity of observations over vast areas, and the effect of weather elements themselves on measurements. Ships may avoid bad weather when possible (Quayle, 1974), thus decreasing the amount of bad weather, thus taking more observations and increasing the data sample

From a survey of data available for this analysis, it is observed that the surface wind is the element most commonly observed and recorded. The percentage of observations containing other basic weather elements is as follows.

Element	Percent
Air temperature	98
Sea temperature	92
Total cloud amount	78
Sea level pressure	56
Wet bulb temperature	36

Records of sea surface temperature values are affected by various methods of recording, which tend to decrease the reliability (Saur, 1963; Crawford, 1969). Air temperature values are considered to be generally reliable. However, in the tropics, as the result of poor instrument exposure, observed temperatures on transient ships under sunny conditions appear consistently high. Dew point temperature also are likely to yield over-estimation (Lamage et al., 1972). Because of the uncertainity of these above mentioned discrepancies and following Lamage et al. (1972) and Roden (1974), no corrections were applied to these parameters. Since there are no weather stations in the Indian Ocean, comparisons can not be made with the compiled

the ship observations for their accuracies. Dunker (1976) for Atlantic data (from the same tape deck) has found that the merchant mariners measure higher sea and dew point temperatures and lower wind speeds and cloud cover data.

The density of observations is shown in Fig.1. Areas of highest concentration (Ed) found in the Red sea and in the China sea, the areas coinciding with the shipping channels. The area north of 10°S is found to have a good coverage of data. The total number of observations show large variations. Marsden square 068 with maximum observations of 36,1768 numbers in the Gulf of Aden and marsden square 439 with a minimum of 10,663 observations in the southern Indian ocean show enormous variations. Dunker (1976) has shown that means and fluxes should be determined from atleast a minimum of 500 observations, in order to be considered reliable. About 10% error is estimated for evaporation computations. Hence at least 6000 observations are needed for twelve monthly averages. Moreover, the observations of parameters like dew point temperatures etc., occur in small percentages. Hence each marsden square is divided into four 5° grids. The data is provided in the form of averages for 1° and 2° squares. Monthly means for the twelve months were not available throughout the area of study for many of the small grids. Hence though the need for higher resolution is much recognised in this study, a 5° grid resolution is adopted.

Fig.1. Number of ship observations used for flux computations, based on climatological averages formed from NCC TDF 11 Tapes, in each Marsden square sub division (5° square).

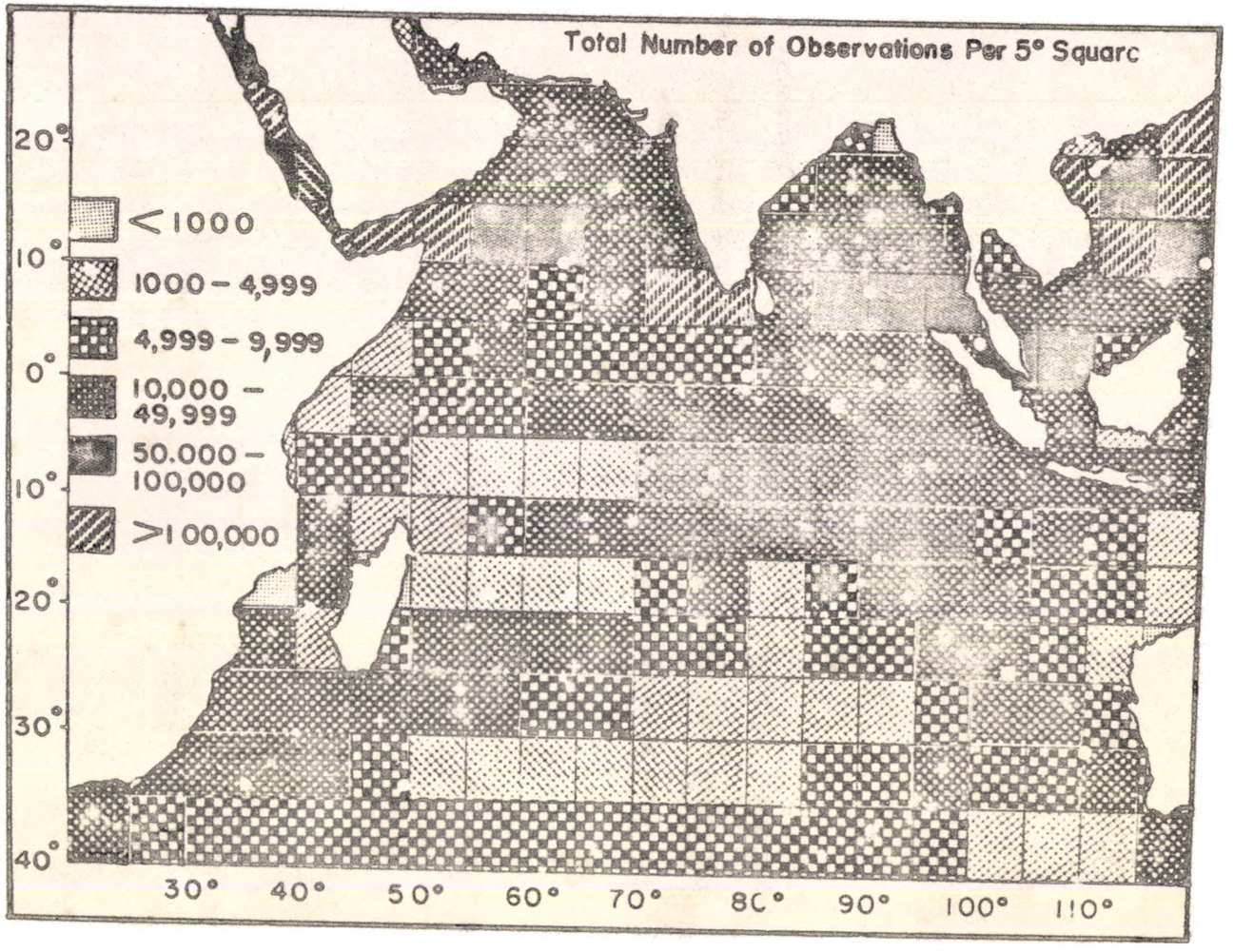
Total Number of Observations Per 5° Square
<1000
1000 – 4,999
4,999 – 9,999
10,000 – 49,999
50.000 – 100,000
>100,000
20°
10°
0°
10°
20°
30°
40°
30°
40°
50°
60°
70°
80°
90°
100°
110°

A computer program was written to sort the 1° square averages and select the means with necessary quality checks to give a 5° grid average, compute fluxes using the equations and the tables and form annual and seasonal averages of fluxes and variations.

The second set of data which was made use of, in the time series analysis was unprocessed. Sorting and shuffling of the data, period-wise, location-wise and element-wise were done. Extreme values were checked and erroneous values were eliminated. Consistency checks were given using standard deviation of the observations, before sorting and averaging for monthly means, for different years, for the given area.

Fig.2 gives the locations of the areas for which detailed time series analysis was attempted. These locations which represent different parts of North Indian Ocean are selected on the basis of availability of data. In the Marine Climatic Atlas of the World Vol.III Indian ocean U S Navy (1976) which was made using the same tape deck, these areas are given as representative areas, for which detailed presentation of data is made. The yearly data is found to be more consistent from 1965 onwards. The time-series analysis was attempted to get the year-to-year variations of the heat budget components and the related parameters. The heat balance of the sea surface for each location under study, for each year is computed using the formulae employed for evolving the climatic models, and

Fig.2. Areas in the North Indian Ocean for which yearly variations of heat budget components and related parameters are studied and harmonic constants are computed.

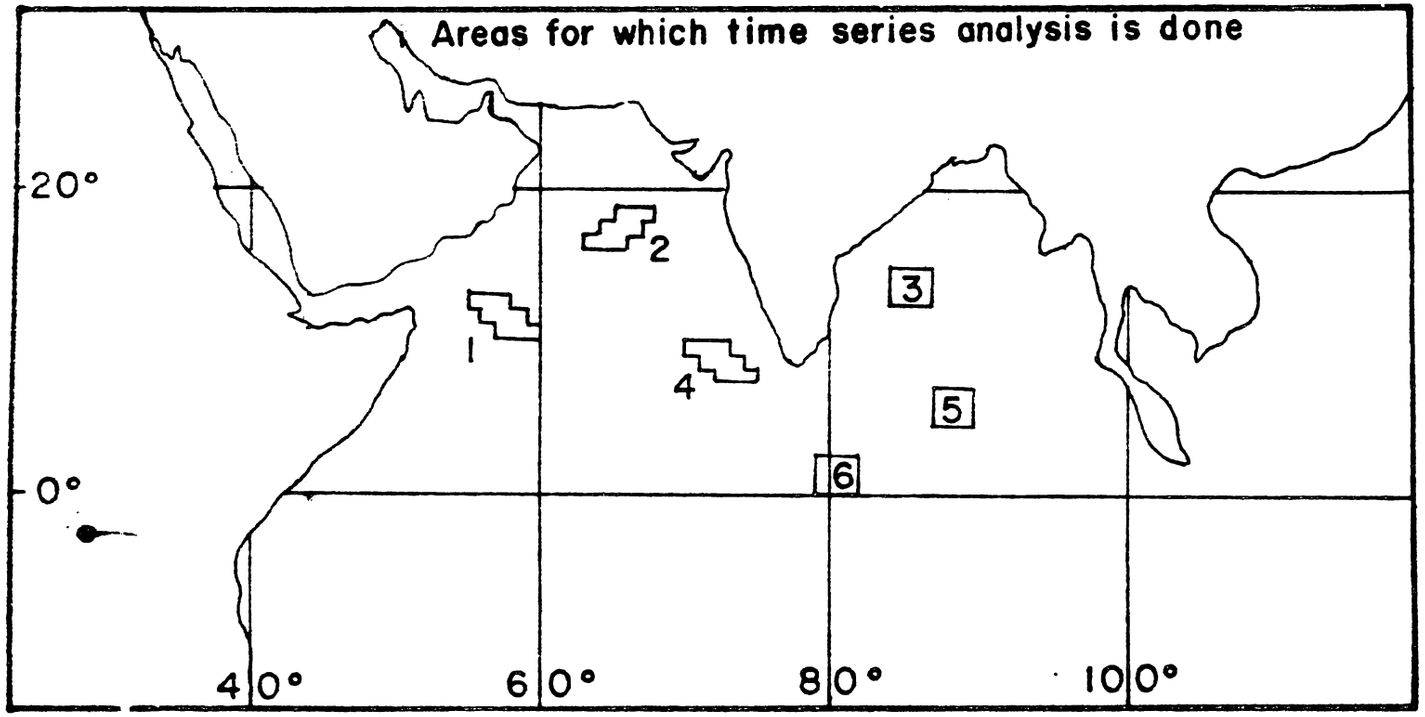
Areas for which time series analysis is done
20°
0°
40°
60°
80°
100°
1
2
3
4
5
6

than averaged for the entire period of study from 1948 through 1972. The annual and the long term course of the heat balance components and the related climatic parameters were constructed based on the results.

Harmonic analysis of the climatic parameters of the area under study is done based on Conrad and Pollak (1950), for the years 1948-72. The parameter at any time t (t indicates months; values of t varies from 0 to 11) of the year is represented by the relationship..

$$P_t = (P) + a_1 \sin\left(\frac{1}{6}\pi t + \phi_1\right) + a_2 \sin\left(\frac{1}{3}\pi t + \phi_2\right)$$

where (P) is the mean annual value of the parameter, a_1 and a_2 are the amplitudes of the annual and semi-annual waves, ϕ_1 and ϕ_2 are respective phase angles. It is assumed that the mean monthly value of the parameter refers to the middle of each of the months and that the months are all of equal length.

Empirical formulae

Many investigators have tried to derive empirical equations relating the elements of standard marine meteorological observations to the heat budget at the ocean surface. All the equations suffer from lack of accurate direct measurements of the budget components.

in particular, during periods of strong winds and high seas. A review of these formulae has been given by Laevastu (1960), Malkus (1962), Tabata (1964), Bell (1965), Kitaigorodskii (1970), Kraus (1972) and others.

For a given area and time period, the equation for heat balance at the air-sea interface is

$$Qn = Qs - Qr - Qb - Qe - Qh$$

The heat exchange processes are expressed in units of gm cal cm^{-2} day^{-1}.

Where Qn is the net heat balance at the sea surface in gm cal cm^{-2} day^{-1}.

Qs Rate of heating at the sea surface from incoming short wave radiation, modified by total average cloud cover.

Qr Rate at which radiation is reflected from the sea surface

Qb Rate of emission of back radiation from the sea surface.

Qe Rate of cooling at the sea surface from evaporation.

Qh Rate of sensible heat loss from the sea surface to the atmosphere.

Energy exchange calculations presented here do not take into account changes in heat brought about by advection.

The manner in which these terms are calculated depends upon the time scale of interest. Here investigations are made on large-scale air-sea interactions and time history of the flux fields using bulk aerodynamic formulae and radiation equations. The radiation equations used in this work are based chiefly on the work of Budyko (1956) and Raden (1959) which were adopted by Ramage (1972). The unit of time is month. Monthly values of energy exchange parameters are computed. Air-sea interface fluxes of sensible heat and moisture are calculated using bulk aerodynamic equations. A drag coefficient varaible with wind speed is used as suggested by Wu (1969). The mean net radiation gain $R_n = Q_s - Q_r - Q_b$, where as mean heat equivalent heat loss $Q_e = LE + H$. The net heat balance at the ocean surface can therefore readily be obtained for each 5^0 grid by substracting the sum of latent and sensible heat losses from net radiation gain. Although the patterns of heat exchange derived from the equations are probably realistic, the absolute values and magnitude of gradients qualify only as approximations (Garstang, 1965).

Radiational Exchange equations

Total (direct + diffuse) incoming radiation is frequently measured by pyrheliometers at certain meteorological stations. From time-series of such measurements incoming radiation with a clear sky and with a sky covered by clouds of various amount, height and thickness may be evaluated. It has been found by

Kimball (1928) and Budyko (1956) that the ratio of incoming radiation of a clear to a cloudy day depends linearly upon cloudiness. Budyko considering all available stations in the northern hemisphere, found that the ratio decreases towards the poles. Average monthly values of total incoming radiation with a clear sky, as determined by Budyko (1963) employs a table of solar radiation received at the surface on cloudless days and calculates empirically the diminution caused by the average total cloud cover. The difficulties are caused by the variability of cloudiness as well as the primitive nature of observations of ships at sea. Observations at sea include an estimate of total cloud cover regardless of type. Thus the presence of cirroform clouds with a high transmittance cause an under estimate of the calculated radiations using total cloudiness. Quinn and Burt (1968) found this to be a problem in the tropical Pacific where cumulus and cirroform clouds predominate. North eastern Indian Ocean is no exception, especially with the active convective clouds prevailing during the monsoon months.

Incident Solar Radiation for observed cloudiness

In the present investigation, the equation

$Q_s = Q_{so}(1-bc^2)$ ———— (1), computing the solar radiation received at the surface of the earth on a cloudy day, used values of Q_{so} (the solar radiation, received at the surface, of the earth on cloudless days) obtained from a table given by Berliand (1960)

TABLE 1. TOTAL INCOMING RADIATION WITH A CLEAR SKY IN CAL CM^{-2} DAY^{-1} (AFTER BERLAND, 1960)

North Lat. Month	1	2	3	4	5	6	7	8	9	10	11	12
30	410	508	613	703	763	780	771	716	628	530	430	373
25	463	562	660	730	784	788	760	729	653	572	482	431
20	511	590	663	720	740	750	743	716	673	608	520	484
15	555	624	681	705	721	724	721	709	688	636	572	530
10	595	650	695	698	696	692	694	698	698	661	610	575
5	635	671	704	688	667	656	662	680	701	681	643	618
0	666	698	707	672	635	618	623	660	696	696	672	656
South												
5	695	704	704	654	602	580	580	634	687	704	698	693
10	722	715	694	631	567	535	550	602	670	705	717	726
15	744	722	679	601	527	491	507	568	648	700	734	753
20	762	726	660	566	485	442	464	531	622	690	746	774
25	776	726	639	527	439	395	416	491	589	679	755	793
30	787	719	611	489	392	348	366	447	558	662	760	810
35	792	701	578	447	343	297	316	398	522	642	760	822
40	792	680	540	401	287	241	265	350	482	616	752	830
45	789	654	499	353	233	180	206	297	439	584	738	832
50	779	622	454	302	178	125	150	241	393	547	720	824
55	762	586	406	245	125	75	98	180	340	507	702	811
60	743	548	353	194	79	32	52	124	280	464	690	804

TABLE. 2

ANNUAL MEAN VALUES OF K AND K' AT STATED LATITUDES

5	10	15	20	25	30	35	40	45	50	55	60	65	70	75	Stockholm	U.S.A.
).66	0.66	0.67	0.67	0.68	0.68	0.68	0.67	0.66	0.64	0.62	0.60	0.55	0.50	0.42	0.61	0.71
).52	0.55	0.57	0.59	0.63	0.63	0.65	0.68	0.70	0.72	0.74	0.76	0.78	0.80	0.82	0.83	-
					Sadyko(1956)										Asklof (1920)	Kimball (1928)

and used by Budyko (1963) (Table 1). The value of k which is a function of latitude, is obtained from Budyko (1956) (Table 2). $\bar{c}$ is the monthly average cloud cover in tenths.

Reflected solar radiation

The amount of radiation absorbed by the ocean is $Q_S - Q_R = Q_S (1-A)$ ————(2). where A is the albedo of the ocean, which varies with water turbidity, roughness of the water surface, solar altitude, and cloudiness. The effects of water turbidity were measured by Ter-Markaryants (1960), who found that, for a solar altitude of 25 degrees, reflected solar radiation increased by a factor of 4 when its transparency decreases by a factor of 10. Actual values of reflected radiation, however, were small. They increased from 0.0015 gm Cal/cm^2/day to 0.0065 gm Cal/cm^2/day as transparency decreased from about 10 m to 1 meter. Estimates of effects of roughness vary considerably. Actual corrections for albedo for different solar altitudes and roughness by Burt (1954) and Ter-Markaryants (1960), but Degtyarev et al. (1964) and Pivovarov et al. (1965) did not find any significant effect of roughness upto a sea state of at least 3 (wave height of about 1.5 meters). Beard and Wiebalt (1966) also concluded that waves have very small effect on the magnitude of reflected solar radiation.

Because the effects of turbidity and roughness were

Table 3

Reflected Solar Radiation for Cloudless Days (ly day^{-1}) (Portman and Rynnar (1970)

Incident Solar Radiation	Average Diurnal Albedo (in percent)	Reflected Solar Radiation
300	7.6	22.8
400	7.0	28.0
500	6.3	31.5
600	5.7	34.2
700	5.0	35.0

uncertain, and because reliable quantitative information on their distributions in space and time was unknown, these two factors were neglected in the computations of reflected solar radiation discussed below. The albedo of cloudless skies was computed only in relation to solar altitude. Pivovarov et al. (1965) who showed along with many others, that the albedo of water for a cloudless sky decreases as solar altitude increases, conducted albedo measurements at Black sea, and arrived at an empirical expression

$$A = \frac{b}{\sin a + b},$$

A = albedo; b = 0.04 an empirical constant; a = solar altitude. Computations were made by Postman and Ryznar (1971) of the average divisional albedo for the different geographical locations in the Indian Ocean. Hourly albedo values were computed and multiplied by corresponding hourly averages of incident solar radiation as measured. The resulting hourly averages of reflected solar radiation were totaled for each day and divided by daily totals of incident solar radiation to obtain the average diurnal albedo. The results are reproduced in Table.3. The albedo was least when the daily solar input was greatest; and, in fact, the relation was found to be linear. The values varied from 0.076 to 0.050. The corresponding increase of reflected solar radiation was about 12 gm cal cm^{-2} day^{-1}. The stations closer to

TABLE. 4. ALBEDO OF THE SEA SURFACE FOR TOTAL (DIRECT + DIFFUSE) RADIATION (AFTER BUDYKO, 1956)

Lat / Month	I	II	III	IV	V	VI	VII	VIII	IX	X	XI	XII	Year
70	-	0.23	0.16	0.11	0.09	0.09	0.09	0.10	0.13	0.15	-	-	(0.13)
60	0.20	0.16	0.11	0.08	0.08	0.07	0.08	0.09	0.10	0.14	0.19	0.21	0.13
50	0.16	0.12	0.09	0.07	0.07	0.06	0.07	0.07	0.08	0.11	0.14	0.16	0.10
40	0.11	0.09	0.08	0.06	0.06	0.06	0.06	0.06	0.07	0.08	0.11	0.12	0.08
30	0.09	0.08	0.07	0.06	0.06	0.06	0.06	0.06	0.06	0.07	0.08	0.09	0.07
20	0.07	0.07	0.06	0.06	0.06	0.06	0.06	0.06	0.06	0.06	0.07	0007	0.06
10	0.06	0.06	0.06	0.06	0.06	0.06	0.06	0.06	0.06	0.06	0.06	0.07	0.06
0	0.06	0.06	0.06	0.06	0.06	0.06	0.06	0.06	0.06	0.06	0.06	0.06	0.06

equator showed smaller change. Hence it was found suitable to adopt a value of 6% of albedo in the computations. Table used by Budyko (1956) also showed the same value to be alright, for low latitudes, inspite of a latitudinal variation which is much evident (Table 4).

<u>(b) The effective back radiation</u>

Effective back radiation is the difference between long wave radiation from the sea surface and the long wave radiation from the atmosphere. It decreases with increasing humidity and stability of air and for the range of humidities commonly observed at sea, it decreases also with increasing temperature. The following semi-empirical equation proposed by Berliand and Berliand (1952) and later used by Budyko (1956), Roden (1959) and Ramage et al (1972) is used here.

$$Qb = -\left[\varepsilon \sigma (T_s)^4 (0.39 - 0.050 \sqrt{e_a}) (1-kc^2) + 4 \varepsilon \sigma (T_s)^3 (T_s - T_a)\right] \quad \text{---------- (3)}$$

the values of k' which depends on latitudes are taken from Budyko (1956) (Table.2). The first term represents back radiation which consists of the longwave radiation from the sea surface, which is proportional to the 4th power of the absolute sea surface temperature, minus long wave radiation from the sky and takes into account the effect of temperature, humidity and cloudiness.

It varies, for the ranges generally found in oceanic regions, between 20 and 200 Cal cm^{-2} day^{-1}. The constant k^* has been evaluated by considering also the vertical extent of clouds as well as the height of the cloud base from the surface of the earth; it was found that k^* increased from the equator to the pole (Table 1). The second term considers the effect of stability. Owing to the small air-sea temperature differences observed over the oceans, this term is rather small and varies for the most part only between - 20 and 20 cal cm^{-2} day^{-1}. A number of empirical formulae exist for the computation of Q_b, most of which were derived for overland conditions. Uncertainities are primarily introduced by the cloud factor in the empirical equations (Kraus, 1972) that is given both as a linear and quadratic function of cloudiness. Because of its common application for the computations of large-scale air-sea interactions equ (3), Brunt's equation with the empirical constants of Budyko (1956) is used here.

Bulk aerodynamic equations

The importance of an accurate knowledge of evaporation in the study of atmospheric energetics needs no emphasis, water vapour being the most important single agent of heat transfer between atmosphere and oceans and in the redistribution of heat over the surface of the earth. The turbulent flux of water vapour between the ocean and atmosphere, besides Q_E is the most important

process affecting Δn. It has been estimated (Jacobs, 1951) that of the total solar energy absorbed at the sea surface during the course of a year, approximately 50% is used for the evaporation of sea water that becomes available to the atmosphere in the form of energy latent in water vapour.

Bulk aerodynamic formulae were used in the computation of fluxes of latent and sensible heat. The bulk aerodynamic exchange equations developed principally by Sverdrup (1937), Jacob (1942) and Budyko (1963) can be expressed in the following forms.

$$Q_e = \rho_a C_e L (q_s - q_a) W \quad \text{---------- (4)}$$

$$Q_h = \rho_a C_h C_p (t_s - t_a) W \quad \text{---------- (5)}$$

where Q_e and Q_h are fluxes of latent and sensible heat energy (gm cal cm^{-2} day^{-1}) respectively. ρ_a is the density of air (assumed to be constant) (gm cm^{-3}); C_e and C_h are the exchange coefficients for water vapour and sensible heat; W is the average wind speed at 10 m or ship anemometer level; q_s and q_a are average of mixing ratios of air in contact with salt water and at 10 m or deck level respectively; t_s and t_a are the average temperatures of the sea surface and air at the upper level respectively. C_p is heat capacity (cal g^{-1} K^{-1}) and L is the latent heat of vaporization at average sea surface temperature. Many field experiments and theoretical works have been carried out which show that the

coefficients are not identical and that they vary with wind speed and atmospheric stability. Despite of the large amount of work done, the values of the coefficients are not known exactly. In most of the studies C_e and C_h are assumed to be equal to C_d, the exchange coefficient for momentum (drag coefficient).

The aerodynamic resistance, or drag coefficient C_d depends upon the height at which the wind speed W is measured. In practise, it is customary for a reference level of 2 or 10 m to be chosen; then, providing the wind is not so strong that stream lining occurs, or light that viscous effects are considerable, Cd is independent of wind and a function only of vertical stability of the atmospheric boundary layer and the aerodynamic roughness of the surface over which the wind is blowing (Sethuraman & Raynor, 1975). Hence for a particular surface and thermal stability condition, the value of Cd is unique. However roughness of the sea surface is determined by the wave conditions prevailing while the wind is acting upon the surface; in turn the wave conditions themselves depend upon the wind situations. Therefore, Cd for a water surface is indeed a function of wind speed. Moreover, when the sea is not fully - developed, it is also a function of wind duration and fetch.

Although there have been numerous experimental investigations and analytical studies of wind-stress upon the sea-surface (Kitaigorodskii, 1970), a relationship which describes satisfactori

the variation of Cd with wind speed has not yet been found. Despite increasingly sophisticated instrumentation for measuring Cd, only trends and orders of magnitudes have so far been established with any degree of certainity. In view of the problems involve in empirical investigations of the atmospheric boundary layer over the sea, discrepancies among results are perhaps inevitable.

Wilson's (1960) compilation of the results of fortyseven wind-stress investigations revealed wide scatter in the values of Cd obtained by field measurements. He concluded that Cd increases with wind speed, probably in a non-linear manner, until, when wind speed W=25 m sec^{-1}, a value of approximately 2.6 x 10^{-3} is approached asymptotically.

After careful consideration of the various lines of evidence available upto 1960, Deacon and Webb (1962) concluded that there is probably a slight increase of Cd with wind speed represented by $C_D=(1.00 + 0.07\ W \times 10^{-3})$. Ball (1965) extended Wilson's survey and improved upon it by tabulating and averaging values of Cd, distinguishing between methods of derivation. He decided that in light winds the methods involving measurement of sea surface tilt is less reliable than other methods commonly employed. The methods (Wind profile method, geostrophic departure method, eddy correlation method, surface film method) and their limitations are discussed by Ball (1965) and Kraus (1968). Ball suggested that the bulk aerodynamic coefficients are nearly equal to each other, for near

neutral conditions.

As the methods improved and the data grew, many empirical formulas were developed to express the relationship between the wind and the coefficients. (Wu, 1968; 1969; Pond et al., 1971; Hicks, 1972; Hidy, 1972; Smith and Banke, 1975; Garratt, 1977). Most of these formulas apply to a small range of light to moderate winds and do not agree well with the estimates available for strong or hurricane winds. An exception to this statement is the scaling of Cd by the Froude number $U(gz)^{1/2}$ by Wu (1968) who used both laboratory and field observations to obtain.

$$C_d^{-1/2} = 1/k \ln (1/a\, C_d F^2)$$

Where U is the wind speed at height Z above the surface, g the acceleration of gravity, F the Froude number, K the Karman constant and a the proportionality constant for the relationship between aerodynamic roughness length (Zo) and friction velocity (Us). Viz. $Zo = a\, Us^2/g$ suggested by Charnock (1955).

When the value of a is near 0.013, the relationship agrees well with values of the drag coefficient found by Palmen & Riehl (1957) in the maximum wind region of hurricanes.

Wu (1969) suggested that for 1 $\leq$ W $\leq$ 15 m Sec^{-1}, Cd increases with wind speed and proposed the approximate formulae $10^3\, C_d = 0.8\, W^{1/2}$. He further thought that for W $\geq$ 15 m Sec^{-1},

Cd is constant and recommended the value Cd = 2.6×10^{-3} 'for oceanic application'. (Fig 3). On the other hand, his conclusion that a discontinuity in the variation of Cd with wind exists at a wind speed of 15 m Sec^{-1}, differed from Wilson's impression that Cd approaches a constant value asymptotically at W =25 m Sec^{-1}. Smith and Banke (1975) also did not find the discontinuity in their studies which proposed the relationship 10^3 Cd = 0.63 + 0.66 W $\pm$ 0.23 for the range 3 $\leq$ W $<$ 21 m Sec^{-1}.

The quest for an indisputable relationship continues. Garratt (1977) who studied observations of wind stress and wind profiles over the ocean reported in the literature for the past few years, has postulated that they are consistent with Charnock's (1955) relation $z_0 = a\, U^2 g$ with a = 0.0144 with a Von Karman Constant = 0.41 $\pm$ 0.025. Main reviews of the neutral drag coefficients over the sea till the first half of seventies show that Cd variations obey Charnock's relation and Charnock's relation with a = 0.016 coincides with Wu's results. More recent observations of neutral drag coefficient values using techniques using eddy correlation and wind profile methods and that for hurricane and Vorticity - mass budget data analyses showed that they are almost consistent with the Charnock's relationship. For practical purposes, this relation is closely approximated over the range 4 $<$ W $<$ 21 m Sec^{-1} by a neutral drag coefficient (referred to 10 m) varying with W (m/sec) either by a power law relation.

Fig.3. Variation of drag coefficient with wind speed according to Wu (1969).

Curve A: $C_d = (0.5 \times 10^{-3})\, w^{1/2}$

Curve B: $C_d = 2.6 \times 10^{-3}$

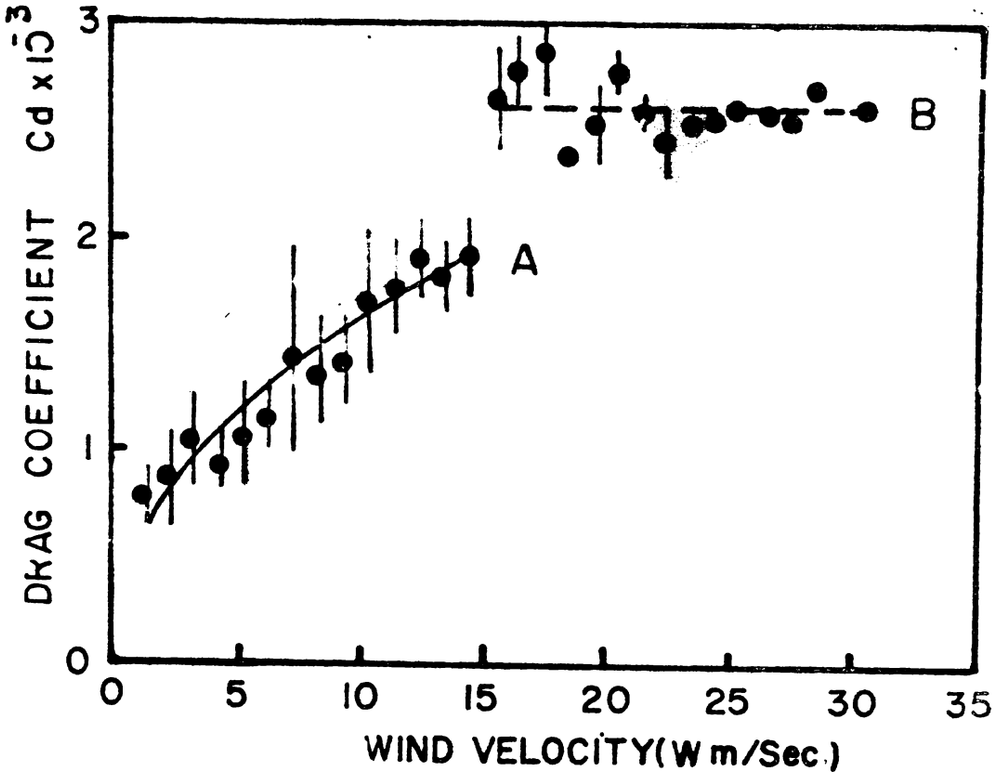
DRAG COEFFICIENT Cd x 10^-3
3
2
1
0
A
B
0
5
10
15
20
25
30
35
WIND VELOCITY(W m/Sec.)

$$Cd\ (10) \times 10^3 = 0.51\ W^{0.46}$$

or by a linear form

$$Cd\ (10) \times 10^3 = 0.75 + 0.067\ W.$$

These relations are close to those proposed by Deacon and Webb (1962) (the linear form) and Wu (1960) for wind speeds $\leq$ 15 m sec^{-1} and do not support a constant Cd above 15 m sec^{-1} as deduced by Wu (1969).

As described above, much of the work is done on Cd. Rather less work has been done on the sensible heat and moisture exchanges due to greater experimental difficulties and perhaps in part because many of the investigators have been oceanographically oriented and hence more interested in the momentum exchange. Our knowledge of the coefficients of exchanges of water vapour and heat are rather limited (Phillips, 1972[66]).

Kraus (1959[3]) has drawn attention to the fact that over large areas of the trades the mean wind speed is marginal in the sense that it is very near the critical value of 6.5 m sec^{-1} at which the sea surface is generally supposed to change from a hydrodynamically smooth to a rough surface. This would mean that small changes in the mean wind speed might produce comparatively large change in evaporation. Pisharoty (1965) has pointed out that the magnitudes of the evaporation as deduced from the various empirical cum theoretical formulae, appears to be significantly less than the evaporation called for by the flux

computations, when the precipitation over the sea as well as the flux upward, through the 450 mb layer are considered, based on his analysis of the 1963 data. He wanted, the k value (evaporation coefficient) of the order of 12.5 to be adopted for the 1963 data.

Values of evaporation coefficient used by different authors for Indian Ocean are given in the Table 5. Budyko (1963) used a value of 7.81. Venkateswaran (1956) computed k empirically for the Indian Ocean area by a method, adopted earlier by Jacob (1951) for the Atlantic. A region of the ocean is selected, when the ocean currents are weak. The evaporation is computed from the estimated solar energy absorbed by the water surface decreased by the amount used up for eddy transfer. The value of E and $(q_s - q_a)$ are estimated from climatic charts, k is then computed. This assumes that there is no storage of heat or transport of heat by the water bodies. The value obtained for k by Venkateswaran is 6.25. The studies by Suryanarayana and Sikka (1965) suggests the use of a high evaporation coefficient than the one they used (5.06), since during south west monsoon period, the value of wind strength exceeds in certain parts of the Arabian sea, which favours higher evaporation. Colon (1965) also recognises the need to adopt a drag coefficient which varies with wind, after studying the large variations of the wind speeds in winter and summer.

Table - 5

Values of evaporation coefficient K according to different authors; $Q_e = K (\bar{e}_s - \bar{e}_a) W$ where Q_e is expressed in gm Cal cm^{-2} day^{-1}; $(\bar{e}_s - \bar{e}_a)$ in millibars and W in m Sec^{-1}

Authors	Evaporation Coefficient K
Budyko (1963)	7.81
Venkateswaran (1956)	6.25
Privett (1959)	4.39
Ramanadham et al., (1969)	5.37
Suryanarayana and Sikka (1972)	5.06
Ramage et al., (1972)	5.17
Colon (1964)	
a) for $W < 7.5$ m Sec^{-1}	5.25
b) for $W > 7.5$ m Sec^{-1}	7.5
Shanmukhar (1978)	7.5
(for south west monsoon season)	~~9.8~~
*Present work	
a) When $W \leq 15$ m Sec^{-1}	Values varying from 2.65 to 7.09
b) When $W > 15$ m Sec^{-1}	9.5

*a) When $W \leq 15$ m/Sec $K = \frac{547.62}{(273+\bar{t}a)} W^{1/2}$

Where $\bar{t}a$ is the monthly average of air temperature expressed in ^{o}C; W the wind speed in m Sec^{-1}; K value varies from 2.65 (for values, $W = 2.20$ m Sec^{-1}, $\bar{t}a = 32.42^{o}C$) to 7.09 (for values, $W = 15$ m Sec^{-1}, $\bar{t}a = 26.30^{o}C$)

b) When $W > 15$ m/Sec, $K = \frac{2847.672}{(273 + \bar{t}a)}$ for an average value of $\bar{t}a = 26^{o}C$; K=9.5.

In the light of above discussions, Wu's values of C_d which varies with wind speed, derived for near-neutral conditions is substituted for the bulk aerodynamic coefficients for latent and sensible heat exchanges. The range of windspeed which is encountered in the Indian Ocean, which usually is neither less than 1 m sec^{-1}, nor more than 15 m sec^{-1}, permits the usage of Wu's results. Since, here only the climatic averages are dealt with, the wind maximum over the western Arabian Sea, seldom increases 15 m sec^{-1}. In the time-series analysis in the western Arabian Sea, values greater than 15 m sec^{-1} are encountered during south west monsoon months for individual years. Wu's relation for greater winds 2.6×10^{-3} is made use of, in the evaporation computation.

Garratang (1967) has shown that when a drag coefficient with a dependence on stability is used, then the changes in the drag coefficient produce an increase in the latent heat transfer during disturbed weather conditions, eventhough the wind speeds and specific humidity differences are similar to those of undisturbed condition. In the present studies, the effects of stability is not fully accounted for, though disturbed weather conditions are encountered during monsoons. However, Pant (1977), using the IIMEX (1973) data inferred that prevalance of stronger surface winds over a large part of the Arabian Sea, during the monsoon season would maintain a near neutral stability in the surface layer.

After substituting the values $Cd = 0.5\ W^{1/2} \times 10^{-3}$ (Wind velocity in m sec^{-1}) L = 595 Cal/gm where L is the latent heat of vaporisation in Cal/gm ; $\rho_a = 1.2 \times 10^{-3}$ gm cm^{-3} R = 2.8704×10^6 erg/gm/K^0 ($\frac{1}{\rho_a} = \frac{RT}{P}$; R is the gas constant for dry air; T temperature; P pressure; ρ_a is the density of air) and converting ($\bar{q}_s - \bar{q}_a$) to ($\bar{e}_s - \bar{e}_a$) is the vapour pressure difference between sea and atmosphere, $C_p = 0.24$ Cal gm^{-1} deg^{-1} where Cp the specific heat of air at constant pressure, the bulk aerodynamic equations could be established as,

$$Q_e = \frac{547.61}{(273+\bar{T}_a)} (0.98\ \bar{e}_s - \bar{e}_a) W^{3/2} \quad \text{---------- (6)}$$

$$Q_h = \frac{261.32}{(273+\bar{T}_a)} (\bar{T}_s - \bar{T}_a)\ W^{3/2} \quad \text{----------(7)}$$

e_s the water vapour pressure (mb) corresponding to sea surface temperature, and e_a the water vapour pressure corresponding to dew point temperature is computed using Smithsonian meteorological tables. e_s is multiplied by 0.98, in order to adjust for the effect of salinity. (Sverdrup, 1951).

The values of evaporation coefficient obtained varies from 2.65 to 7.09 for different conditions (when $W \leq 15$ m Sec^{-1}). During south west monsoon months, when $W > 15$ m Sec^{-1} is observed from the west Arabian Sea, this evaporation coefficient rises up to 9.5, which is much high a value, though not as high as the value suggested by Pisharoty (1965) for rough seas with strong

winds. The drag coefficient values vary from 0.74 to 1.96, for the wind speed values encountered during the calculations. Sensible heat coefficient varies between 1.75 and 4.69. The coefficients of evaporation and sensible heat is influenced by the air temperature. As the air temperature increases, the coefficients decrease. This roughly coincides with the stability of air. The lowest values of the coefficients are observed in the Persian Gulf during south west monsoon months and the highest values near the core of high wind speeds observed in the west Arabian sea.

Though the equations (6) and (7) are ideally suited for computations of synoptic measurements, here the equations are made use of, to obtain a large scale energy exchange picture. Computations of air-sea fluxes using means and fifty-nine three hourly ship observations (Wyman - Woodcock (1946), Caribean data), reveal that use of mean values for the constant and of climatological data in the transfer formulae for heat and moisture fluxes are satisfactory within the purposes for which such long period calculations are made use of. Covariances between elements can make the product of averages, as used in Qs and Qe calculations here, differ from the average of products (Bunker, 1976); however, this effect is also not of considerable importance.

Accuracy of heat exchange computations

Accuracy of the air-sea interaction values derived from marine surface meteorological parameters depends both on the correctness of the formulae and the quality of data used. Discrepancies connected with observations by merchant vessels, and the uncertainties connected with the empirical formulae used are discussed earlier.

Estimates of the radiation from sun and sky Qs, have been uncertain, because marine cloud observations are of subjective nature. Better measurements of cloudiness such as the amount of opaque clouds or the percent of possible sunshine are not reported and information regarding the thickness of cloud layers is generally not observable, from ships. The corrections, derived are usually evolved in mid latitude and over the land, which might produce erroneous results, as reported by Quinn and Burt (1968).

As in the case of short wave radiation, the formula which attempt to account for the modification of the long wave radiation flux, when cloud is present are expressed only in terms of fractional cloudiness, with no provision for variation in cloud height and type. This can lead to even more serious errors in the case of long wave radiation, since the clouds themselves are a source of such radiation, the intensity being principally

determined by the temperature and therefore, indirectly, by the height of the cloud. Any attempt to take account of the influence of varying cloud height and amount in the long wave radiation is handicapped, of course, by the fact that at night time, when long wave radiation is most easily measured, cloud observation is difficult and the results somewhat uncertain. The table of clear sky radiation constructed by Berliand (1960) when compared with Portman and Rymar (1971) values based on radiometer observations show that Berliand tables are 5–20% too high (Bunker, 1976). Variations in stability and wave spectra, and the assumptions that the transfer coefficients of heat, water vapour, and momentum are equal, increase the uncertainity in the magnitudes of the derived turbulent exchange processes. Since there are not many direct measurements to compare with the computed evaporation, determination of the accuracy cannot be made. Measurements of vertical eddy fluxes during BOMEX (Holland, 1972) indicate that the derived evaporation is of the correct order of magnitude.

The conduction of sensible heat (Qh) is subject to the same limitations, but is of relatively small magnitude. Errors in Qn due to uncertainities in Qh are expected to be smaller than those contributed by the other heat exchange processes.

Qn is the difference of large numbers. The relative error in Qn is therefore potentially much larger than that for the individual exchange processes.

Chapter 3

Annual climatic models of energy exchange parameters

Energy exchange charts of the Indian Ocean, leading to the study of annual surface energy budget of the region bounded by 30°N to 40°S and 20°E to 120°E have been constructed. Normals of the energy budget components, as solar radiation absorbed by the Ocean, net infrared radiational exchange at the surface, and the net radiative heat balance, following Budyko's method, latent heat flux and sensible heat flux, following bulk aerodynamic method during the twelve months of the year are evaluated using the available marine climatological data. The resultant net heat gain by the ocean for the twelve months are computed. Charts giving annual coverages of the net heat gain by the ocean, radiational, latent and sensible heat (Fig 4) and related meteorological variables and sea surface temperature are presented (Fig 5 and 6).

Annual distribution of Ocean-surface heat exchange parameters

The relationship between the major components of the energy budget can be written as,

$$Rn = Qh + Qe + Qst + Qv$$

where Rn is the balance of radiant energy on an area of the ocean surface. This is chiefly distributed between ocean-

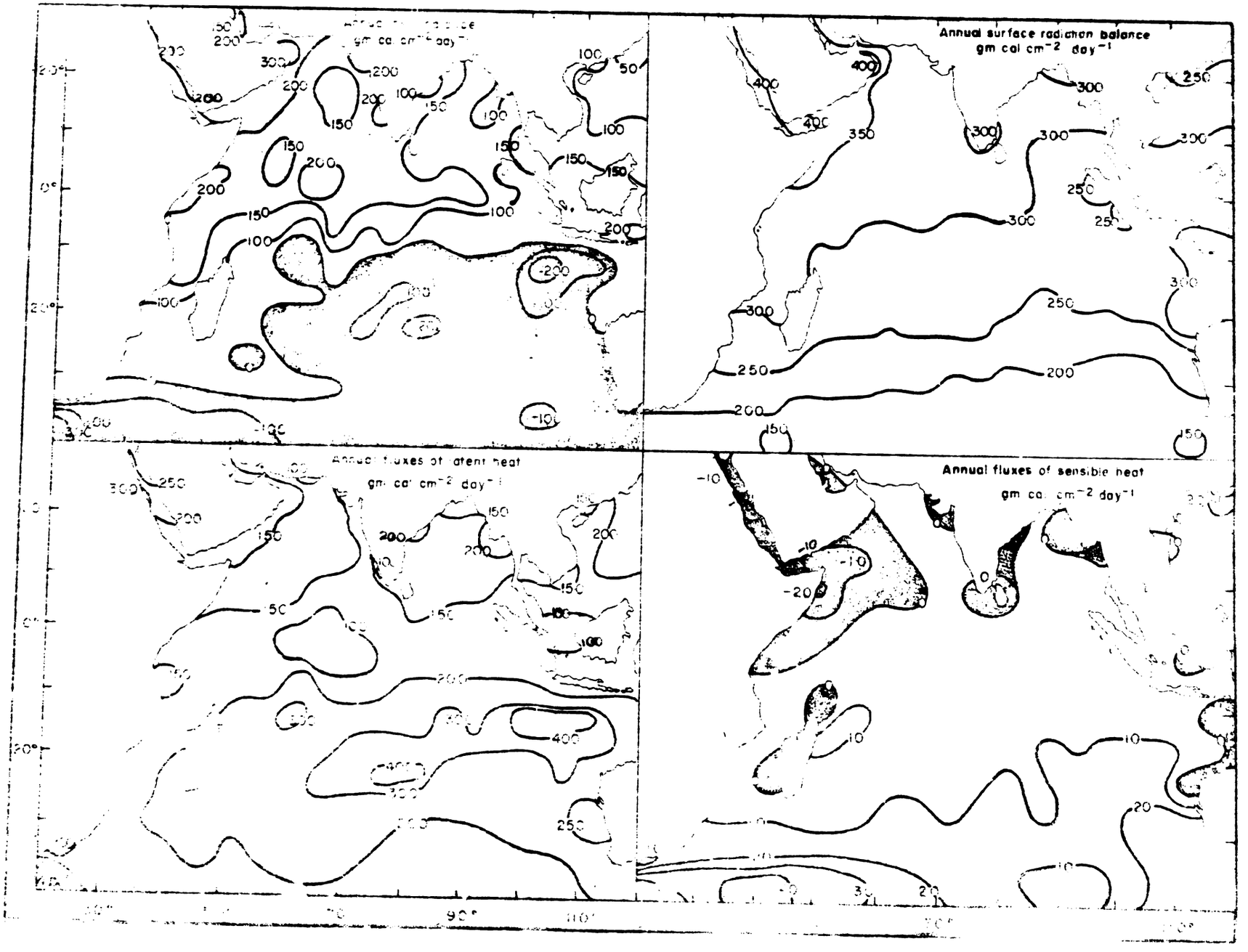
Annual surface radiation balance
gm cal cm⁻² day⁻¹
Annual fluxes of latent heat
gm cal cm⁻² day⁻¹
Annual fluxes of sensible heat
gm cal cm⁻² day⁻¹

[redacted]nual average heat balance

b) Annual average latent heat flux

c) Annual average radiation balance

d) Annual average sensible heat flow

at the Surface of Indian Ocean
expressed in gm cal cm^{-2} day^{-1}

atmosphere transfers of the sensible and latent heat (Qh and Qe respectively), storage of heat in a cloumn of the ocean (Qst) and the horisontal divergence of heat by sea currents (Qve). Rn the net radiative heat energy input, is the balance of radiant energy components holding the relationship

$$Rn = Qs - Qr - Qb$$

where Qs is the rate of heating at the sea surface from the incoming short wave radiation, modified by the total average cloud cover, Qr is the rate at which radiation is reflected from the sea surface and Qb is the net infared radiational exchange at the surface. The methods for evaluating individual components are given in detail in the chapter 2.

Net heat balance

The contoured distribution of the annual heat gain is presented (Fig.4.a). The positive value of the term net oceanic heat gain signifies gain of heat for the sea, where as negative values signify the loss of heat. This residual term of the heat balance is arrived at, as the balance between net radiative heat gain by the ocean, and the total heat, lost to the atmosphere.

$$\text{ie } Rn - Qe - Qh \neq Qs + QVe$$

Thus the residual term comprises of the sum total of lateral

heat transport and the storage of heat. The mean condition of the ocean-atmosphere system varies but little from year to year, so that in climatological calculations of annual energy budgets it is permissible to neglect oceanic storage of heat. For annual picture, heat storage does not have much of a significance. For periods much more or less than a year, however, the fluctuations of heat storage cannot be ignored. Secular changes of oceanic heat storage, although small in magnitude, are probably of some importance in the mechanism of climatic change, and seasonal values of Qs can exceed Qa/3 (Newell et al., 1970; Nathan, 1971).

The chart (Fig.4 a) shows the strongest heat loss area over the Agulhas Current, south of Africa (maximum > -300 gm Cal cm^{-2} day^{-1}) and the south equatorial current region between Eastern coast of Madagascar to southern region of Indonesia. South of Indonesia between 10 - 20°S a strong (> -300 gm Cal cm^{-2} day^{-1}) heat loss is observed. The central southern Indian Ocean region of negative heat balance is again quite remarkable. West North-west Australian coast and the waters around Madagascar show areas of weak heat gain. The equatorial waters of the southern Indian Ocean in the western part show comparatively low values of heat gain and this extends to the Eastern Indian Ocean north of 10°S and East of 80°E. Arabian sea on the whole, shows high values of heat gain except the central part of the sea. The east African and Arabian coasts show the maximum heat

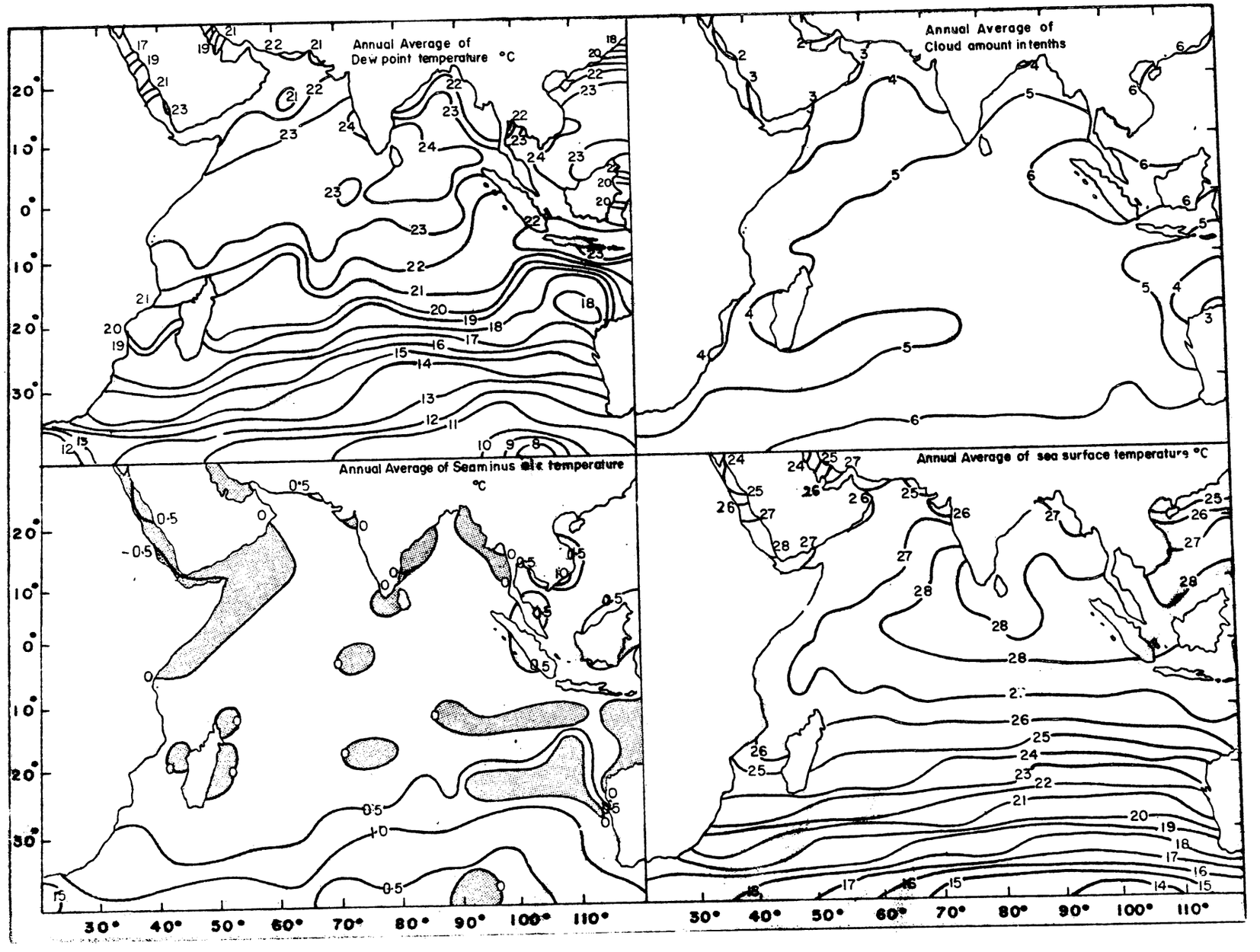
Annual Average of
Dew point temperature °C
Annual Average of
Cloud amount in tenths
Annual Average of Seaminus air temperature
°C
Annual Average of sea surface temperature °C
20°
10°
0°
10°
20°
30°
30°
40°
50°
60°
70°
80°
90°
100°
110°

Fig.3. a) Annual average dew point temperature (°C).

b) Annual average sea minus air temperature (°C).

c) Annual average sky coverage by clouds (in tenths).

d) Annual average sea surface temperature (°C)
over the Indian Ocean.

gain. The northern Indian Ocean shows positive values of heat balance. There is a marked decrease in the values of heat gain towards the east, the western Arabian Sea showing the maximum and the south China sea showing comparatively low values. This zonal gradient causes the isopleths to orient towards north east.

The strong heating of the waters of the Western Arabian sea is the result of the upwelling of cold water (Fig 5 b). The cold water inhibits evaporation and reverses the usual direction of the sensible heat flux. The stability of air prevents the formation of many cumulus clouds and insolation reaches a maximum. The South-west coast of Indian sub continent also show a region of maximum positive heat balance. This area is also marked for its cool, upwelled waters during the south-west monsoon months, though not to the extend of western Arabian Sea. Since the cloud coverage is more, the insolation values are low. Another area of comparative high positive heat balance is Bay of Cambay area which shows negative temperature gradient (Fig 5 b & 5 d). The low sea surface temperature forms the cause for low evaporation and hence, comparatively high positive values of heat balance. The equatorial waters, except for the Somali coast show very low values. The net annual heat loss can be better understood by noting the contributions of radiation, latent heat and sensible heat fluxes shown in the charts (Fig 4b, c & d).

The net radiation balance

The distributions of net radiation annual average values are presented in Fig (4 c). The contours of equal radiation balance are strongly dependent upon the latitude, but are modified, by the local cloudiness. The effect of cloudiness shown in Fig (3.a) associated with ITCZ is apparent in the equatorial region of southern Indian Ocean. Southern Indian Ocean values of net radiation balance are latitude dependent. There is a decrease in the values of radiation heat input towards the higher latitude. The cloud distribution does not show much of a variation except in the West coast of Australia, where it is noted for the low cloudiness and relatively high surface radiative balance. In the southern Indian Ocean south of the subtropical anticyclonic gyre, in the region of westerlies it is always overcast. Very low values of mean annual radiative balance are observed.

In the Northern Indian Ocean, where the monsoonal influences are felt, the cloud distribution shows a zonal variation and zonal differences ~~in~~ as seen in the radiative heat balance. The Western Arabian sea is noted for the high radiative balance. The Arabian coast and the Red sea record maximum radiative heat balance of 400 gm cal cm^{-2} day^{-1}. The cloud amount observed in the Red sea drops to a minimum with seasons and shows a very low

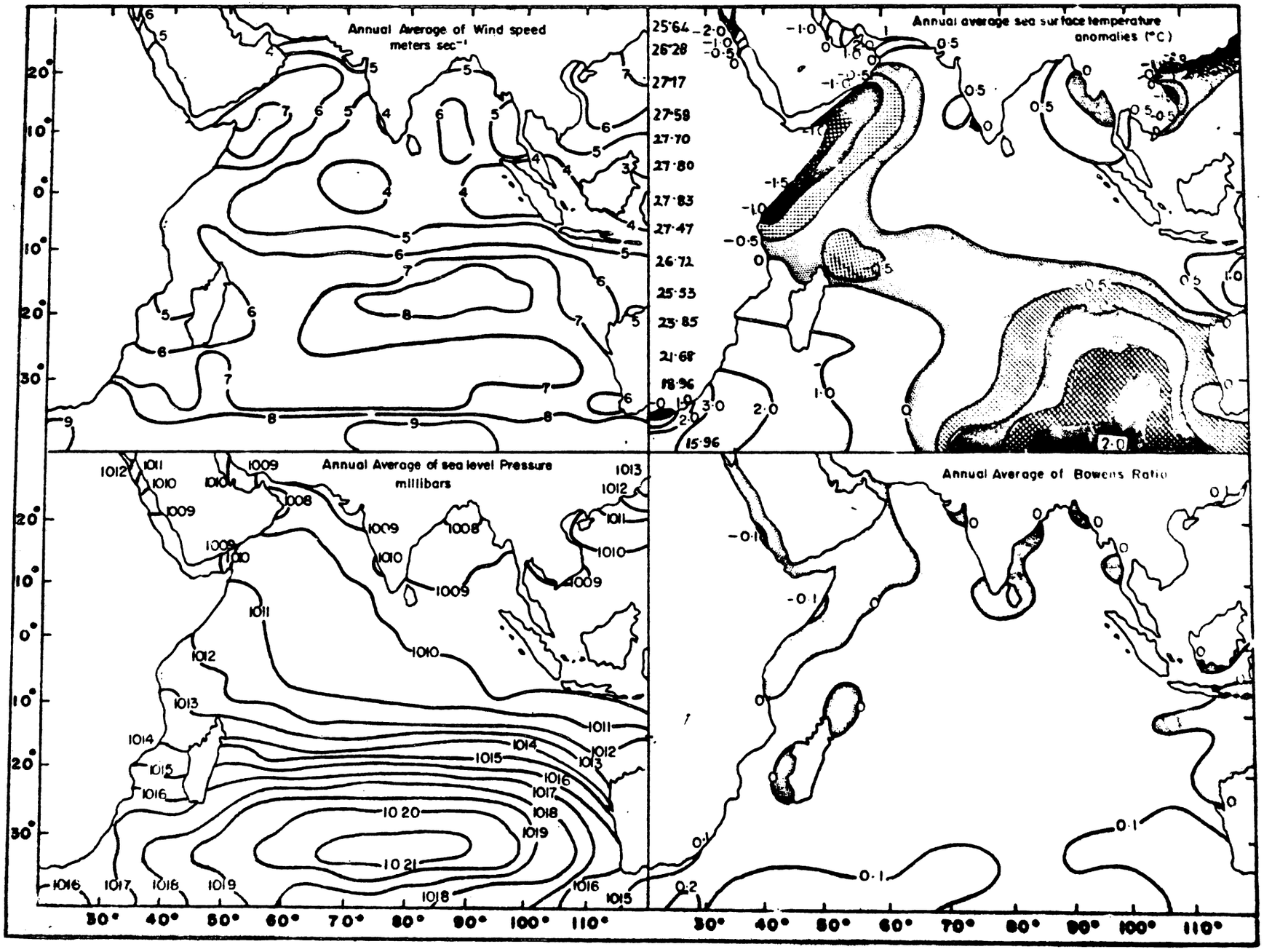
Annual Average of Wind speed
meters sec⁻¹
Annual average sea surface temperature
anomalies (°C)
Annual Average of sea level Pressure
millibars
Annual Average of Bowens Ratio
25·64
26·28
27·17
27·58
27·70
27·80
27·83
27·47
26·72
25·53
25·85
21·68
18·96
15·96
20°
10°
0°
10°
20°
30°
30° 40° 50° 60° 70° 80° 90° 100° 110°

Fig.6. a) Annual average scalar wind speed in (m Sec^{-1}).

b) Annual average sea level pressure (mb)

c) Annual average zonal anomalies of sea surface temperature (^{o}C) as calculated as deviations from the latitudinal averages of annual mean sea surface temperature. (given on the ordinate at 5° latitude interval in °C)

d) Annual average Bowen's ratio over the Indian Ocean.

(less than 20%) mean value. The Indonesian waters and the south China sea show comparatively lesser gain of radiative heat. The area of maximum cloudiness spreads from 10°S - 10°N in the Eastern Indian Ocean. Zonal anomalies of the cloudiness corresponds to that of sea surface temperature (Fig 5 c & d). The recent studies by means of satellite data by Saha (1970, 1971 a, 1971 b, 1972 a, 1973) reveal the zonal anomalies of the cloudiness in the tropical ocean. The distribution of sea surface temperature (Fig 5 b), the distribution of sea level pressure (Fig 6 b) and the distribution of sea minus air temperatures (Fig 5) could also be noted. Saha has observed asymmetry and discontinuity of cloud amount over areas which are affected by cold currents and monsoons. As a rule, cloud bands do not appear over cold oceans. Somali Current maintains a cold ocean surface in the Western Indian Ocean, especially in Western Arabian sea west of about 65°E. Saha observed, during the southwest monsoon season that the cloud cover over the Indian Ocean region has a sharp cut - off at about 65°E and the occurance of ITCZ over the Indian Ocean which varies between 10°N - 10°S, east of about 60°E. According to his surmise its occurance appears to form in warm equatorial Ocean where boundary layer convergence in a conditionally unstable atmosphere arising largely from the thermal - wind effect due to ocean surface temperature, causes increased lifting of moisture and condensation to form concentrated cloud zone a few degrees away from the equator.

Turbulent fluxes of latent heat

Turbulent fluxes of latent heat (evaporational cooling) is of the same magnitude as net heating due to radiation. This component of thermal energy - exchange is presented in Fig (4b). The strongest areas of evaporation are the south equatorial current (10 - 25°S) especially the area between Madagascar and Java and the Agulhas Current regime, off South Africa. The rate of latent heat exchange decreases towards north and south. The rate of latent heat flux is comparatively high in the southern China Sea. The equatorial region and the western Arabian Sea show low values of latent heat exchange. South west coast of India, the Gulf of Cambay region and the coast of Pakistan also exhibit low values of latent heat flux. The annual mean values of wind speed (Fig 6a) and the dew point temperature values, the sea surface and air temperatures difference Fig (5 a and b) and the sea surface temperature values are presented for the appraisal of the condition influencing evaporational cooling. Humidity content decreases with latitude from the maximum at the equator, towards the subtropical high pressure cells, where adiabatic heating of subsiding air keeps the humidity content low, away from saturation. Unlike the other Oceans, the western parts of north Indian Ocean is less humid than the eastern parts which is warmer. Very high values of vapour pressure gradient are observed in the Red sea. The eastern part of the area between 10 - 30°S is always

marked for moderately high vapour pressure gradient. The wind speed values which shows a high maximum during South west monsoon season, increases the annual average. This compensates for the cold waters off the Somali and Arabian coasts. Southern Indian Ocean exhibits more humidity in the western side. The stable south east trade winds along Bay of Bengal exhibits slightly higher values than the Arabian sea excluding the Red sea values which are comparatively higher. The western Arabian sea latent heat exchange values are lesser compared to that of eastern Arabian sea. These results confirm the qualitative explanation of Saha (1971)[a,b] of the differential distribution of cloud and sea surface temperature and the subsequent air-sea interaction. The centre of maximum evaporation noted in the subtropical anticyclonic region of southern Indian Ocean is associated with the clear skies and the dry subsiding air characterstic of this region. Another area of maximum evaporational cooling in the region of Agulhas Current, reflect the cooling of the waters of warm current exposed to cold dry continental air in the wintertime.

Sensible heat exchange

The fluxes of sensible heat exchange from the ocean to atmosphere is considerably large in the south China Sea and in the southern most portion of the Indian Ocean under investigation. The chart of annual averages of sensible heat is given (Fig 4d).

The area between Java and Australia, western side of Madagascar,

south of Borneo, eastern Bay of Bengal, southern and Northern parts of west coast of India and the western Arabian sea show negative heat exchange. The area off Somali coast exhibits the strongest negative flux. The direction of the fluxes of sensible heat are governed by the temperature gradient and the relative magnitude of the wind speed. Western Arabian sea is characterised by the winds of great speed and negative temperature gradient. Other areas are characterised by seasonal upwelling and subsequent gradients in temperature along with moderately high values of wind speed which favours sensible heat exchange. The areas of negative fluxes of heat almost follow the regions of negative gradients of temperature.

Annual average sea surface temperature anomalies

The geographical distribution of the latitudinal anomalies of the annual sea surface temperature is depicted in Fig 6 c. The distribution sea surface temperature anomaly $\Delta \bar{T}s = (\bar{T}s - \bar{\bar{T}}s)$, where Ts is the sea surface temperature and $\bar{T}s$ is the latitudinal average of sea surface temperature over the area under study in the Indian Ocean, shows the east-west differences, in the sea surface temperature values. The value of $\bar{\bar{T}}s$ is marked at the left hand edge of the map. The distribution of sea surface temperature anomalies, as shown in the map, shows a close relationship to the oceanic circulation in the surface layers as given in Fig (7 a and b). Horizontal advection of water,

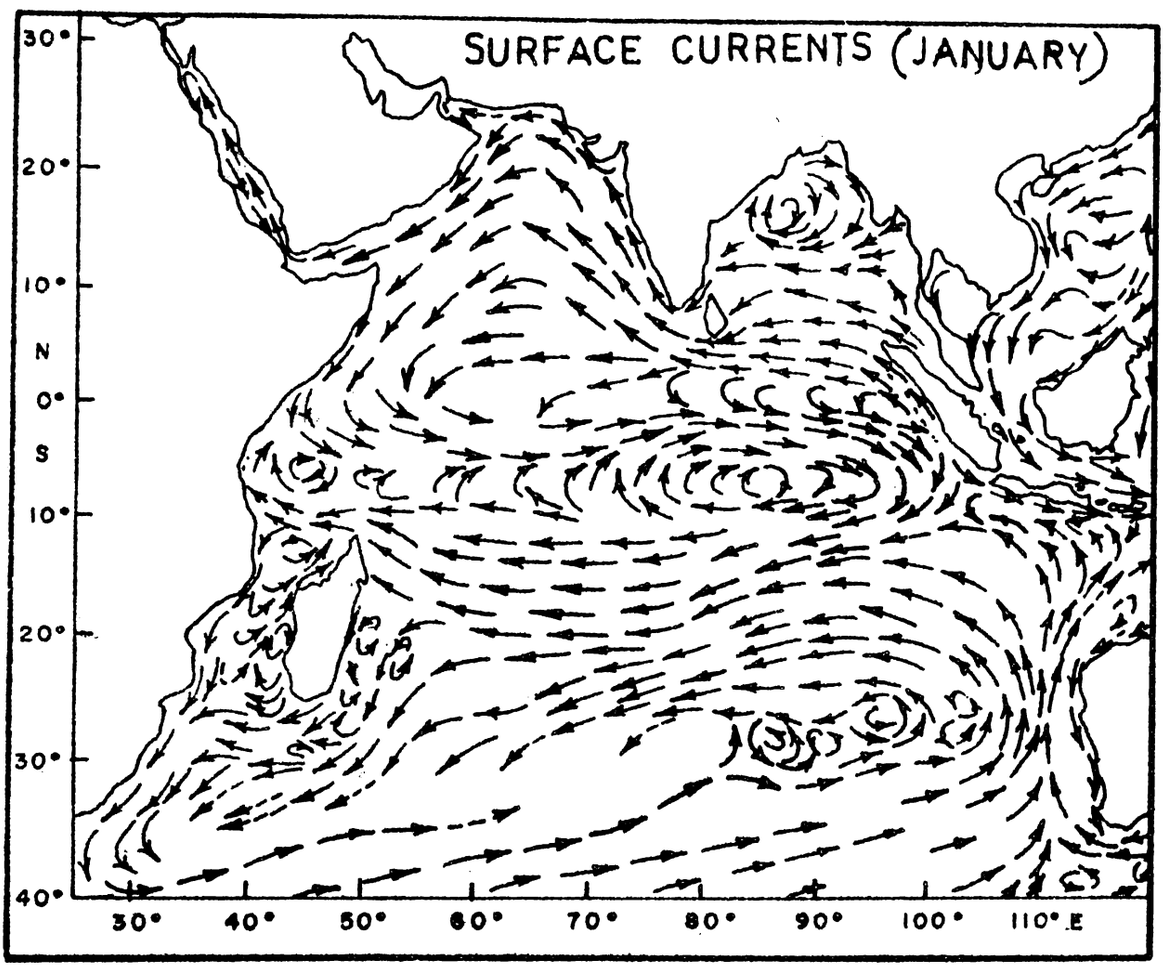
SURFACE CURRENTS (JANUARY)
30°
20°
10°
N
0°
S
10°
20°
30°
40°
30°
40°
50°
60°
70°
80°
90°
100°
110° E

Fig.7.a. Prevailing surface currents in the Indian Ocean, during January (northeast monsoon) (U.S.Navy Marine Climatic Atlas of the World Vol XII Indian Ocean).

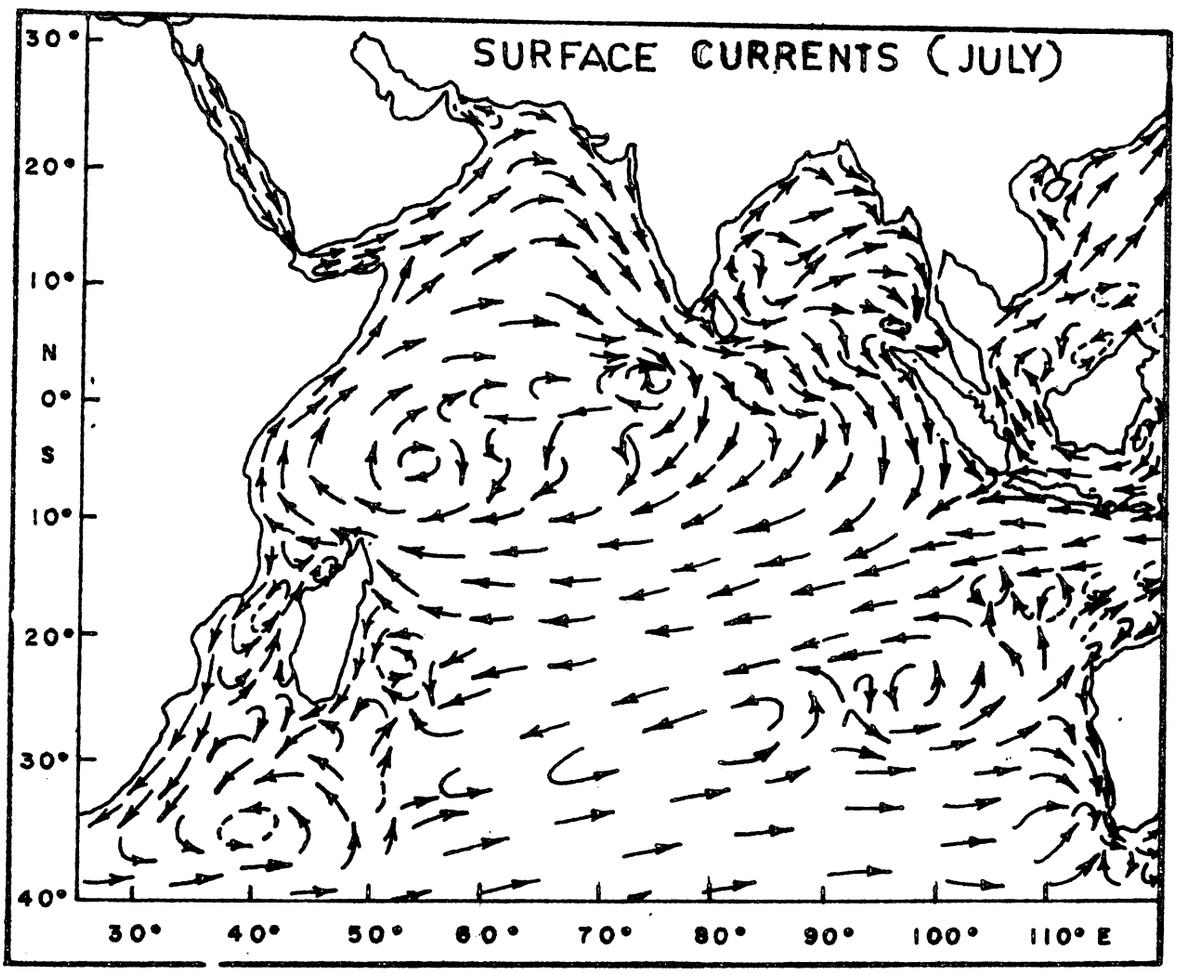
SURFACE CURRENTS (JULY)
30°
20°
10°
N
0°
S
10°
20°
30°
40°
30°
40°
50°
60°
70°
80°
90°
100°
110° E

Fig.7.h. Prevailing surface currents in the Indian Ocean, during July (south west monsoon) (U.S. Navy Marine Climatic Atlas of the World Vol XII Indian Ocean).

the slope of isotherms as related to the currents and vertical upward motion in regions of upwelling (surface divergence) or sinking motion in regions of convergence, influence the temperature distribution. The region of upwelling near the east coast of Africa and Arabia is of special interest, for the temperature fluctuations of this region is noted to be influencing the atmospherics circulation of the North Indian ocean and hence the precipitation pattern.

Bjerknes (1969) while studying the geographal distribution of sea surface temperature anomalies from the charts of Dietrich and Kalle (1957), which depicts the difference between the sea surface temperature and its average global value along the part of each latitude circle situated over the oceans, observed no appreciable negative sea surface temperature anomalies. But the anomalies pertaining to the Indian Ocean data presented here, shows negative anomalies mainly in the western equatorial waters Arabian sea and an extensive area off Australia in the eastern south Indian Ocean. The equatorial cold water in the Indian Ocean is observed in the western side of the ocean, unlike Atlantic and Pacific. It stretches eastward from the coast of east Africa to about 65°E longitude.

Bowen's Ratio

Bowen's ratio was calculated and the distribution of the annual mean values are presented (Fig 6d). The negative values

indicate that heat is conducted from the atmosphere to the sea. Southern Indian Ocean exhibits latitudinal variations of Bowen's ratio. It increases with higher latitude. The spatial distribution of Bowen's ratio follows the trends of sensible heat. Negati values of Bowen's ratio are observed in the western Arabian sea, western Bay of Bengal and other areas where negative fluxes of sensible heat are observed.

Conclusions

The annual models of energy-budget components as compared with that of Budyko (1956) show comparisons and contrasts. The largest annual radiation balance observed anywhere in the world, a net income of more than 400 gm cal cm^{-2} day^{-1} located in the north-western part of the Arabian sea is observed in the present study also. The present study shows the same amount of radiation balance for the Red sea too. Values of almost the same magnitude is observed off west north-west coast of Australia as computed by Budyko is presented in the present studies also. The low values observed, near the Indonesian region also coincides with Budyko's observations. Values obtained by Budyko for Bay of Bengal and the South Indian Ocean are higher. Budyko observed same values of net radiation for the cloudless western equatorial waters and the southern Bay of Bengal, marked for heavy cloudiness. This discrepancy might have occured presumably because of the few data points used and an unrealistic extrapolation of isopleths.

The annual map of net latent heat flux of Budyko did not show the low values of latent heat exchange near the upwelling regions of south-west coast of India and Arabian coast and high values of Red sea as observed in the present studies. The areas of highest evaporation near the southern tip of African continent is not well brought out in Budyko's charts. But the other region of high latent heat exchange in the eastern subtropical region of South Indian ocean shows almost similar values. Budyko's work shows similar values of latent heat flux for Arabian sea and Bay of Bengal. The present study shows greater values for Bay of Bengal. Since Bay of Bengal is observed to be warmer, more evaporation could be expected. Values of Budyko for the North Indian Ocean as a whole, are higher. The isopleths of sensible heat values are scanty in Budyko's charts. The downward heat exchange of the sensible heat in the western Arabian sea and other areas are not brought out. The mean annual distribution of ocean heat balance of Budyko showed similar distribution as that of the present study, except for the isopleths of negative heat balance including the southern Bay of Bengal in his studies. The maximum of heat loss near the Agulhas Current region off so Africa is a lesser magnitude, as computed, by Budyko. The maxim region of heat gain in the upwelling region of Arabian Coast is not brought out by Budyko. Since the rest of the work by other authors giving annual models of heat budget components are for individual years the values can not be compared. The net radiat

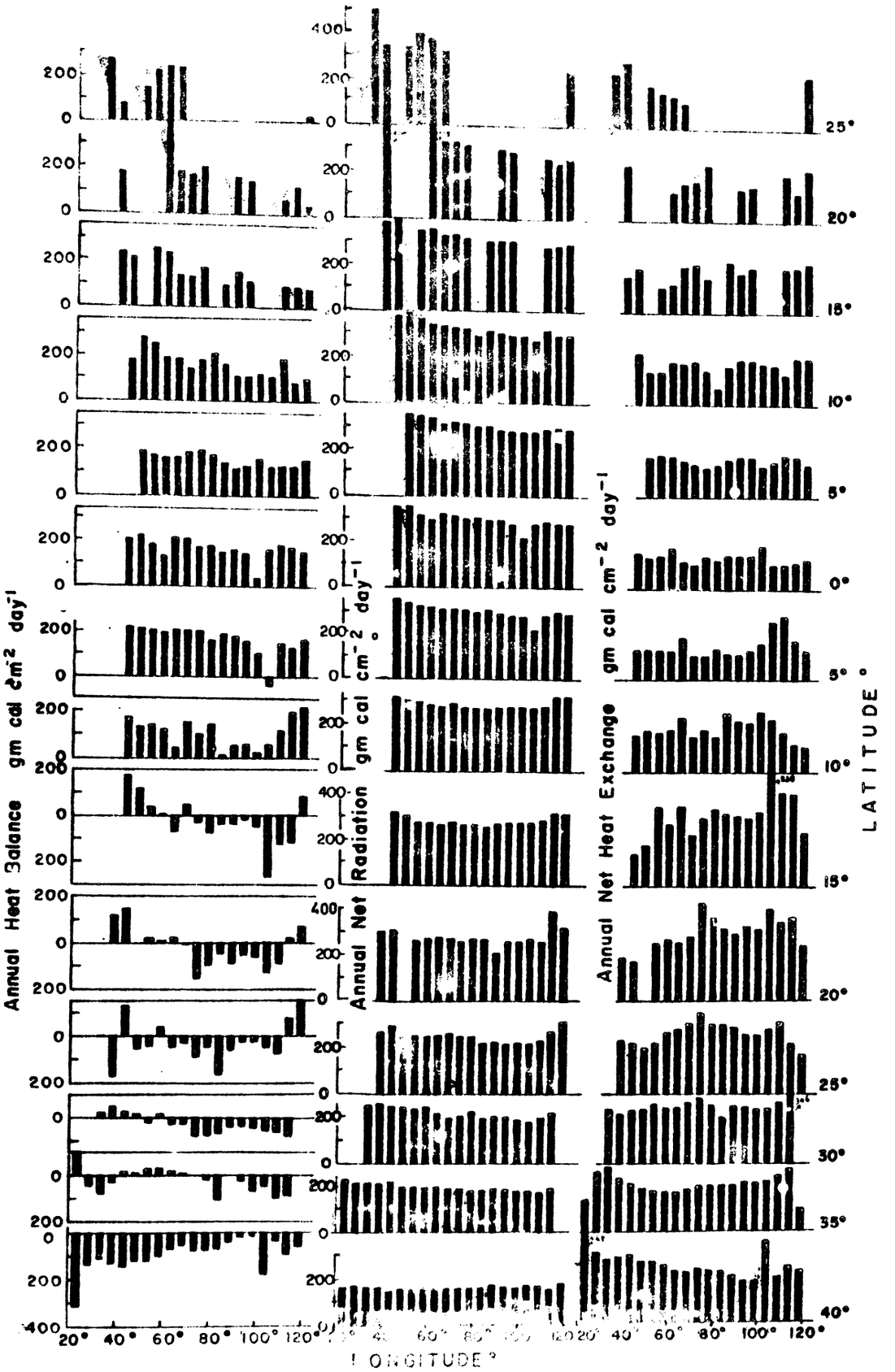
Annual Heat Balance gm cal cm⁻² day⁻¹
Annual Net Radiation gm cal cm⁻² day⁻¹
Annual Net Heat Exchange gm cal cm⁻² day⁻¹
LATITUDE °
LONGITUDE °
20° 40° 60° 80° 100° 120°
25° 20° 15° 10° 5° 0° 5° 10° 15° 20° 25° 30° 35° 40°

Fig.8. Climatograms of heat budget components

a) annual heat balance

b) annual net radiation balance

c) annual total heat lost in the Indian Ocean for different latitudes.

heat balance computed by Mani et al., (1965), combining observations and estimations showed lesser maxima near West Arabian sea and the north west coast of Australia.

A summary of geographical distribution of net radiative heat input, total thermal energy exchanged and the subsequent heat balance have been given in Fig.8. This figure gives a more clear picture of the total annual heat balance and its main components in different latitudes and longitudes than the other figures given earlier.

Indian Ocean could be divided into three regions as far as the air-sea interaction studies are considered. Starting from the southern Indian Ocean 1) region of westerlies beyond $30^{o}S$ 2) South-east trade wind region 3) Region of the monsoons.

In the region of Westerlies a permanent cloudiness beyond $30^{o}S$ which is marked by low values of radiative heat input is observed. The moderate evaporative cooling and high values of the fluxes of sensible heat mark this region. Very high values of latent heat and sensible heat fluxes are observed in the Warm Aghulhas Current region. This area of low radiative heat exhibits maximum negative heat balance in the Indian Ocean. This region of heavy heat loss which is associated with the region of Warm Aghulhas Current conforms with the studies of Malkus (1962) by means of Budyko's (1956) charts for global heat exchange values. The eastern

part of this region shows moderate heat loss.

The values of clouds associated with the ITCZ in the equatorial region is high and it decreases towards the subtropical high pressure areas of 20 - 30° latitude where subsiding air movements dissolve clouds, since the air is warmed adiabatically. This combines with the latitudinal variations of heat balance from equator to subtropical high in the southern Oceans which is in the south-east trade wind region. Considerable heat exchange is observed from the eastern part of this region and hence remarkable heat loss too. The south-east trade wind regions where dry trades of considerable speed favour maximum evaporation in the eastern part since the subtropical high is more in the eastern region (Nieuwolt, 1977). Thus western and eastern peripheries of the subtropical anticyclone (Fig 6b) show contrast in the heat exchange processes. Western part shows less of evaporation than the eastern part. The sensible heat fluxes are downwards in the eastern part than the western.

The region of monsoons covers almost all the areas of northern Indian Ocean. Here the monsoonal influences and their consequences make this part of the ocean differ from the Atlantic and Pacific. Unlike the other two seas the western part of the ocean is colder. The distribution of mean sea surface temperature in the equatorial Indian Ocean appears to exercise a profound influence on the properties and circulation of the overlying

atmosphere through air-sea interactions. Saha's papers on this annal differences in temperature, cloudiness and pressure values, based on the satellite evidence give a qualitative explanation in terms of ocean-atmosphere interactions. It is suggested that the equatorial westerlies which are observed in the equatorial Indian Ocean during practically the whole year, may have its origin as strong thermal winds that are created by steep meridional ocean surface temperature gradient on either side of the equator in the equatorial Indian Ocean. He observed upward fluxes of sensible heat in the equatorial eastern Indian Ocean and downward fluxes of sensible heat in the equatorial western Indian Ocean. Contrary to his observations which show western Indian Ocean as a major source of water vapour and the eastern Indian Ocean a major sink of water vapour for 1964 monsoon months, the annual values show slightly more evaporation in the eastern north Indian Ocean. Here the sea surface temperature is greater than the air temperature almost all over the eastern north Indian Ocean. Upward fluxes of sensible heat in equatorial eastern Indian Ocean and downward flux of sensible heat in the western Indian Ocean are observed.

The climatic model of net annual heat balance gives contrasting picture of the northern and southern parts of the Indian Ocean. Where as the northern Indian Ocean shows unique behaviour in its distribution of marine meteorological parameters

and subsequent interaction with the atmosphere, the southern Indian Ocean conforms with the general pattern. The latent heat exchange is found to be the major component of the heat balance picture. Sensible heat exchange is found to be contributing less. The influences of monsoons and the ocean currents are obvious from the climatic models of northern Indian Ocean. Zonal differences are much obvious in the northern Indian Ocean. The strong heating of the waters off the East African and Arabian coasts is observed contrary to the moderate warming of the eastern parts. The cold waters of Somali cold current lessens the evaporative cooling and reverses the direction of sensible heat exchange. The stability of air prevents the formation of many cumulus clouds and insolation reaches a maximum. The reversal of the wind systems and change in their strength along with distribution of other oceanic and meteorological parameters due to the advent of monsoonal winds are obvious from the above studies. Thus Indian Ocean presents an interesting picture of air-sea interaction, which reveals the influence of several elements and links between the elements which regulate their own behaviour by the operations of internal feedback mechanisms. The sources and sinks in the system of Indian Ocean and the atmosphere above could be located by this diagnostic studies which gives a quantitative estimation of the physical processes taking place, which contribute to the thermal interaction mechanism.

Chapter 4

The Seasonal Climatic models of the energy exchange parameters

The diagnostic treatment of the thermal energy exchange of the atmosphere and ocean is presented as seasonal models. Energy fluxes through the surface of the Indian Ocean which have been calculated using bulk aerodynamic equations with exchange coefficients which vary with seasons, and radiation equations, with the climatic data available for the twelve months of the year is presented here in the form of seasonal climatic models of energy exchange. Well recognising the semi-annual reversal of general circulation over the Indian Ocean to the north of 10°S, the seasonal models are made combining the winter monsoon and summer monsoon months. December, January and February values are clubbed together to get the resultant picture for the winter season. The summer monsoon circulation which actually starts from May and ends in September, is well developed during June, July and August. Hence these three months are combined to get a representative picture for the south west monsoon season. The pictures for transition seasons, winter as well as summer, represented by (March-May) and (September-November) respectively are also made. The seasonal models for the energy exchange parameters and the related climatic variables are presented (Fig.9-18).

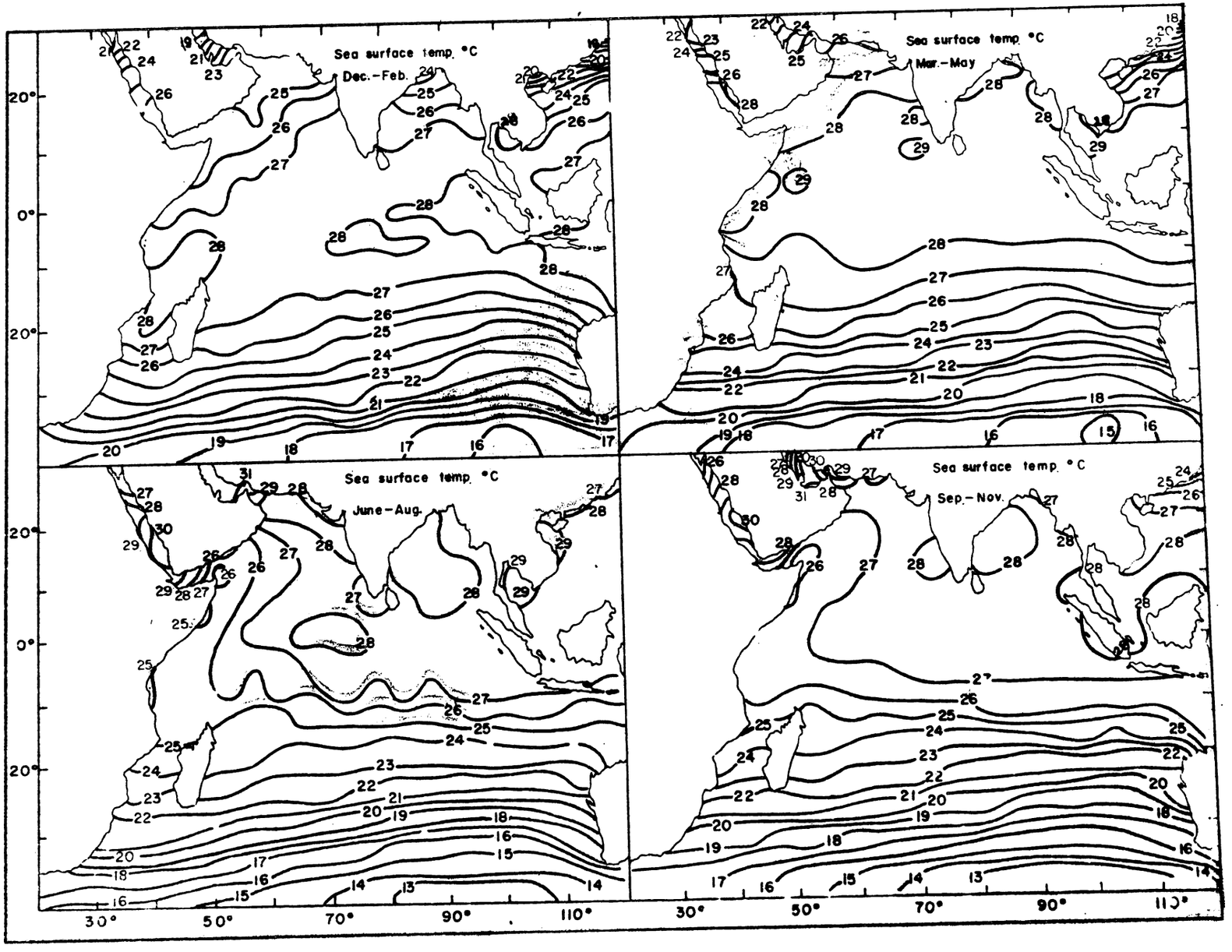
Sea surface temp. °C
Dec.–Feb.
Sea surface temp. °C
Mar.–May
Sea surface temp. °C
June–Aug.
Sea surface temp. °C
Sep.–Nov.
20°
0°
20°
30°
50°
70°
90°
110°

Fig.9. Seasonal distribution of the sea surface temperature (°C).

The seasonal variations of the climatic parameters could be discussed first, so as to get the overall climatic conditions prevailing over the Indian Ocean, which have a profound influence over the energy-budget of the Indian Ocean and which in turn will influence the climatic system, through feedbacks.

Sea surface temperature

Sea surface temperature is the main indicator of atmospheric dynamics and thermo dynamics (Fig 9). During December-February the typical winter conditions are observed. The northern parts of the Persian Gulf and the Red Sea show low values of temperature. Towards the Arabian Sea basin it shows higher values. The isotherms 26°C - 27°C run South-west to north-east in the Arabian Sea since western part is colder than the eastern part. In the Bay of Bengal the isothermal distribution is zonal. The South China Sea shows maximum temperature gradient. The equatorial region is uniformly warm (28°C) except near the Somali coast, where the temperature is slightly less. The southern hemisphere which experiences the summer season, has its maximum prevailing from East Africa to the south of Indonesia and extending southwards to northern Australia. There is a decrease in the temperature towards the south. The isotherms run southwest to northeast, since the western side is warmer.

During summer transition, the northern hemisphere

receives more heat energy and temperature above 28°C is observed in the equatorial region and the southern part of Arabian Sea. Bay of Bengal is uniformly warm. The northeast monsoon retreats and by May the conditions are ready for southwest monsoon. Upwelling starts in the places of major horizontal advection, though the rainfall sets in only by the last week of May starting from southern Bay of Bengal.

During south-west monsoon season, the marginal seas of Arabian Sea reach to maximum temperature (31°C). An increase in temperatures is observed in the South China Sea. The rest of the North Indian Ocean including southern equatorial waters show sudden drop in temperature. Waters of very low temperature (25°C) extends from Somali coast to the Arabian coast, due to intense upwelling. Synoptic values upto 16°C are reported to have been observed (Stommel & Moorster, 1964). Low values of Sea surface temperature are observed in the south of Gulf of Aden. Comparatively low values of sea surface temperature are observed near the south-west coast of India, due to upwelling and considerable reduction in the incoming radiation. There is a marked zonal temperature gradient in the equaterial waters. The Bay of Bengal and South China Sea are uniformly warm. South of 30°S the isothermal distribution is similar to that of winter, though the values are lesser. During winter transition, the zonal temperature gradient is much less. There is a decrease in sea surface temperature towards the north. There is not much of a difference

in the southern hemisphere. The winter transition model almost resembles that of annual model. The spatial variations of sea surface and air temperature follow the movement of thermal equator. The thermal equator is located in the northern equatorial waters during summer transition. Hence very high values of sea surface temperature are observed in the northern equatorial waters. During southwest monsoon season the thermal equator moves northward up to 25°N to the continental region (Hamm, 1976; Saha, 1973). Very low values of sea surface temperature are observed in the equatorial western Arabian Sea and hence high pressure ridges occupy the Arabian Sea tropical belt. The zonal temperature gradient in the equatorial waters is maximum during the summer monsoon season, (25-29°C), when the equatorial upwelling is at its maximum. A marked contrast in the values of sea surface temperature is observed between Western and Eastern parts of the Arabian Sea. The temperature gradient prevails, though the intensity decreases throughout autumn. Very high temperature values are observed in the Indonesian region (29°C). During winter transition, the latitudinal decrease of temperature starts showing throughout the Northern Indian Ocean. There is little variation in the equatorial waters, except along the Somali coast and adjacent regions, due to intensive upwelling. Maximum variations of temperature values are observed in the northern Indian Ocean. Southern Indian Ocean exhibits the same pattern with slight changes in magnitude. Maximum seasonal

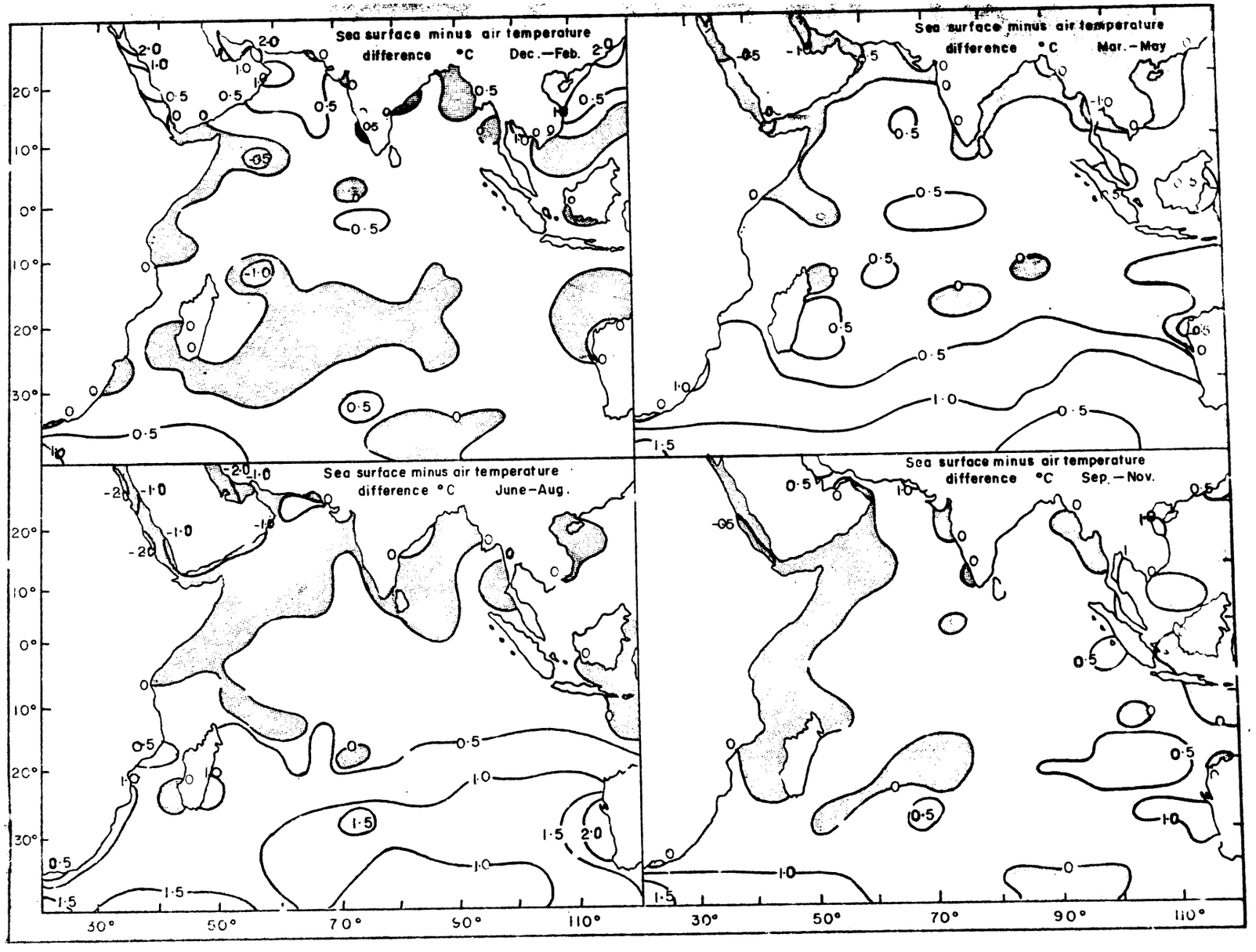
Sea surface minus air temperature
difference °C Dec.—Feb.
Sea surface minus air temperature
difference °C Mar.—May
Sea surface minus air temperature
difference °C June—Aug.
Sea surface minus air temperature
difference °C Sep.—Nov.
30°
50°
70°
90°
110°
20°
10°
0°
10°
20°
30°

Fig.10. Seasonal distribution of the sea and air minus temperature difference (°C).

changes in the magnitude of temperature are observed in the marginal seas of northern Indian Ocean and South China Sea. The pronounced seasonal differences in heating and cooling of the sea surface by absorption of solar radiation are much more pronounced as a result of greater seasonal changes of the zenith distance of the sun and stronger effects of back radiation due to less cloudiness.

Sea surface and air temperature difference

The air temperature closely follows the changes of sea surface temperature so that the isotherms nearly coincide over much of the ocean. Because of this, the air-sea temperature difference is presented which is widely used in the computations of air-sea exchange (Fig 10). During winter, negative temperature differences are found over the southern Indian Ocean, western Arabian Sea, North western Australian coast, South China Sea and north eastern part of the Bay of Bengal. During summer transition the negative temperature difference area extend westward. The whole of western and northern Arabian Sea, Bay of Bengal and South China Sea are marked by values of negative sea minus air temperature. With the advent of summer monsoon the area of negative sea minus air temperature difference covers almost allover the basins of Arabian Sea and Bay of Bengal. The south of Indonesian region shows negative sea minus air temperature differences. During winter transition, the values of negative

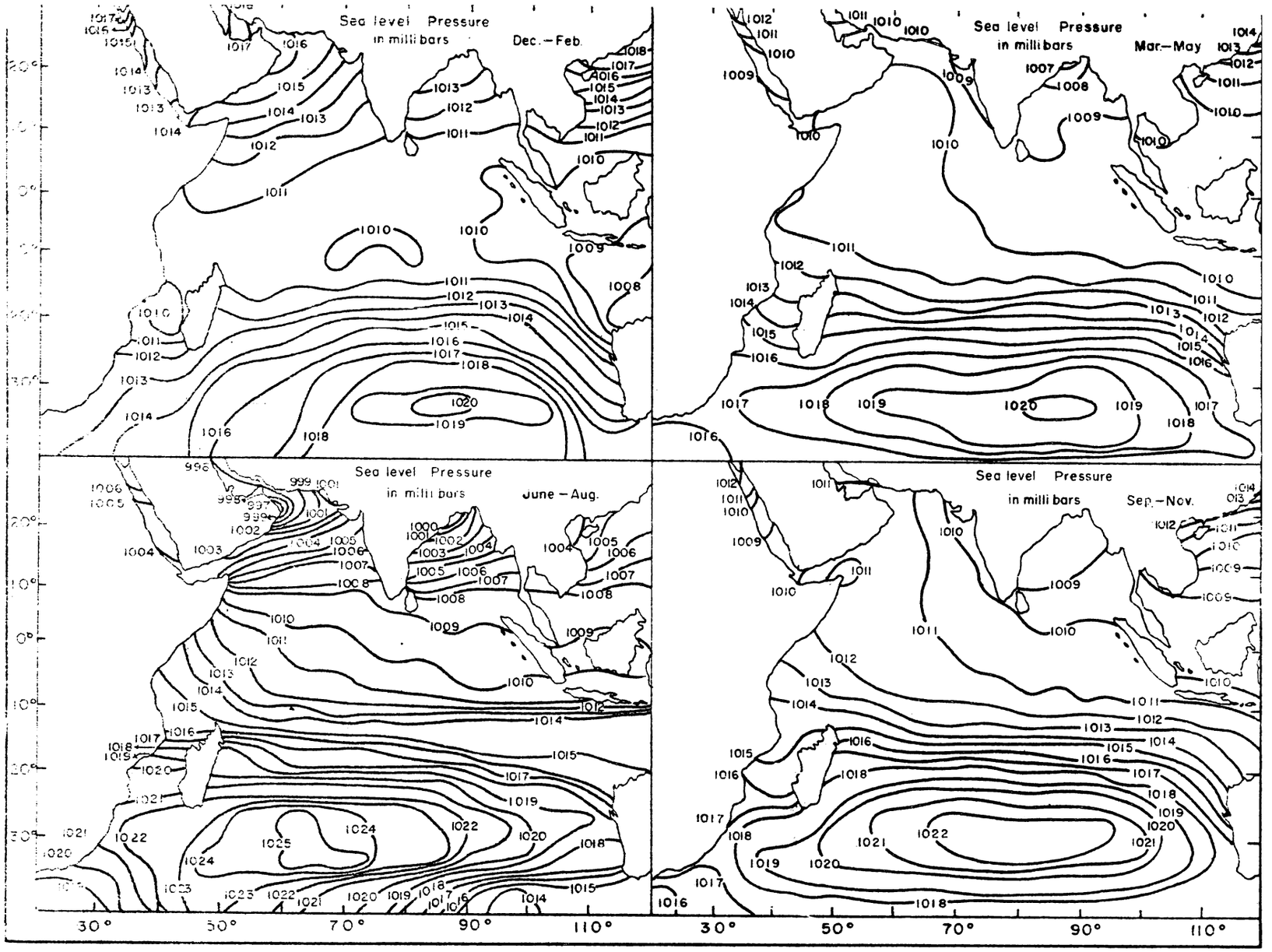
Sea level Pressure
in millibars
Dec.–Feb.
Sea level Pressure
in millibars
Mar.–May
Sea level Pressure
in millibars
June–Aug.
Sea level Pressure
in millibars
Sep.–Nov.
30°
50°
70°
90°
110°

Fig.11. Seasonal distribution of the sea level pressure (mb).a

temperature difference are seen prominently over the western Indian Ocean. A small area of negative temperature difference is observed in the southern Indian Ocean. Southern Indian Ocean shows a contrast during summer and winter months with a high negative heat difference in winter and a high positive difference in summer. The western Arabian Sea has a negative temperature difference, throughout all seasons, with maximum intensity and areal extension during summer monsoon months.

Annual Variation of sealevel pressure, surface circulation and surface winds.

A constant feature observed in the seasonal pictures of sea level pressure, is the subtropical high pressure area between 30-35S (Fig 11). It decreases towards the north forming a trough. The equatorial low pressure area is prominent throughout all seasons, and an east-west pressure gradient is noted throughout. The high pressure area show maximum values (1025 mb) during south west monsoon months and minimum (1020 mb) during winter. The pressure gradient is also maximum during the monsoon season. The damming action of the large island of Madagascar on the steady flow of the SE trades is clearly shown by a ridge of high pressure on the windward side and a trough to leeward. The mean pressure gradient seems to be strongest between 15-20°S. During north-east monsoon period the Arabian Sea, the Bay of Bengal and the south China Sea are occupied by subtropical high

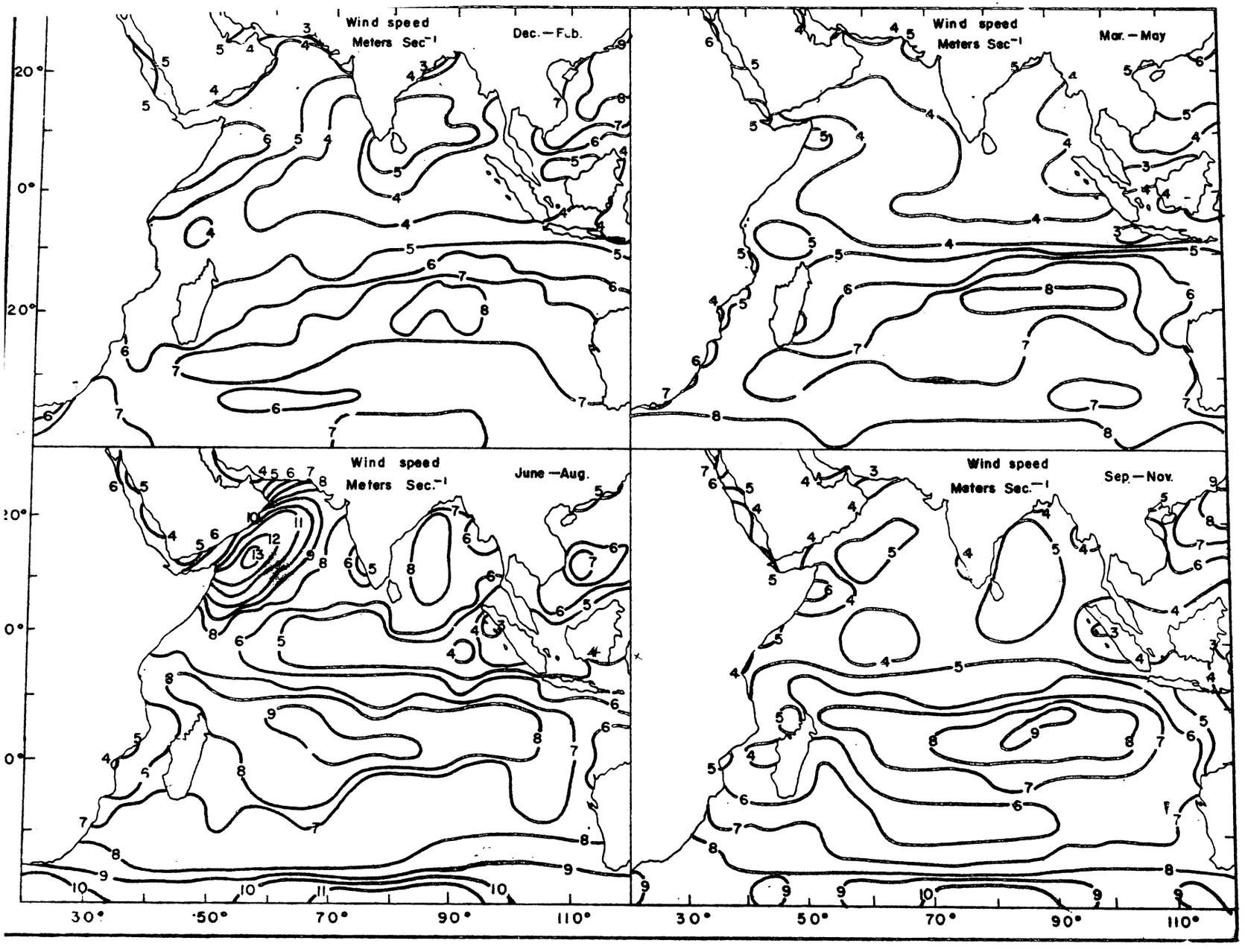
Wind speed
Meters Sec⁻¹
Dec.—Feb.
Wind speed
Meters Sec⁻¹
Mar.—May
Wind speed
Meters Sec⁻¹
June—Aug.
Wind speed
Meters Sec⁻¹
Sep.—Nov.
20°
0°
20°
0°
30°
50°
70°
90°
110°

Fig.12. Seasonal distribution of wind speed ($m.Sec^{-1}$).

pressure. During summer transition when the northern Indian Ocean gets heated up, low pressure areas prevail over the northern Indian Ocean. The pressure drop gets intensified during south-west monsoon season and the pressure drop over the seas adjacent to Indian subcontinent is lower than that of equatorial waters. A low pressure area over the northern Arabian Sea and the Bay of Bengal with minimum values during the summer monsoon months are observed. A contrasting picture during winter monsoon season, is noted. A ridge of high pressure over the western Arabian Sea with an area of conspicuously low pressure near the coast of Somali-land is noted during summer monsoon months. Lowest minimum sea level pressure of all the seasons is observed over the north Arabian coast.

Drastic seasonal variations of windspeed are observed in the northern hemisphere southward upto 10°S (Fig 12). Annual variations over the southern Indian Ocean is comparatively much less.

Once the season changes over to winter the low heat capacity of the land relative to the sea causes the surface air over land to be colder than that over the sea. A gradient of pressure causing northerly air flow is established. The mountain blocks in the north prevent the intrusion of cold air and makes the north east monsoon a gentle phenomenon. Over the central and eastern Indian Ocean the monsoon spirals into a weak low pressure trough just north of the equator. The influence of

Africa on the atmospheric circulation, persisting 800 km east of the continent and merging with the influence of Asia farther north, extends the northeast monsoon of the Arabian Sea far into southern hemisphere. The African continent spans the equator and so due to winter cooling high pressure cells over the Sahara and Arabia and low pressure area over the Kalahari Desert in the summer hemisphere cause a pressure gradient. Since the heat low is found in the same latitude as that of anti cyclonic high and constant subsidence occurs near the subtropical anticyclone, clouds are not formed and hence the low is maintained throughout the season. Northeast trade winds blow outward from the Asiatic high pressure region into northern Indian Ocean. Unobstructed by mountain ranges, the vigorous northeast monsoon of southeast Asia blows out from the intense polar anticyclone creates greater pressure gradient between the continent and China Sea. Very high speed winds are observed, in the South China Sea and off the Somali coast. As the winter monsoon season intensifies the speed maximum of the western Arabian Sea shifts southward. There is a southerly shift of the equatorial troughs, as the winter monsoon intensifies. Australia experiences summer monsoon, with a continental heat low and southward moving air from northern hemisphere.

As it changes to summer transition, subtropical anticyclone moves equatorward. The continental heat low developed during

summer and the equatorial cold upwelled waters off the coasts of Somalia and Arabia creat the summer monsoon. The upwelled waters intensify the southwest monsoon, by increasing the summer time reversal of land-sea temperature gradient. The low and high pressure areas exchange places, due to the change of season and a south-north pressure gradient is set up, which initiates a southerly flow which merges with the south east trades over the southern Indian Ocean and with the south west monsoon north of equator. The southwesterly flow of the monsoon current shows the maximum wind speeds and the core of wind speed is observed off the coasts of Somalia and Arabia. The whole of North Indian Ocean shows a speed maximum, during the peak monsoon periods June-August. But the invasion of cool air from north and tropical cyclones from east lessens the temperature and pressure gradient between adjacent land and South China Sea. Hence the influence of summer monsoon is less, and the wind speed values are comparatively lesser. The core of intensity is observed in the western Arabian Sea. The intense upwelling causes the summer monsoon to be stronger than the winter monsoon. It is observed by many workers that the south easterly winds of southern hemisphere change over to south westerly winds in the northern hemisphere and sweep over the Arabian Sea and the Bay of Bengal. A pressure gradient with low over Indonesia and high over Australia, due to the eastward moving anticyclones intensifying over the cold continental interior is observed, which causes cross-equatorial flow towards southeast Asia.

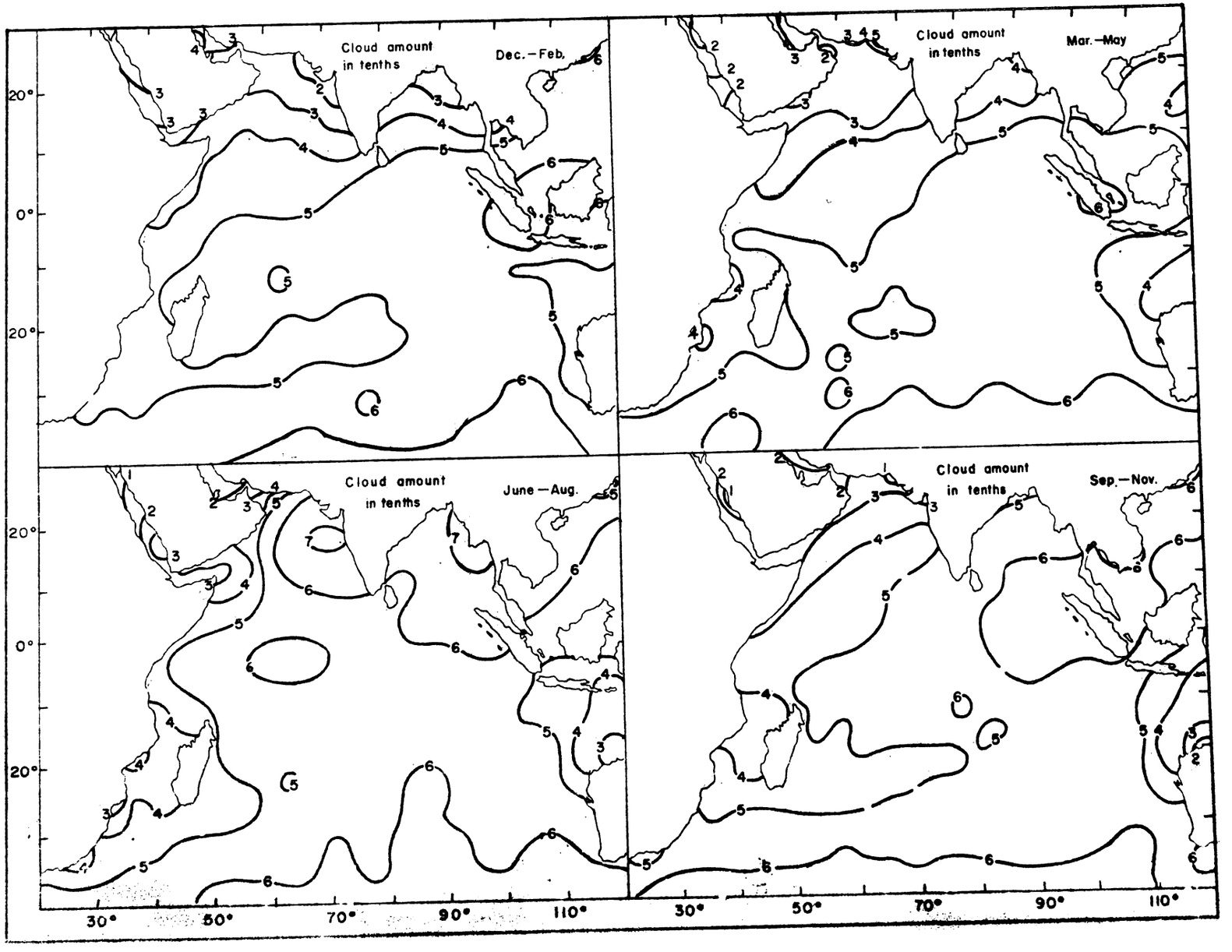
Cloud amount in tenths
Dec.—Feb.
Cloud amount in tenths
Mar.—May
Cloud amount in tenths
June—Aug.
Cloud amount in tenths
Sep.—Nov.
20°
0°
20°
30°
50°
70°
90°
110°

Fig.13. Seasonal distribution of sky coverage by clouds (in tenths).

Cloud amount

In the northern hemisphere, the cloud cover changes greatly by seasons (Fig 13). During the period of north east monsoon the cloud cover over the Arabian Sea and the Bay of Bengal is much less. In winter greatest cloud activity occurs in equatorial Africa, Indonesia and South China Sea. With the advent of summer monsoon, a dense cloud cover is observed from the eastern Arabian Sea to South China Sea. In winter months, Indonesia lies in the realm of semi-permanent westerlies which is fed by the trade winds of both the hemispheres. By the advent of summer monsoon this area of cloudiness shifts northear to South China Sea. Relatively large total cloudiness occurs in most of the equatorial belt between about 10°N and 20°S throughout the year. During northern summer less cloud cover is observed west of Australia. This persists till the winter transition months.

An east-west decrease in cloudiness is observed throughout all seasons. The maximum decrease is observed during the summer monsoon months with a pronounced cloudiness minimum near the Somali coast and extensive cloud coverage over eastern Arabian Sea where the south west monsoonal flow converges. A pronounced maximum of cloudiness is observed in the Bay of Bengal and the China Sea also. The cloud amount follows the

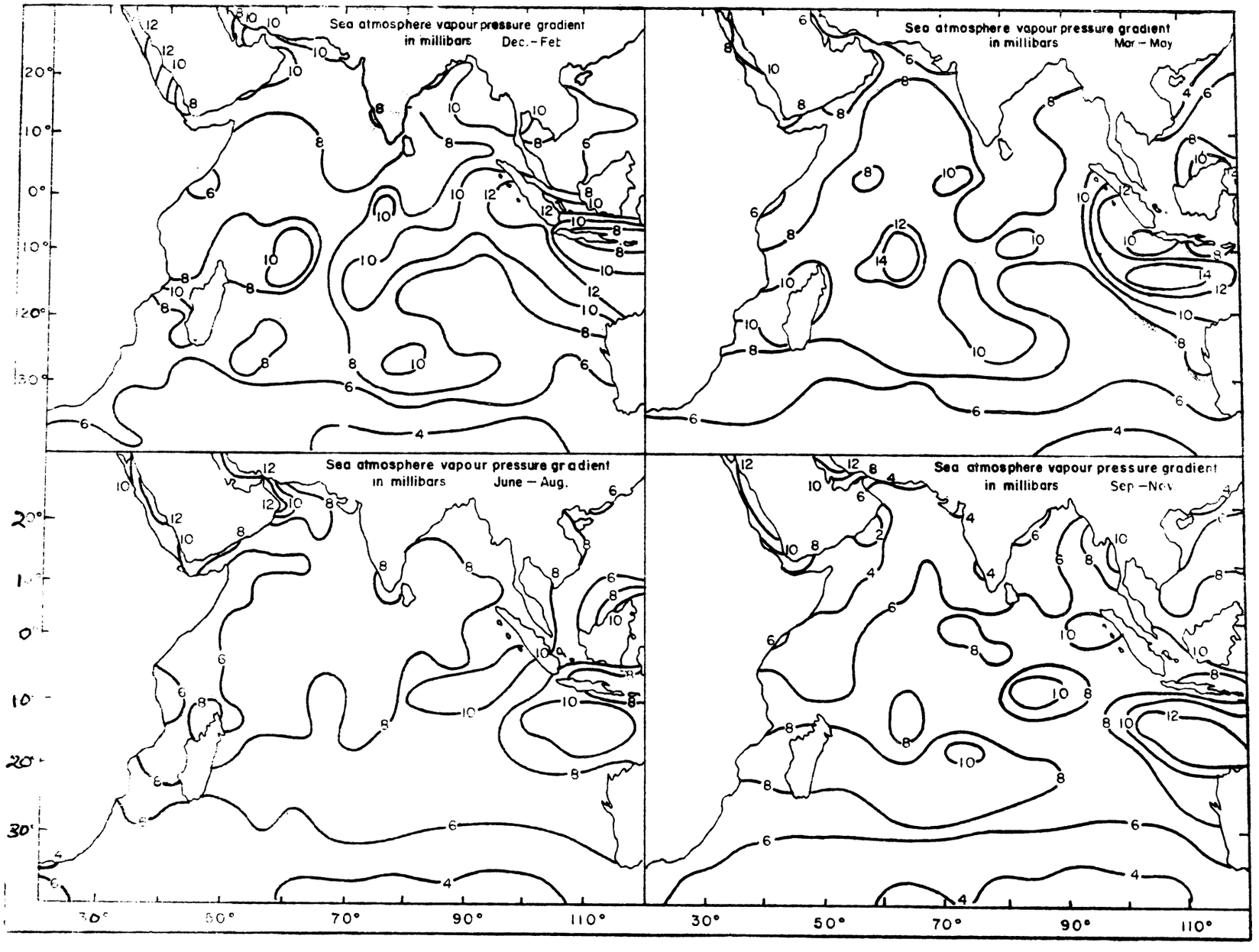
Sea atmosphere vapour pressure gradient in millibars Dec.–Feb
Sea atmosphere vapour pressure gradient in millibars Mar – May
Sea atmosphere vapour pressure gradient in millibars June – Aug.
Sea atmosphere vapour pressure gradient in millibars Sep –Nov
20°
10°
0°
10°
20°
30°
30°
50°
70°
90°
110°

Fig.14. Seasonal distribution of vapour pressure gradient (in mb).

precipitation pattern. During summer monsoon season, high amount of cloudiness is observed. As the winter transition approaches, the maximum cloudiness changes to minimum cloudiness. But the same state is reached in the Bay of Bengal only during the winter monsoons.

The Red Sea and Persian Gulf region show less cloudiness throughout all the seasons. Incidentally, this region of the north Indian Ocean gets maximum incident radiation observed anywhere on earth (Budyko, 1956). The area south of 30^{0}S is a region of high cloudiness. This area shows seasonal variation and during south west monsoon season, it reaches maximum northward.

Vapour pressure difference between Sea and air

Throughout all the seasons the vapour pressure gradient between Sea and air is much high over the equatorial belt, since the satuation vapour pressure of the sea surface is controlled by the sea surface temperature (Fig 14). Eastern side of the sub-tropical anticyclone exhibits quite high values of vapour pressure gradient with a maximum in the southwest monsoon months. The Somali coast is marked for its low values of vapour pressure gradient. During winter transition the Arabian Sea shows lesser gradients of vapour pressure. As winter approaches, the vapour pressure gradient sears up. The marginal seas show invariably high values of vapour pressure gradient.

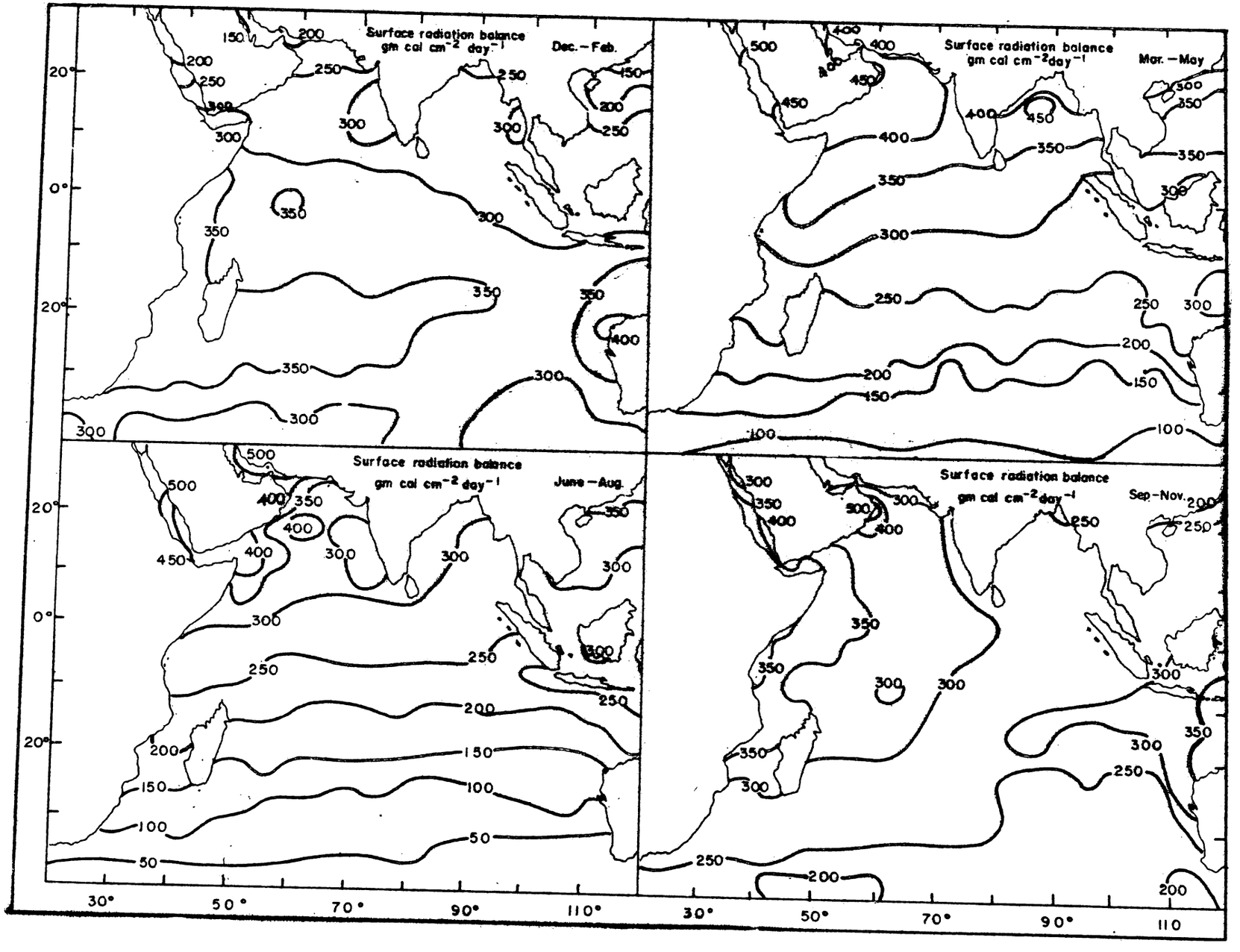
Surface radiation balance
gm cal cm⁻² day⁻¹
Dec.–Feb.
Surface radiation balance
gm cal cm⁻² day⁻¹
Mar.–May
Surface radiation balance
gm cal cm⁻² day⁻¹
June–Aug.
Surface radiation balance
gm cal cm⁻² day⁻¹
Sep.–Nov.
20°
0°
20°
30°
50°
70°
90°
110°

Fig.15. Seasonal distribution of net radiative balance (gm Cal Cm^{-2} day^{-1}).

Annual variations of the heat budget components

The heat budget components for the four seasons of the Indian Ocean are given in Fig (15-18).

The net radiative balance

During northern winter, very high values of surface radiation balance is observed near the west coast of Australia due to small amount of cloudiness (Fig 15). Southern Indian Ocean (0-35°S) experiences high radiative balance. In the norther hemisphere, higher latitudes show low values of radiation balance. As it turns to summer transition, very low values of radiative balance are observed over the southern hemisphere. The northern parts of Arabian Sea and Bay of Bengal and the marginal seas experience enormous radiative energy since the cloud amount presen gets decreased. There is an increase of radiative heat input in the China Sea also.With the advent of summer monsoon, northern hemisphere shows such changes. Southern hemisphere shows lesser values, as summer season progresses.With the presence of large amounts of convictive clouds present in the west coast of India, the area east of 60°E shows a sudden decrease in net radiative balance values. Bay of Bengal also show lesser values. Since the upwelling region of somali and Arabian coasts are marked for lesser cloudiness, the net radiative heat balance values appear up. The marginal seas also show extremely high values. During the sout

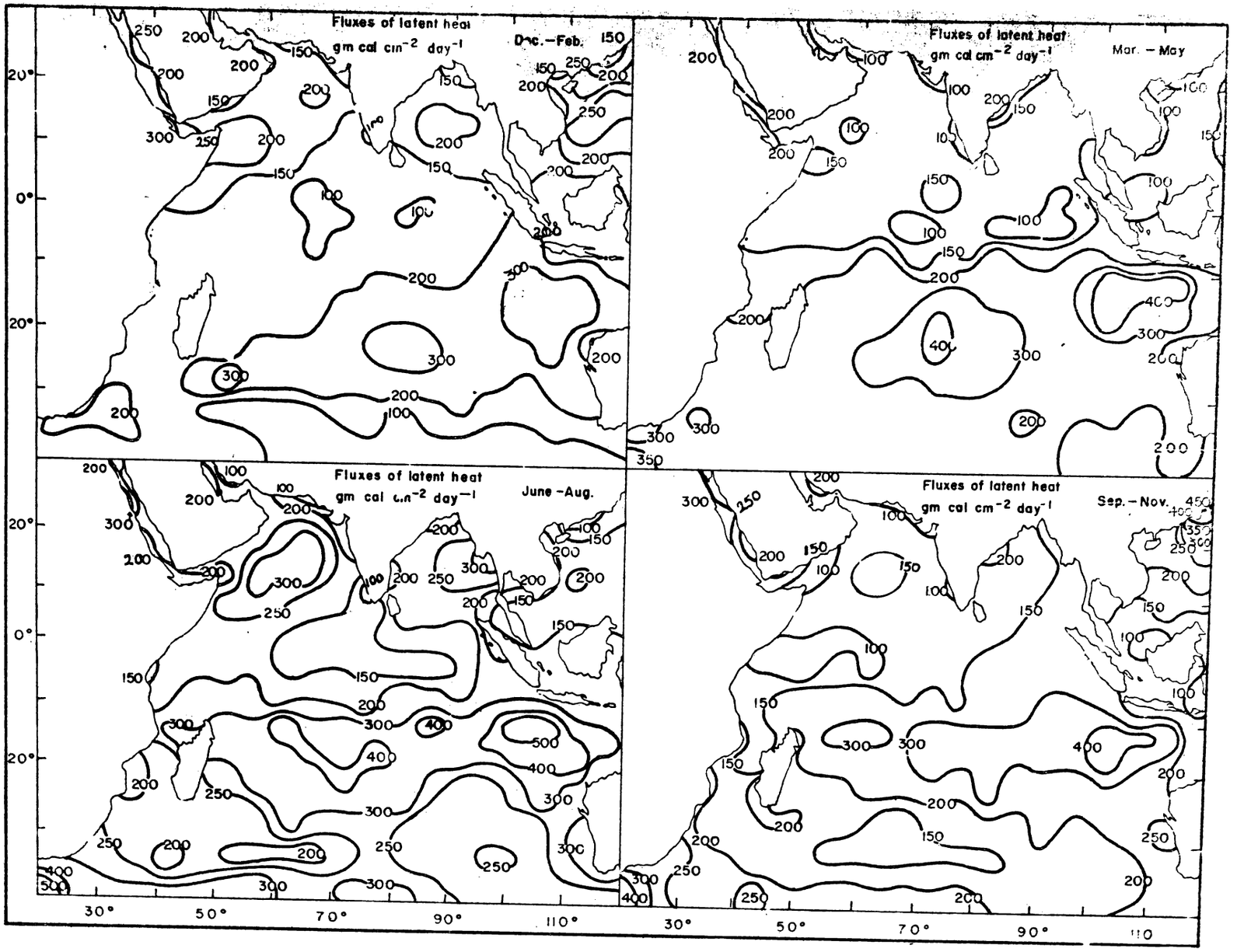
Fluxes of latent heat
gm cal cm^{-2} day^{-1}
Dec.–Feb.
Fluxes of latent heat
gm cal cm^{-2} day^{-1}
Mar. – May
Fluxes of latent heat
gm cal cm^{-2} day^{-1}
June – Aug.
Fluxes of latent heat
gm cal cm^{-2} day^{-1}
Sep. – Nov.
20°
0°
20°
30°
50°
70°
90°
110°

Fig.16. Seasonal distribution of fluxes of latent heat (gm cal cm^{-2} day^{-1}).

west monsoon season, the northern Red Sea shows cloud amount values almost equal to 10%. South China Sea does not show much of a variation. As the monsoon withdraws, and winter starts in the Southern hemisphere values show an increase. The area near Australia and Indonesia shows an increase. There is a decrease of value in the northern Indian Ocean. However, western Arabian Sea especially North Arabian coasts shows very high value The east-west zonal differences in radiative heat input are maximum during south-west monsoon. The differences are minimum during winter monsoon months. The zonal anomalies correspond to sea surface temperature and the distribution of ocean currents. The radiative heat balance observed in the equatorial region shows less variations.

Latent heat flux

The seasonal values of the latent heat flux, during northern winter show a maximum in the southern Indian Ocean (Fig 16). This area of maximum is oriented in the north eastern direction from southern Madagascar to the southern area of Java extending to western Australia. The equatorial waters show very low values of latent heat exchange. Western and central Arabian Sea, the marginal seas, central Bay of Bengal and South China Sea show remarkable amount of evaporative heat transfer. The northern part of Arabian Sea and Bay of Bengal exhibit low values during summer transition, the North Indian Ocean values are much

less. The southern Indian Ocean retains the area of maximum evaporation. Aghulhas Current region south of Africa also shows high values of evaporation. With the advent of monsoon, this area of maximum gets accentuated and shifts westward. The equatorial region also shows higher values than the previous seasons. The western and central Arabian Sea and eastern Bay of Bengal show all time maxima. South China Sea shows considerably high values. The winter transition values again resemble that of summer transition, except for South China Sea where the values are much high due to the interaction of the cold air blowing from the polar regions.

The area of maximum evaporation migrates between 10°S and 30°S. During summer and winter transition it moves northward and is seen between 10°S - 20°S. The main centre of maximum is always observed in the eastern part of the subtropical anticyclone between 15-20°S. This centre is associated with clear skies and dry subsiding air characteristic of the anticyclonic conditions prevailing in these latitudes.

The Aghulhas current region shows maximum values throughout all seasons except during northern winter. During southern winter maximum latent heat exchange takes place between this warm current and cold air prevailing in the southern latitudes. Another area of maximum is in the western Arabian Sea. Maxima developed are prominent during summer and winter monsoons.

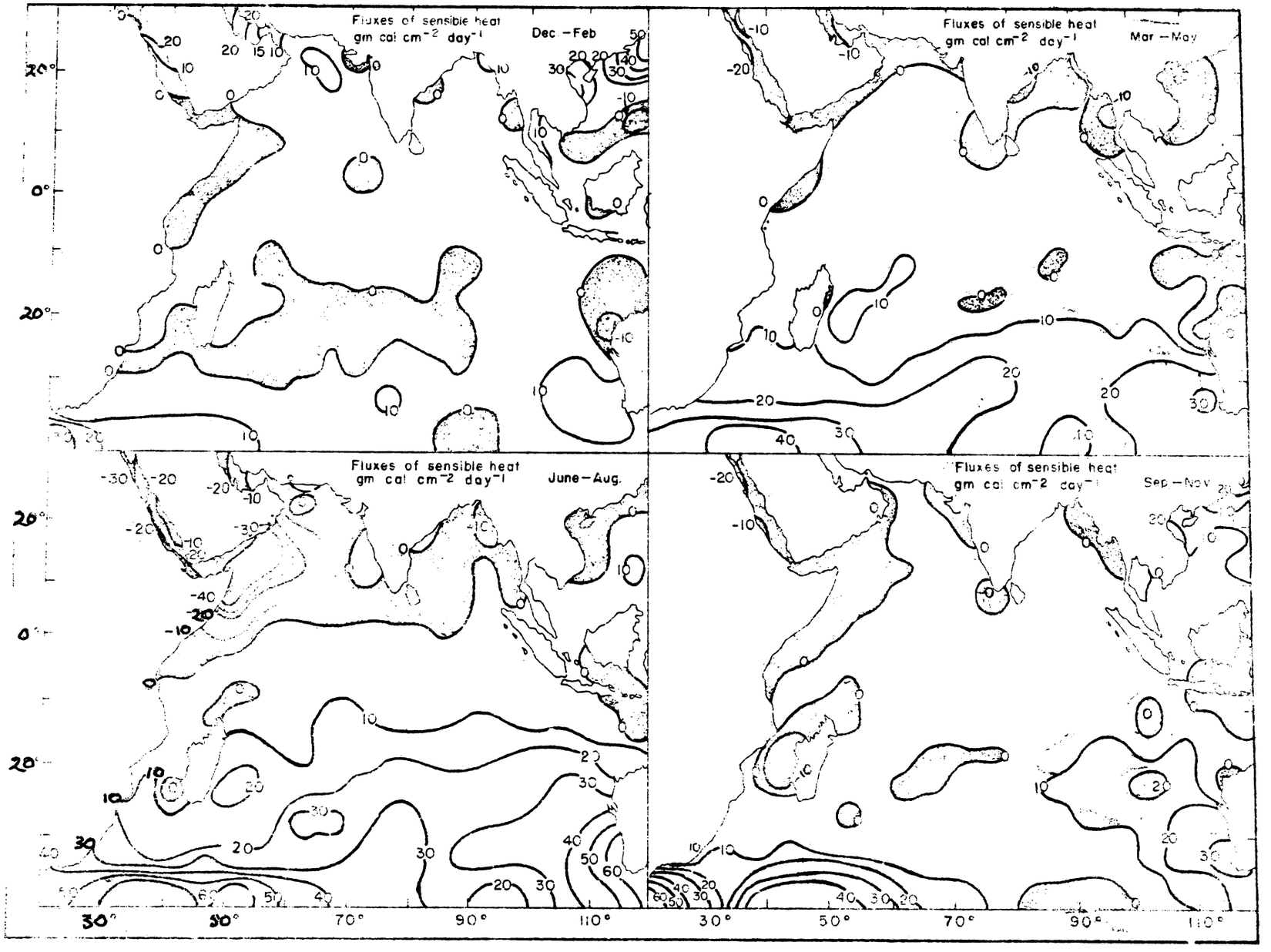
Fluxes of sensible heat
gm cal cm⁻² day⁻¹
Dec – Feb
Fluxes of sensible heat
gm cal cm⁻² day⁻¹
Mar – May
Fluxes of sensible heat
gm cal cm⁻² day⁻¹
June – Aug.
Fluxes of sensible heat
gm cal cm⁻² day⁻¹
Sep – Nov
20°
0°
20°
30°
50°
70°
90°
110°

Fig.17. Seasonal distribution of fluxes of sensible heat (gm Cal Cm^{-2} day^{-1}).

Sensible heat flux

During northern hemisphere winter, negative fluxes of sensible heat are observed along the African coast, northwest coast of India, west northwest Australian coast, southern most part of South China Sea and western part of South Indian Ocean subtropical anticyclone. Large positive fluxes are observed in northern South China Sea and Agulhas Current region (Fig.17). As the summer transition approaches, the area of negative heat flux spreads to the marginal seas and northern part of Arabian Sea. Most of the Bay of Bengal and southern most part of west coast of India and West South China Sea show negative fluxes of sensible heat. The area of negative heat flux of southern Indian Ocean vanishes. The northwest coast of Australia shows a prominent negative heat flux. Higher latitudes of southern Indian Ocean show high values of positive heat flux.

As the circulation pattern over northern Indian Ocean changes over to summer monsoonal circulation, the western Arabian Sea shows a prominent area of negative values of sensible heat exchange. Except for the region of Indonesia and southern part of South China Sea the whole of northern Indian Ocean, shows negative sensible heat exchange. Area in between Indonesian Islands and West northwest Australia shows a region of negative sensible heat exchange. Very high values of sensible heat exchange are observed in the southern Indian Ocean. As the season turns to winter transition, areas of negative heat flux starts forming

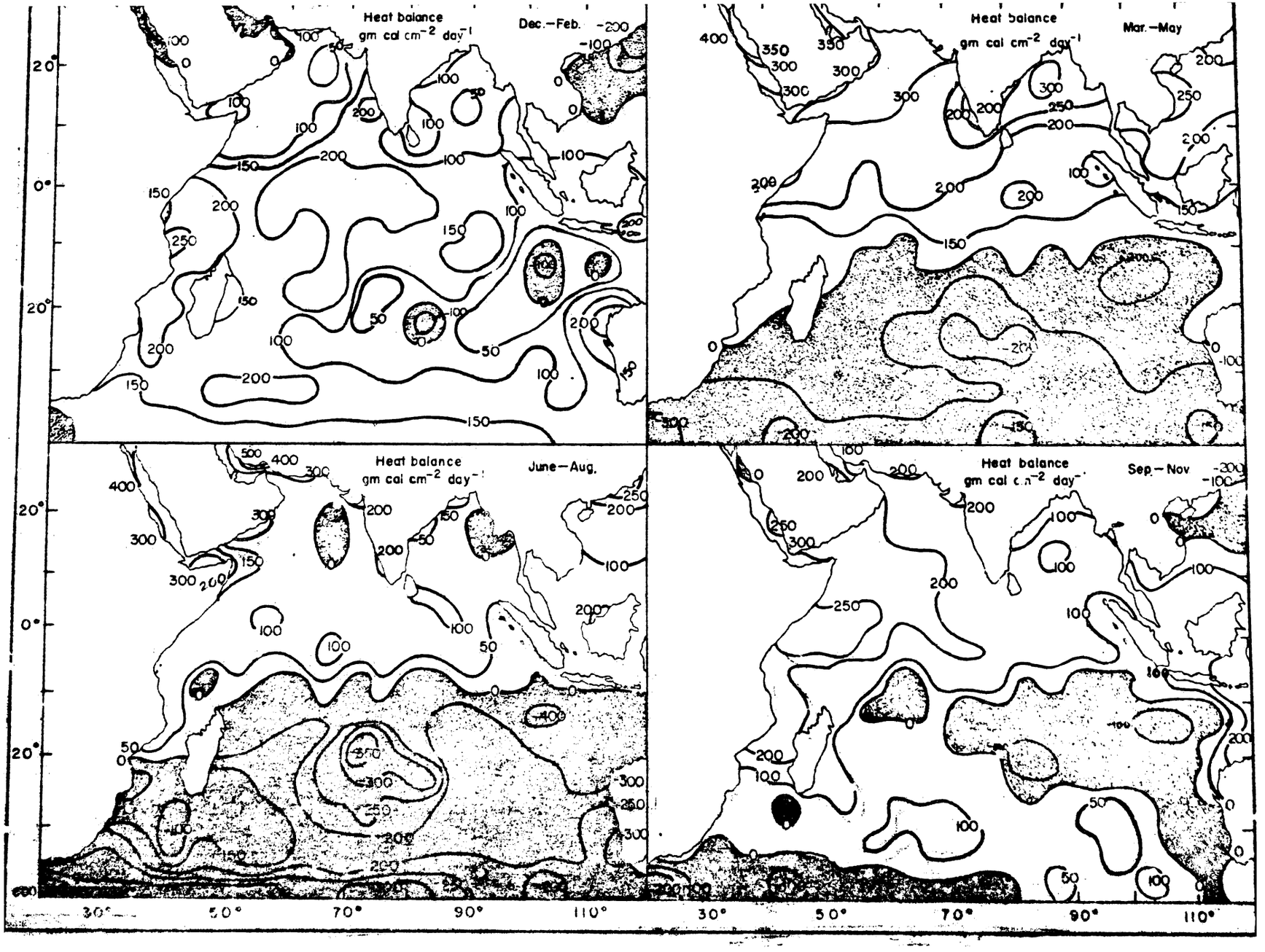
Heat balance
gm cal cm^{-2} day^{-1}
Dec.—Feb.
Heat balance
gm cal cm^{-2} day^{-1}
Mar.—May
Heat balance
gm cal cm^{-2} day^{-1}
June—Aug.
Heat balance
gm cal cm^{-2} day^{-1}
Sep.—Nov
20°
0°
20°
30°
50°
70°
90°
110°

Fig.18. Seasonal distribution of fluxes of heat balance (gm cal cm^{-2} day^{-1}).

in the southern oceans. The areal extension of these areas in the northern Indian Ocean gets reduced. South China Sea shows high values. The area of highest sensible heat is invariably found in the Agulhas Current region.

Net heat balance

During northern winter, solar radiation balance is least in the northern hemisphere. Still sea gains heat since lesser amount of cloud favours more radiative heat input, and the low wind speed values do not favour high evaporation (Fig.18). The marginal seas experience loss of heat due to less radiative heating and comparatively greater evaporative cooling. Since the cold and dry north east winds are favourable for intense evaporation and the net radiative heat input is not considerable. Due to clouds in the South China Sea, the heat loss is experienced here. Negative heat balance is observed in the region between southern Madagascar and south of Java, where it coincides with areasof highest evaporation. During the summer transition, the entire southern ocean losesenergy. The gain in the equatorial region, south of 10^{0}S, is not very remarkable (less than that of winter). Much gain of heatis observed in the northern part of Arabian Sea and Bay of Bengal. Once the summer monsoon sets in, considerable heat gain is observed in the west Arabian Sea. The strong heating of the waters off the Somali and the Arabian coast is the result of the upwelling of cold water. The cold water inhibits the evaporation and reverses the usual direction

of the sensible heat flux. The stability of the air prevents the formation of clouds and the insolation reaches maximum. Another,but weak area of upwelling is noted along the south west coast of India. The central Arabian Sea experiences loss of heat. Here the strong winds, which brings cool upwelled water is cooled and hence cause intense evaporation which exceed the summer radiative heat input and loss of heat is resulted. Simila is the case in Bay of Bengal too. South China Sea gains heat due to less evaporation due to mild winds, though the insolation is not favoured by cloud conditions.Butduring the winter transition as north-east winds start blowing the evaporation exceeds insolation andheat loss is experienced. The tongue extending from west African Sea to the equatorial waters experience moderate heating, since the upwelled waters still persist and move eastward. The other areas show lesser heat gain in the North Indian Ocean, Southern Indian Ocean, shows areas of heat loss at Agulhas Current region, the eastern part of subtropical anticyclone and the west coast of Australia. Incidentally, these areas show maximum evaporation.

Time-latitude sections of the latent heat exchange

The above studies on heat budget components,reveal that the exchange of latent heat is a main component in determining the distribution of heat divergence in the ocean, which influences the circulation of the oceans, which in turn influences

the general circulation of the atmosphere. Colon (1964) has suggested that energy exchanges between the Arabian Sea and the monsoon air have considerable influence on the monsoon flow and the synoptic weather patterns over India. Walker (1978) has concluded that the monsoon system of western Indian Ocean can exist only by interaction with the convective troposphere.

The time-latitude pictures of the variations of evaporation over Indian Ocean is presented (Fig 19). The meridional variation of evaporation over the northern and southern Indian Ocean along the longitudinal blocks of 40-50°E, 50-60°E, 60-70°E, 70-80°E, 80-90°E, 90-100°E, 100-110°E, 110-120°E during different months are shown in Fig.19.

<u>40-50°E longitude</u>

The winterpeak of evaporation in the northern hemisphere is more prominent in this meridional belt. This maximum extends from Nov-Feb with a peak in December around 15-20°N latitude. The summer maximum of evaporation is comparatively weak and it occurs in the same latitude range. The southern Indian Ocean exhibits a maximum near the 35-40°S latitude belt. The equatorial waters show minimum evaporation except for the south west monsoon months.

<u>50-60°E longitude</u>

The northern hemisphere maximum occurs in June at the equator (0-5°N) and 10-15°N. The same latitudinal belt shows

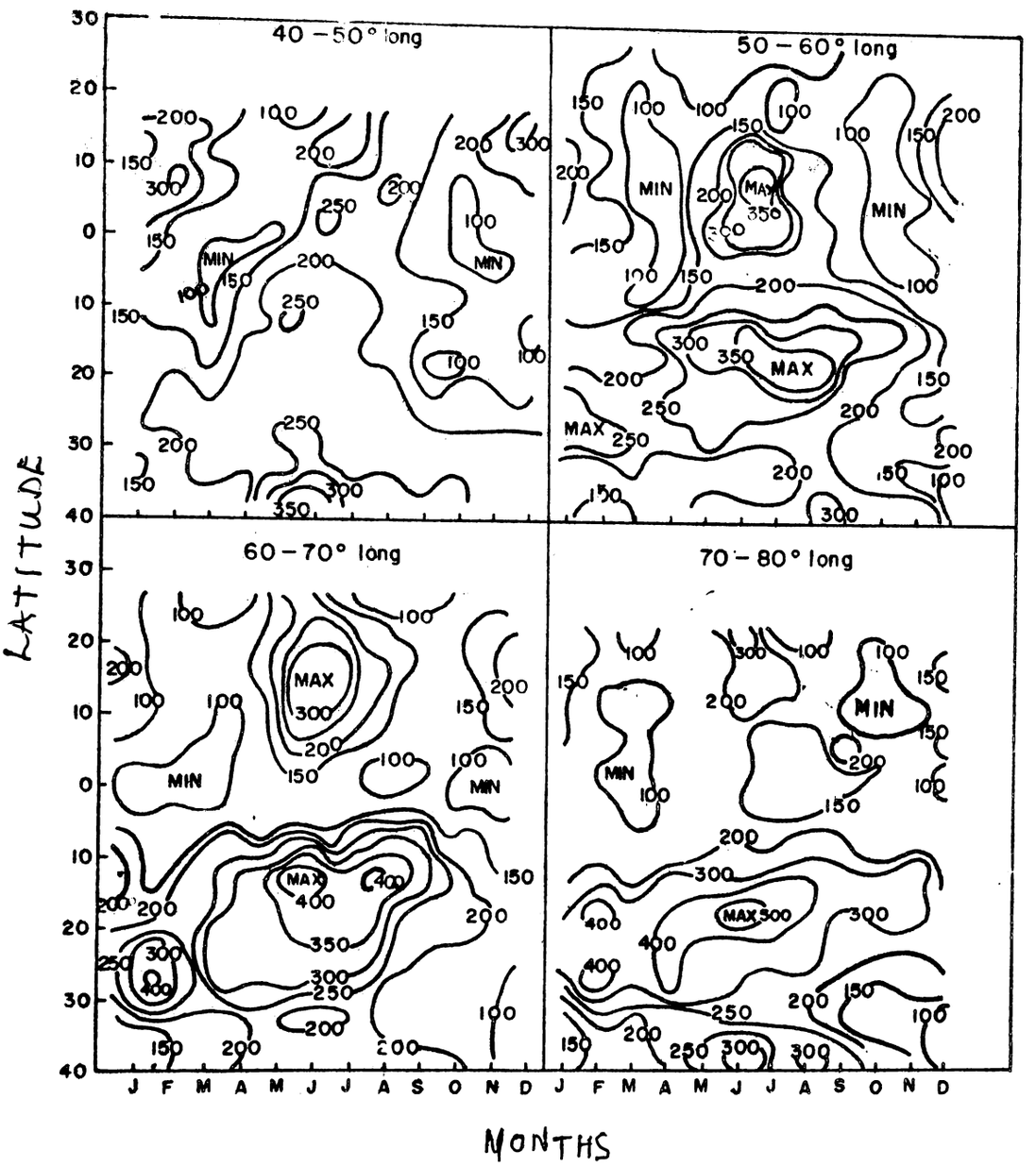
40 – 50° long
50 – 60° long
60 – 70° long
70 – 80° long
MIN
MAX
LATITUDE
MONTHS
J F M A M J J A S O N D

maximum areas for December and January. The summer and winter maxima are separated by transition minimum. This gives a bimodal picture typical of northern hemisphere. The southern hemisphere winter maximum occurs at 25–30° latitude. The summer peak is greater and it is found near 15–20°S. The winter transition maximum occurs at about 10–15°N. There is a shift from winter to winter transition along the south west direction.

<u>60–70°E latitude</u>

The northern hemisphere summer maximum is found at 10–15°N. The southern hemisphere summer maximum is found symmetrically placed at 10–15°S. The winter maximum is lesser and is found in the northern oceans at 15–20°N. Equatorial zone show minimum evaporation. There is a summer transition maximum in southern hemisphere at 20–25°S. Winter transition maximum is found at 10–20°S latitudinal zone. The south west shift is again observed here.

<u>70–80°E latitude</u>

The northern hemisphere monsoon maximum is very feeb (20–25°N). Winter maximum is absent in northern hemisphere, where as in southern hemisphere it is observed at 25–30 and 15–20°N. The summer maximum of southern hemisphere is very strong and is found to be around 15–20°S. The winter transition is at 10–20°S. The shift is much apparent. The area 10–30°S

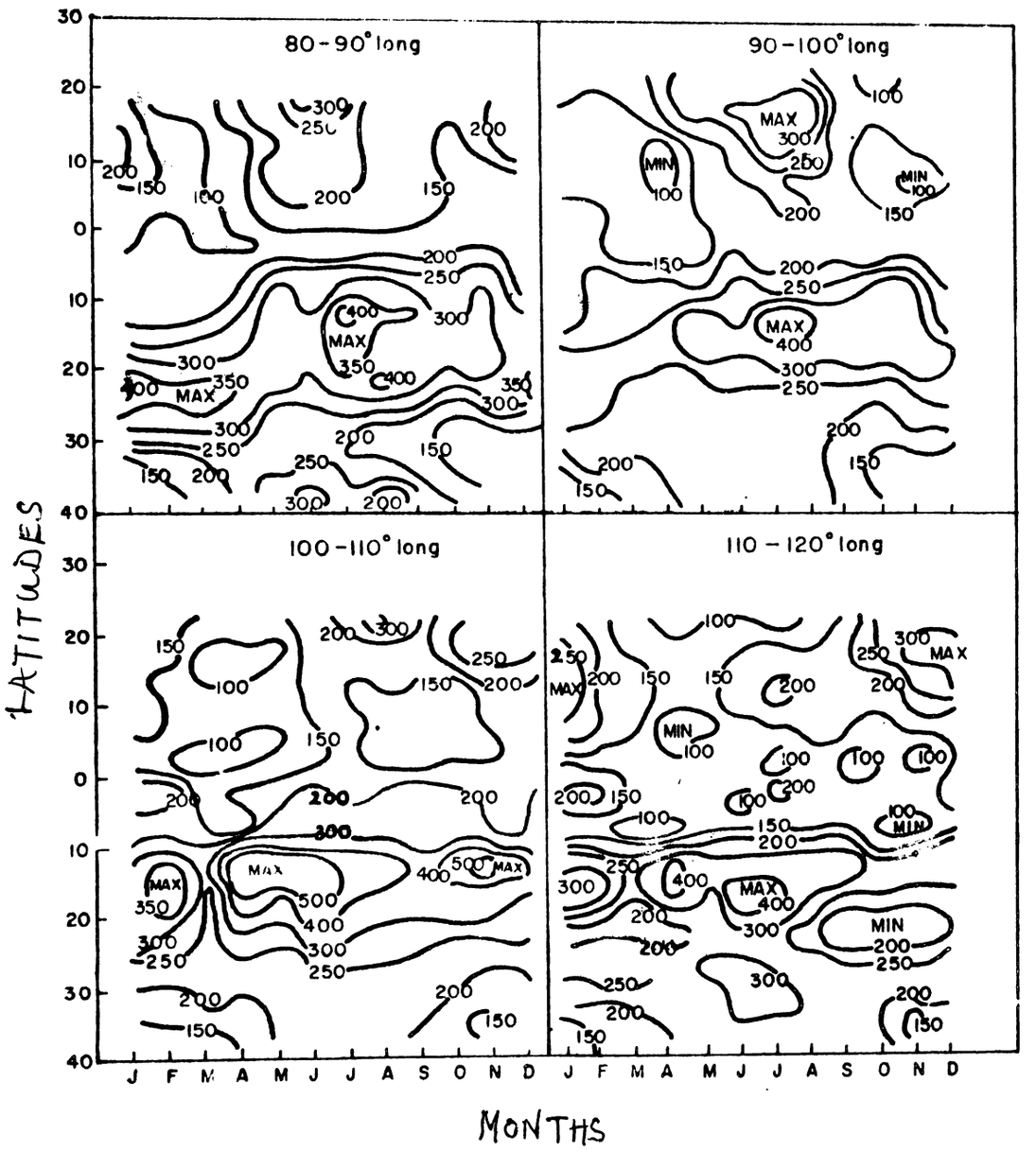
80-90° long
90-100° long
100-110° long
110-120° long
LATITUDES
MONTHS
J F M A M J J A S O N D
MAX
MIN

Fig.28. Time-latitude sections of the latent heat exchange - Eastern Indian Ocean.

a maximum through out, where as the northern and southern areas show a minimum uniformly.

80-90°E latitude

Similar distribution as that of 70-80°E block is observed in the northern hemisphere. The southern Indian Ocean shows a maximum which extends through out all seasons.

90-100°E latitude

The summer maximum is considerably strong (15-20°N). Winter maximum is feeble (10-20°N). Most of the areas show low values of evaporation. The southern Indian Ocean maximum spreads through all seasons, with summer and autumn values showing highest magnitudes. The south westerly shift is seen here also.

100-110°E latitude

Northern hemisphere evaporation is lesser. Southern Indian Ocean values are higher and intensive evaporation is noted at 10-25°S for all seasons except in spring. South equatorial areas show high evaporation values scattered.

110-120°E longitude

Maximum values of evaporation is observed only during

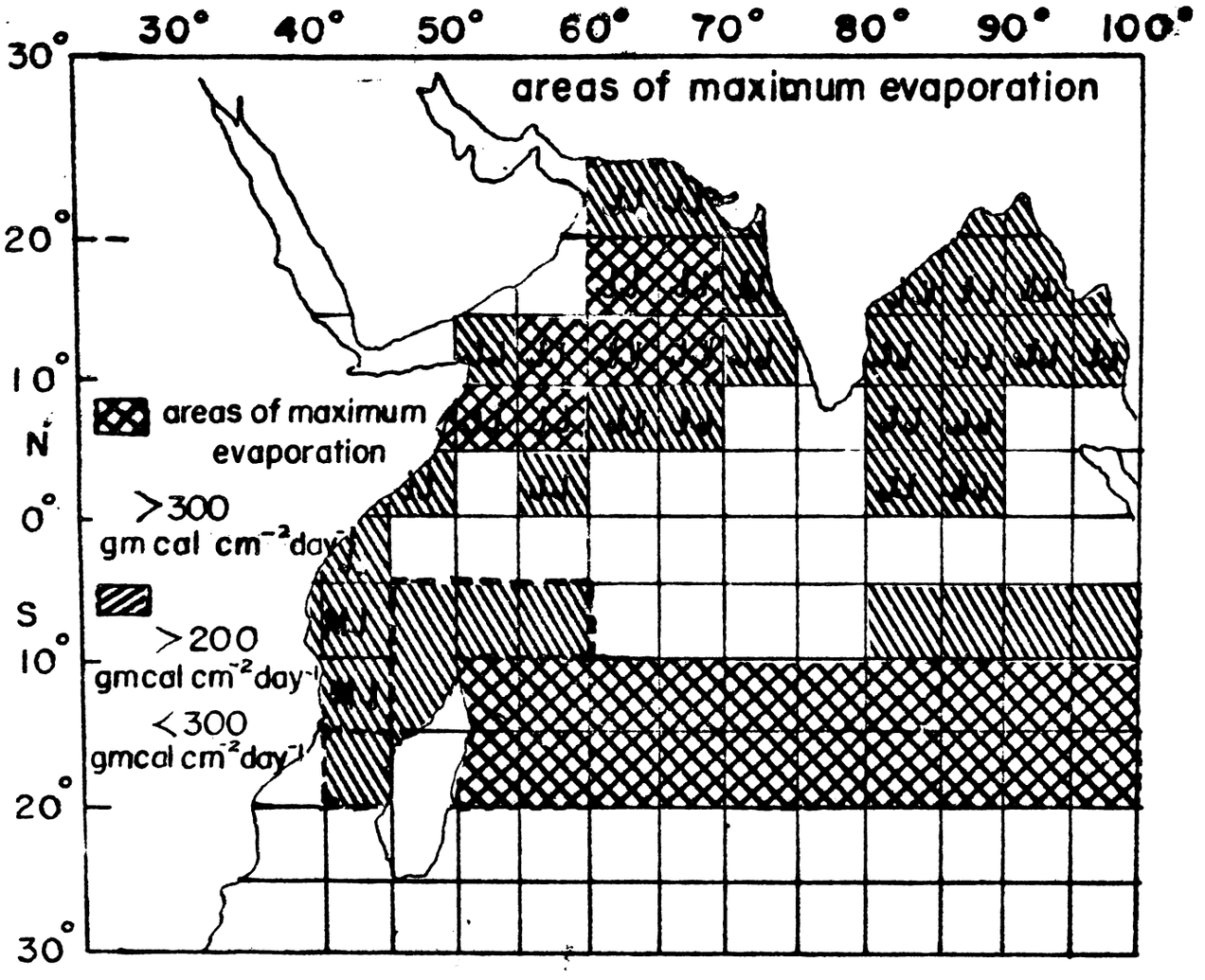
30°
40°
50°
60°
70°
80°
90°
100°
30°
20°
10°
N
0°
S
10°
20°
30°
areas of maximum evaporation
areas of maximum evaporation
>300
gm cal cm⁻²day⁻¹
>200
gmcal cm⁻²day⁻¹
<300
gmcal cm⁻²day⁻¹

Fig.2[illegible]. Areas of intense evaporation in the Indian Ocean. Double hatched areas in the Arabian Sea represent the areas of maximum evaporation, intensity greater than the single hatched areas, during southwest monsoon months. Double hatched area in the southern Indian Ocean represent a semi-permanent area of maximum. The extension of this area towards the beginning of southwest monsoon months is represented in dashed lines. Months of maximum for the rest of the areas are given in the respective 5° grids.

winter and winter transition. The southern Indian Ocean, summer and winter maxima occur at 15-20°S.

The areas of maxima indicated in the above time-longitude sections were plotted for the Indian Ocean area under investigation (Fig.21). It indicates an extension of the area of maximum of the southern Indian Ocean towards west (indicated by dotted lines) during the April-September. The area of maximum of southern Indian Ocean is semi-permanent and shows such intense evaporation during southwest monsoon months. The continuation of this area towards the northern hemisphere, could be due to cross equatorial flow of air, since wind speed is the key factor controlling evaporation. The possibilities are discussed in detail. The area of intense evaporation is observed in the West Central Arabian Sea, due to intense interaction of South-west Monsoon Current with the sea below. Due to intense advection of cold water, July maximum is less than June maximum. Beyond 20°N July maximum is predominent, since the influence of cold water is less.

Seasonal values of heat balance components in different latitude zones

The seasonal values of different heat balance components computed for 5° latitude zones, 30°N-40°S are given as seasonal curves (Fig.22). The seasonal curves of net radiation balance indicate enormous amount of radiative heat input for the Northern Indian Ocean. During warming season of the year, the

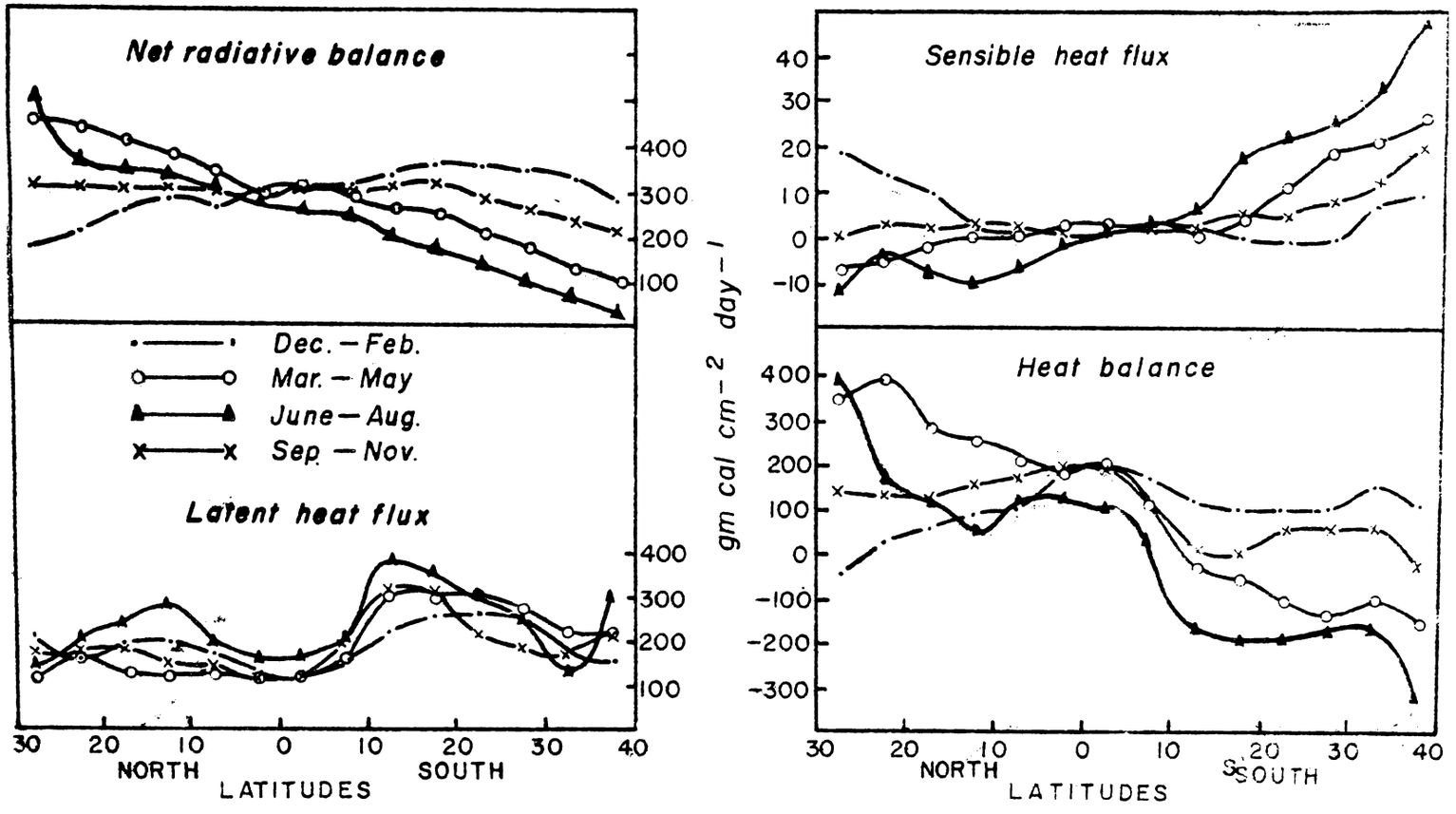
Net radiative balance
400
300
200
100
Dec. — Feb.
Mar. — May
June — Aug.
Sep. — Nov.
Latent heat flux
400
300
200
100
30 20 10 0 10 20 30 40
NORTH
SOUTH
LATITUDES
gm cal cm⁻² day⁻¹
Sensible heat flux
40
30
20
10
0
-10
Heat balance
400
300
200
100
0
-100
-200
-300
30 20 10 0 10 20 30 40
NORTH
SOUTH
LATITUDES

Fig.22. Seasonal curves of the heat balance components for different latitude belts.

North Indian Ocean gains more heat than that gained by southern Indian Ocean, during the warming season of the respective hemisphere. The seasonal variation curves of latent heat exchange shows a main source of water vapour in the 10-20°S latitude belt, throughout all seasons. Unlike North Atlantic and Pacific seasonal curves given by Jacobs (1951), the North Indian Ocean curve for summer (monsoon) shows highest values of evaporation. Southern hemisphere maximum of latent heat exchange also coincides with the same period. Through out all seasons, especially in the higher latitudes, the surface air is warmed in the southern hemisphere the maximum being in winter. Except for winter, warming of the air above is not prominent in northern hemisphere. During spring and summer monsoon period North Indian Ocean receives energy from the atmosphere above. Northern Indian Ocean also show enormous loss of heat along 10-20°N latitude belt, but does not reach negative values, since the radiative heat input observed in that region is quite remarkable. Net heat gain is maximum in the northern most part of North Indian Ocean and the marginal seas.

(Qe-Qp) values (difference of energy used for evaporation and released in precipitation) for different seasons in the Indian Ocean are obtained using the results of the present studies and the precipitation values presented by Jacobs (1951).

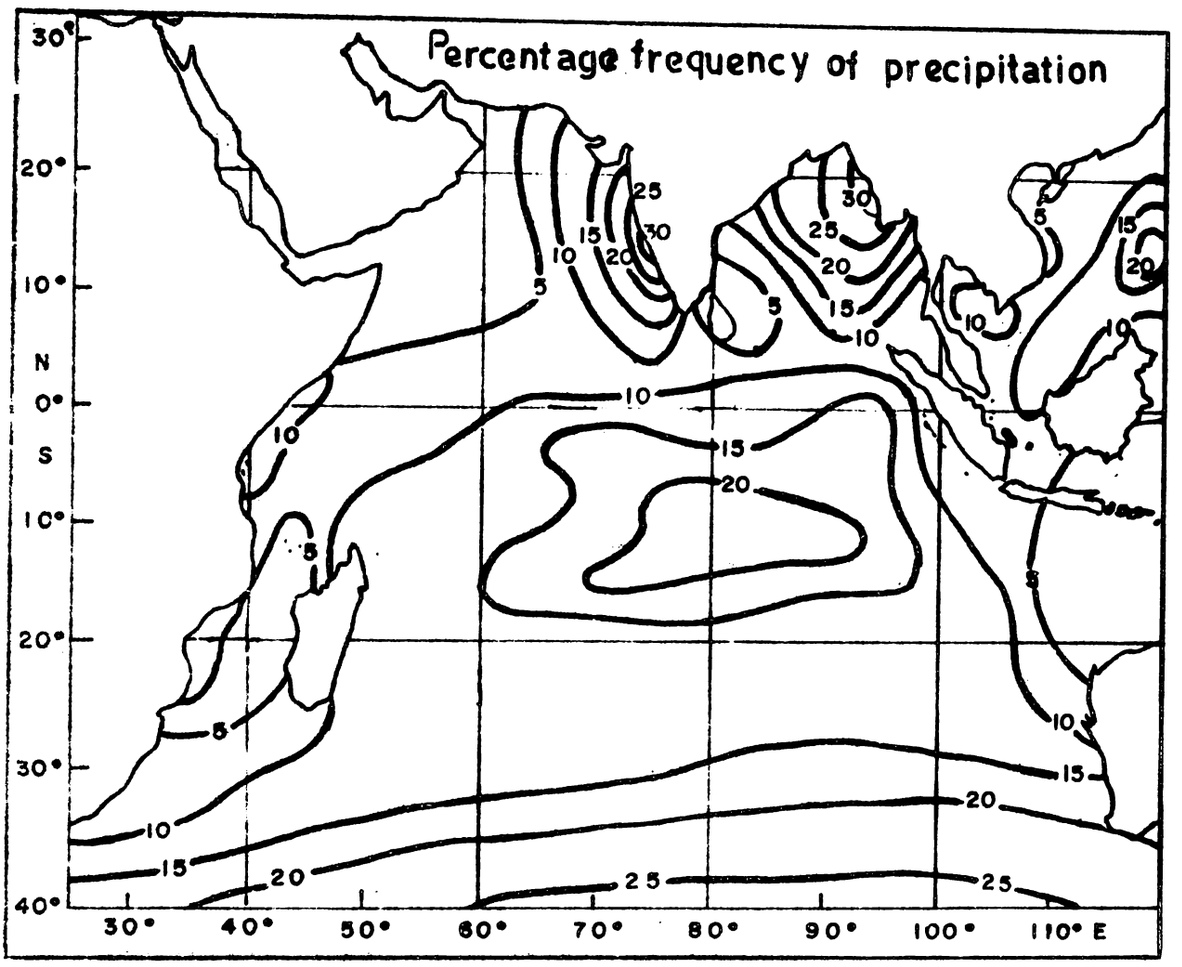
Percentage frequency of precipitation
30°
20°
10°
N
0°
S
10°
20°
30°
40°
30°
40°
50°
60°
70°
80°
90°
100°
110° E

Fig.13. Percentage frequency of observations reporting precipitation during July (U.S. Navy Marine Climatic Atlas of the World, Vol III Indian Ocean).

Table. 6

Seasonal Variation of (Qe-Qr) values over Indian Ocean

Lat. range	Dec-Feb	Mar-May	June-Aug	Sep-Nov	Annual
30-30N	144	116	-9	91	86
10-20N	134	59	-18	-30	36
0-10N	-12	-73	-31	-101	-54
0-10S	-131	-79	-39	-84	-91
10-20S	39	121	-203	186	138
20-30S	171	189	172	158	170
30-40S	95	128	136	103	116

Though precipitation over the ocean is not too well measured, the excess of precipitation over evaporation values obtained give a rough picture. The frequency of precipitation for the month of July, as presented by climatic atlas of the Indian Ocean, Vol III is given (Fig.23) for reference. The negative values of (Ce-Cp) for the equatorial belts show heavy precipitation due to the heavy convective clouds in the doldrums. The seasonal and annual (Ce-Cp) values are given in Table.6. 10-20°S zone shows enormous evaporation excess, during summer monsoon and winter transition months. Throughout ehh seasons the equatorial waters show negative (Ce-Cp) values, caused by low evaporation and heavy precipitation of doldrums. In accordance with Wüst (1936) and Venkateswaran (1956) the present computations indicate a residual annual excess of evaporation over precipitation for the northern Indian Ocean. Though Venkateswaran suggests that this positive value is due to intense evaporation from western Arabian Sea during northeast and southwest monsoons it has to be pointed out that the summer monsoon months show excess of precipitation over evaporation and so are winter transition months.

The values of Bowen's ratio for different seasons is given in the Table 7. The values for low latitudes are smaller. The summer values of Bowen's ratio in the respective hemispheres are negative. Negative values of Bowen's ratio, throughout the

Table.7

Seasonal variation of Bowen's ratio over the Indian Ocean

Lat. range	Dec-Feb	Mar-May	Jun-Aug	Sep-Nov	Annual
25-30 N	0.09	-0.06	-0.09	0.00	-0.02
20-25 N	0.08	-0.03	-0.02	0.02	0.01
15-20 N	0.05	-0.02	-0.03	0.01	0.00
10-15 N	0.01	0.00	-0.04	0.02	0.00
5-10 N	0.01	0.02	-0.03	0.01	0.00
0-5 N	0.01	0.02	-0.02	0.01	0.00
0-5 S	0.03	0.02	0.01	0.02	0.02
5-10 S	0.03	0.02	0.01	0.01	0.02
10-15 S	0.01	0.01	0.02	0.06	0.02
15-20 S	0.00	0.01	0.05	0.02	0.02
20-25 S	-0.00	0.04	0.07	0.02	0.03
25-30 S	-0.00	0.07	0.10	0.04	0.05
30-35 S	0.04	0.08	0.14	0.07	0.08
35-40 S	0.06	0.11	0.15	0.09	0.10

northern hemisphere latitudes for summer monsoon months are seen in the table which differs from Venkateswaran's (1956) values.

Conclusions

The broad patterns of the heat budget components as computed over the Indian Ocean agree generally with the earlier studies. The net radiation seasonal charts are consistent with that of Mani et al., (1965). The regions of high maxima in the western Arabian Sea, west coast of Australia and the equatorial region are identified. Very low values of net radiative input in the higher latitudes of southern Indian Ocean and the areas of maximum precipitation during south west monsoon are also observed. The highest values of radiation over the earth, noticed in the western Arabian Sea, is found to be playing an important role in the origin and maintenance of summer monsoon. Latent heat exchange is observed to be the most important heat budget component especially in the trade wind zone. The general picture of evaporation over the Indian Ocean agrees well with Venkateswaran (1956), Privett (1959), Ramage et al., (1972) and Suryanarayana Sikka (1973). Apart from the main areas of evaporation over Arabian Sea and Bay of Bengal (during summer and winter monsoons) and a permanent region of maximum in the subtropical anticyclone region of South Indian Ocean, a pronounced region of maximum in the area of Agulhas Current which is the most prominent of all the areas.

As identified. Immense evaporation and hence heat loss is observed by Zillman and Bell (1968) also. This is comparable to that of Gulf stream and Kuroshiro except that it is found in southern hemisphere. Seasonal variations and its prominence in the northern hemisphere is noted. The peculiar pattern of evapo ration in the northern Indian Ocean with a summer maximum is als observed.

Arabian Sea and Bay of Bengal show different seasonal values. The net radiation is almost the same for winter and summer transition. As the monsoon invades, Arabian Sea (western part) receives more energy on account of cloudlessness and Bay of Bengal receives minimum, on account of its heavy cloudiness. Eastern Arabian Sea especially west coast of India receives less radiative energy. During south-west monsoon season the flux of latent heat is more in the Arabian Sea on account of enormous evaporation due to the interaction of the intense monsoon current over the west central Arabian Sea. During north-east monsoon season it is almost the same, over both the oceans. During the transitions, when the winds are moderate, the influence of sea surface temperature is more and hence warmer waters of Bay of Bengal are cooled more by evaporation. This does not conform with Suryanarayana and Silda's (1972) findings of higher values of evaporation for Bay of Bengal than Arabian Sea, for south-west monsoon seasons, for the years 1965-67. Very high negativ values of sensible heat exchange are observed in the western

Arabian Sea, where as Bay of Bengal values are lesser. During southern summer, it shows a contrast between North Indian Ocean with high negative values in the western Arabian Sea and south Indian Ocean with high positive values in the Agulhas Current region, marking the cold and warm currents respectively. The impact of monsoon over the North Indian Ocean, the late summer cooling which is found no where else in the world oceans, is indicated in the climatic model of summer monsoon sensible heat.

The magnitudes and distribution of seasonal net heat gain by the ocean generally aids in the studies of oceanic currents and formation of water masses. The main areas of heat gain and loss in general coincide with the cold and warm ocean currents. The maximum cooling occurs off the south east coast of Africa, where warm waters of Agulhas Current are exposed to cold dry continental air in the winter time (southern hemisphere winter). Another area of maximum heat loss is observed in the region of subtropical anticyclone of southern Indian Ocean. Maximum heat loss is observed in the eastern side. The areal extension and intensity of this region is maximum in the southwest monsoon season. This area occurs as two main intense maxima of heat loss separated by contours of lesser magnitudes. In regions of net negative annual heat exchange, the seasonal oceanic thermocline is erased before

the end of winter. In such regions, water masses can be formed by convergence and sinking of the surface water which flows, at depth away from the area of its formation. The Aghulhas Current region of negative heat exchange, which extends eastward coincides with the area of formation and sinking of Antartic Intermediate Water or subtropical subsurface. The negative heat exchange is maintained by warm water of Aghulhas Current which flows southward to replace the sinking water. The intense heat loss area of subtropical anticyclone (western maxima) coincides roughly with the source region of subtropical water. Sharma (1976) states that this high saline water mass which gets cooled due to intense evaporation sinks at about 28°S-35°S and protrudes as a tongue to about 15°S in the depth range of 100-500 m. Arabian Sea water whose source region is identified around 65°E 21°N (Sundara Raman et al., 1968) coincides with the area of heat loss of southwest monsoon season. This area which coincides with the intense area of evaporation due to the interaction of strong monsoon westerlies is marked for salinity maximum. The annual (Oe-Op) value is positive here. This water mass influenced by high saline waters of Red Sea and Persian Gulf, shows a salinity maximum throughout, associated with a thermocline in eastern Arabian Sea and spreads southwards upto 8°N. The Red Sea water of salinity maximum, whose influence is conspicuous in the Arabian

Sea upto 8°N is formed by sinking and spreading in the out flow from Red Sea. The intense evaporation and heat loss during winter indicates the formation of this water mass.

As the narrow and intense Somali Current flows northward and turns east at about 8°N, the intensity of heat gain decreases. It joins the monsoonal current which flows eastward. Upwelling off Somalia and Arabia which begin in May, is intense during July and August, and, through feedback, has so increased the pressure gradient between sea and land that, the south westerlies are the strongest and most sustained surface wind systems on earth (Mcdonald 1938). Even beyond the reach of upwelling, strong winds are observed to be sufficiently cooling the waters by evaporation. North Indian Ocean picture for the southwest monsoon season, as observed by many previous workers, is different from the usual concept of evaporation maximum during winter. Thus Indian Ocean, as a whole experiences intense evaporation during sothwest monsoon.

The ocean-atmosphere exchanges studied in this Chapter, reveal the modification produced by ocean surface on the properties of the moving airmasses. During northeast monsoon months, a dry warm continental airmass flows over the cold waters of the northern part of Indian Ocean and after that reaches warmer waters. Consequently, more latent heat exchange, takes place

as the water-mass reaches equatorward to the western Arabian Sea. Horizontal gradient of temperature in the Arabian Sea is conspicuous. Since the sea and air temperature differences are considerable, the sensible heat values are quite high in the northern parts of Arabian Sea and Bay of Bengal. It is remarkably high over Red Sea and Persian Gulf. The combined effect of sensible and latent heat and low values of radiative heat input create loss of heat in the marginal seas of Northern Indian Ocean. As observed by Saha (1972), the amount of cloud cover increases as the airmass gathers water vapour and heat. During southwest monsoon season, two types of airmasses are found over the Arabian Sea the dry warm continental airmass, from the continents of Africa and Arabia and cool maritime airmass of southern hemisphere. The airmasses travel over the cold surface of western Arabian Sea. As the airmasses gather energy from the western Arabian Sea and reaches the warmer eastern Arabian Sea, large amounts of cloudiness are observed, the cloudcells becoming larger and more vertically developed as the westcoast is approached. The cloud amount chart of present studies for the monsoon months show well defined maxima of clouds in the eastern Arabian Sea 70-80°E and an area of scanty cloud amount in the region, west of 60°E is also observed. Radiation data obtained from Nimbus-II Satellite and studied

by Saha et al.,(1969) for June 1966 also reveal cloudiness in the same areas in northern Indian Ocean. The areas of cloudiness are reported to be coinciding with area of updraft and they concluded that the cloud bands extending into the two hemispheres to be suggesting cross equatorial flow of south east trades into the northern Indian Ocean. Godbole and Ramana Murty (1970) using the pattern of brightness (indicator of the cloud activity) over India, has arrived at a continuity from latitude to latitude from south of equator suggesting that the monsoon air presumbaly comes from the south Indian Ocean and crosses the equator. The large-scale cloud patterns over the Indian Ocean studied by Mishra and Singh (1980) using satellite cloud imagery for the month of June 1967 showed extensive cloud bands, thousands of kilometers in length, originating in south Indian Ocean. These cloud bands were aligned along the south-easterly trades, and curved sharply near the axis of southern hemispheric equatorial trough between Lat.5°S and 10°S. The small scale cloud features, showed the equator-crossing of the deflected south westerly current.

The summer maxima of evaporation, pertaining to the monsoon months, when plotted on a chart, hints the merging of southern and northern Indian Ocean circulation; through interhemispheric mixing in certain preferred latitudes (40-45°E,

55-60°E and 80-90°E). The orientation of intense evaporation regions almost follow the usual path of massive transfer of southern hemispheric air to the west coast of India; which could mean an important part played by the southern Indian Ocean airmasses in the monsoon circulation. According to Miller and Keshavamurthy (1968) the southwest monsoon current in the lower 5 km near India consists of two main branches, which are the Bay of Bengal branch, influencing the weather over the northeast part of India and Burma, and the Arabian Sea branch, dominating the weather over the west, central and northwest parts of India. According to them the latter branch can be further divided into two separate currents. One part of the main low level current flows northward, across the equator between 35°E and 55°E and then, turning northeast flows over the Arabian Sea, crossing the west coast of India north of 15°N. The southern current separates near 10°N over the Arabian Sea and flows eastward across the south Malabar coast to join the Bay of Bengal branch. Langrangian studies of the low level flow over the Indian Ocean during the summer monsoon with constant density low-level balloons by Cadet, etal (1978) also confirm the large-scale atmospheric flow from the southern hemisphere, (southwest part of Indian Ocean). These studies further revealed that typically the air reaching the west coast crosses the equator west of 55°E and goes through the

East African low-level jet. The air crossing the equator in the vicinity or eastwards from 55°E is deflected towards the east in the northern hemisphere and meets the Bay of Bengal branch of the monsoon. This goes along with Findlater's (1969a) findings showing the division of the Arabian Sea branch of the monsoon into two separate currents. The northern current affects the west coast of India north of 15°N and the southern current breaks away at 10°N over the Arabian Sea and flows eastward along the southern Malabar coast. Eastward moving disturbances in the northern hemisphere and westward moving disturbance in the southern hemisphere are also identified. A reversal of flow near the equatorial station of Seychelles is also observed from July 1964 data. This idea of cross-equatorial flow is a controversial subject, and here, in this study it is relevant as to know whether heavy precipitation experienced over the west coast of India is caused partly by the air-sea interaction of southern hemisphere airmasses also. The above mentioned chart of areas of intense evaporation, along with the seasonal latitudinal averages of (Le-Lp) values, indicate the possibility of southern hemisphere airmasses contributing to the process of precipitation in the west coast of India. Though the (Le-Lp) annual values are positive in the northern hemisphere, (Le-Lp) values for the south west monsoon and post monsoon months are negative, indicating excess of precipitation over evaporation.

This indicates that evaporation taking place in the northern Indian Ocean latitudes do not support the whole of precipitation experienced in the west coast of India. Bhumralkar (1978) while studying the relation with the evaporation of the Arabian Sea has observed excess evaporation over precipitation in the western Arabian Sea. The climatic model of evaporation presented here indicates heavy transfer of latent heat energy in the western Arabian Sea and subtropical anticyclonic areas of southern hemisphere. This anticyclonic area is observed in the present studies as extending towards northwest. The area of high winds also extend towards the northern hemisphere area of intense monsoon flow. Increase in evaporation of the anticyclonic region of the southern hemisphere starting from summer transitions and its movements northwest wards indicating transfer of air from southern hemisphere is reported by Privett (1959) and Venkateswaran (1956) and confirmed by present studies. The present studies agrees with Venkateswarans annual (Le-Lp) values for northern hemisphere and the minimum (Le-Lp) values observed in the southern equatorial zone. But (Le-Lp) values for the northern Indian Ocean for the southwest monsoon months are negative in all latitudinal zones in the present studies inspite of a large evaporation coefficient used Agreeing with Jacobs (1951) contention of prependerance of precipitation over evaporation in that particular area, Evaporation minus

precepitation patterns of Bhumralkar (1978) clearly indicate that the supply of moisture from the Arabian Sea alone is not sufficient to explain the recorded rainfall amounts at and near the west coast of India. Precipitable water from the dropsonde soundings of research aircraft taken at some selected locations off the west coast of India, in comparison with actually recorded rainfall, indicated that the rainfall exceeded the amount of precipitable water. Venkateswaran (1956) also found that precipitation exceeded evaporation by over 40 cm, during summer monsoon seasons near the coast of India. All these results, indicate that moisture required to explain the heavy rainfall at the west coast of India, must be sought from other sources. Jacobs (1951) also, while discussing the role of oceans as moisture suppliers for rainfall over land (in the northern hemisphere) concluded that they are not the only sources.

Following the climatological studies of Jacobs(1951) and the negative (Qe-Qp) values observed in the present studies, one has to look for another source of water vapour. It looks apparent that the hot and dry desert land mass bordering the Arabian Sea, with subsiding air over it cannot make any significant contribution of moisture to the monsoon atmosphere. But Pisharoty (1965) ruled out all possibilities of another source. Pisharoty (1965) calculated moisture over the equator

over the Indian Ocean west of Long 75°E in a layer from the surface to 450 mb and over the west coast of India during July 1963 and 1964 and observed that the moisture was about double over the west coast when compared with that over equator. According to him the monsoon current over the Arabian Sea was primarily of northern hemisphere origin, the air from North-east Africa and Arabia picking up moisture while travelling over the sea. Pisharoty and Sreenivasiah (1969) have stated that the air that crosses the equator from the southern hemisphere turns towards the east by the time it reaches about Lat 10°N and so does not apparently participate in the circulation of the heat low over Pakistan and the Gangetic Valley trough. Rama (1968) while studying the Radon content of air as tracers have concluded that the monsoon air over the Arabian Sea north of about Lat 5°N was not a continuation of the air from the southern hemisphere, but was from the northern hemisphere itself from North-east Africa and Arabia as presumed by Pisharoty.

But Findlater (1969) b observed a persistent high-speed air current in the form of a system of low-level jet stream blowing from south to north across the equator exists in the lower layers of the air in the vicinity of the western Indian Ocean during the southwest monsoon season. He found that the variations in the cross-equatorial speed of the current were

found to have important regulating effect on the rainfall producing capacity of the southwest monsoon over India during a two months (July-August, 1962) sample period. Findlaters observations show that the winds over the peninsula upto about 4.5 km and rain over the west coast of the peninsula when the monsoon is active or strong can be understood easily if one considers the south-westerly monsoon current over the Arabian Sea as a continuation of air from the southern hemisphere, crossing equator between 30°E and 60°E.

These jet streams have been connected with the jet off the coast of Somalia and the low level westerly jet stream over India to form a wind system bringing in air of southern hemispheric origin over India in significant quantities (Rao & Desai 1969). The data presented by Findlater (1969) and Rao (1964) also show that in summer the monsoon current accounts for nearly half of the air estimated to be transported into the northern hemisphere across the whole equator at lower levels. Moreover, results of Rangarajan et al., (1969) show that the radioactive fall out debris from the French explosives in Polynesia - 20°S, 138°W during July to September 1966 to 1968 travelled westward into the Indian Ocean and reached India. Rangarajan and Gopalakrishnan (1972) relates these studies on the movement of radio-active debris across the equator to the meteorology of Indian Ocean area. It confirms the cross equatorial flow of

Somali jet' near the African coast which arrives as westerly winds on the west coast of India.

However Fig.2i shows the extension of the area of high evaporation westward starting from May. Areas of considerable evaporation west of 50°E and African coast is observed. As has been putforth by Bunker, the low-level jet that develops off the coast of Somalia during the summer monsoon is the end result of a series of land-air-sea interactions with many size scales from the global to the local dimensions Baskara Rao (1972) using satellite data showed that ITCZ migrates northwards much more during the northern summer in the Northern Indian Ocean than anywhere else in the world and the air of low pressure belt associated with this over south asia at the sea level. Studies by Krishna Rao (1966) have shown that the ITCZ migrates northwar with time during the monsoon period and that a sudden shift to the southern tip of India of the convergence zone near the equat marks the burst of the monsoon over India. Also, it is of interest to note that findings by Findlater (1969a and b) which are in general agreement with those by Rao (1964), have indicated that the southern hemispheric air of differing origins gets accelerated in a well-defined stream which crosses the equator and that variations of the cross equatorial speed of this curren influence the rain producing capacity of the India summer monsoo Findlater (1981) has arrived at strong correlation be the pulses of cross equatorial flow at low-level a Kenya and rainfall of Western India during nor Summers.

With the advent of summer season of northern hemisphere radiational cooling creates high pressure over the Kalhari Desert and radiational heating creats low pressure over the Sahara. A southerly flow is set across equator, eventually merging with the southeast trades and south-west monsoon north of the equator. This flow of air transports the warm surface of the ocean to the eastward, leaving cooler waters on the surface along the eastern coast of Africa. These cooler waters then cool the atmosphere above them there by increasing the atmospheric pressure. The increase of atmospheric pressure causes a weak ridge of pressure to develop along the African coast. The high pressure ridge over Somali coast and the heat low, which develops in May, over Arabia, west Pakistan and northern Indian Ocean (Ramage, 1965) creates persistent wind speed maximum off shore from the zone of upwelling (Bunker, 1968) and defection of inflow to flow parallel to the coast. In, mid July, the heat low is deepest, the southwest monsoon is strongest and west Indian rains are heaviest. The lowest temperature is observed in the month of July along the Somali coast in the present studies. Consequent upwelling of cold water increase the down wind pressure gradient and accelerate the winds. The strong surface winds facilitate downward transport of heat and moisture, despite the great stability of

the air. According to Ramage (1966) the Arabian and Somali troughs elongate the circulation to southwest. The charts of present analysis reveal continuity of isotherms of summer monsoon season except for the coastal regions of Somalia. Unlike other seasons, very steep gradient of pressure is observed in the southwest monsoon pressure chart along the Somali coast. A shift of high wind speed region of south Indian Ocean towards west in the southern equatorial region, which almost looks as a continuation of intense wind speed is observed. It is to be mentioned that the main aim is not a review of works on the genesis of south west monsoon. An attempt is made as to see whether the southern Indian Ocean airmasses contribute towards the intense precipitation observed, with the help of surface values of climatic parameters and computed heat exchange values though, we are fully aware that the surface conditions are not sufficient to explain the precipitation mechanism which depends much on the upper air conditions of rain producing mechanisms. (Ramage., 1966, Miller and Keshavamurty., 1966). The observed near surface characteristics suggest the coming of the monsoon air from the South Indian Ocean crossing the equator. It may, however, be stated that it is not to suggest that the monsoon rainfall is solely caused by southern hemisphere air, but the main aim is to see whether the surface charts and the latitudinal values could give any hints as to whether the contribution is

mainly from the western Arabian Sea or is partly done by Southern Indian Ocean air also. It is obvious that the southern air masses, humid and unstable after their long journey over warm ocean surfaces, can yield large amounts of precipitation. But the precipitation frequency chart (Fig.23) reveals that part of the vapour gathered, is depleted on its way. The (Le-Ep) latitudinal value for the southern equatorial waters is negative. The intense evaporation is usually seen during June, since the cold water observed in the Arabian Sea reaches minimum in July and August. In June the strong monsoon wind offsets the effect of low sea surface temperatures. Beyond 15°N the maximum evaporation is observed in July. A fall in intensity of evaporation beyond 20°N is observed. Sangarajan et al., (1970) (in connection with studies of radioactive debris across equator) that this coincides approximately with the monsoon trough. According to him the transfer east of 60°E is small, the velocities at Oun (8°N, 75°E) being a few knots, as compared to the velocities of Garissa (8°N, 40°E) of about 30 Kt (Findlater., 1969 a). Tentative calculations by Rao (1964) and Findlater (1969 b) indicate that nearly half of the air is estimated to be transported into the northern hemisphere. Saha (1970 b) believes less than 50 percent originates in the northern hemisphere. Saha and Bowadekar (1973) concluded that the influx along the southern boundary was about equal to the total amount of evaporation from the surface of Arabian Sea.

In the light of above discussions, it is seen that the variations of heat balance components and other climatic variables, especially sea surface temperature show maximum variations in the northern Indian Ocean. The proximity of huge land mass in the northern side, the orientation of the vast arid regions in the northwest and the intense upwelling could be the main reasons for the peculiarities observed here.

The intense upwelling not only is one of the causative factors for the genesis of Asian monsoon, but also causes the complete absence of cyclogenesis in the Arabian Sea. Cyclogenesis is maximum in the Arabian Sea and Bay of Bengal before the onset of summer monsoon (April and May) and after the withdrawal of monsoon (October and November). Arabian Sea shows complete absence of cyclones during winter and summer monsoon months. (Tracks of Storms and Depressions in Bay of Bengal and Arabian Sea 1877-1970., IMD-1979). This could be attributed to the drop in temperature observed during winter and summer monsoon months. During winter, the reduced insolation and comparatively high rate of evaporation cause low values of sea surface temperature. During summer monsoon, the higher radiative input is outweighed by the upwelling effect. Along the Somali and Arabian Coasts, where intensity of upwelling is maximum, evaporational cooling is less due to low sea surface temperature values. In the easternside the evaporational cooling plays a prominent role. Eastern Arabian Sea and Bay of Bengal do not exibit conspicuous cooling, since the effect of upwelling and evaporational coolin

is less, though the net radiative input is much less due to heavy convective clouds present during Southwest monsoon. Bay of Bengal is conspicuously warmer and does not exhibit complete absence of cyclones during winter and summer monsoon seasons. During spring and autumn the evaporational cooling is minimum in Arabian sea, and these periods coincide with the periods of cyclogenesis maximum, in these regions. According to Ramage (1974) cyclones always begin to develop in troughs located at high enough latitudes for low level westerly winds to be observed on their equator side. In the height of summer monsoon, due to enormous drop in temperature in the Arabian sea, the trough moves beyond 25°N and is largely over land (Raman, 1970., Ramage, 1974) and storms are rare. Inspite of low sea surface temperature observed, Western Arabian sea shows maximum evaporation due to the gale force winds observed. However, the present studies reveal that inspite of intense evaporation observed in the Western Arabian sea, a significant part of the monsoon water vapour flux across the Indian Peninsula, comes from Southern Indian Ocean. At the same time, the contribution from the Western and Central Arabian sea is very important.

Chapter 5

On Zonal differences in the seasonal variations of the heat budget of the equatorial Indian Ocean

The large-scale climatic models of the World oceans reveal huge anticyclonic gyres, with equatorward flowing cold waters in the eastern and poleward directed warm currents in the western parts of the oceans. The southern Indian Ocean with warm Agulhas Current flowing towards the polar regions in the western side and the cold West Australian Current flowing northward along the west north-west coast of Australia towards the equator, follow the usual pattern, where as in the northern Indian Ocean, it is distorted by the presence of the large continental mass. Large gyres existing in the Pacific and Atlantic are not found in the northern part of the Indian Ocean, (Düing, 1970). The conditions encountered in the North Indian Ocean are unique.

The discussions and the charts presented in the previous chapters, conforming with the works of many others show a different picture for the North Indian Ocean. The northward flowing cold somali Current in the Western part of the North Indian Ocean and the monsoonal influence are found to be creating a different picture in the northern Indian Ocean. The presence of important

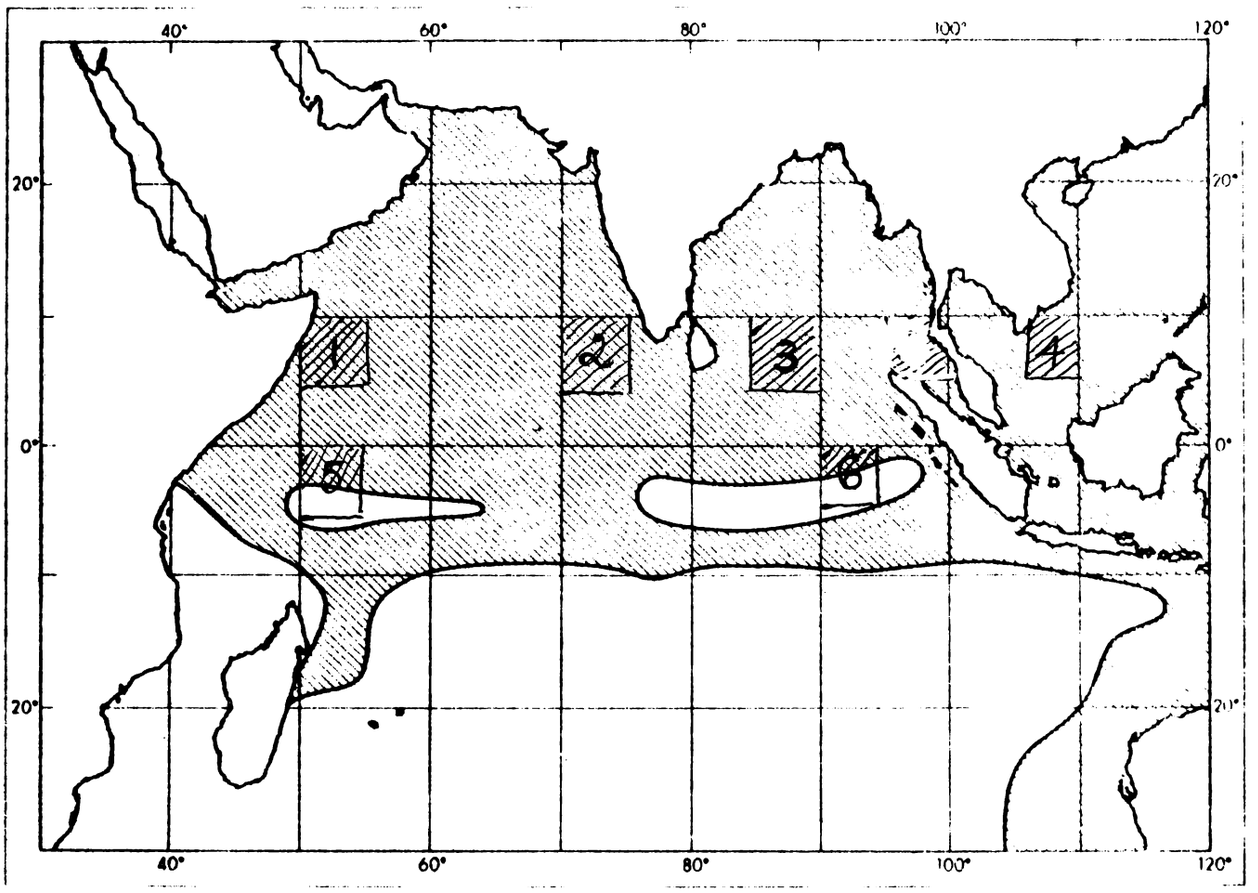
40°
60°
80°
100°
120°
20°
0°
20°
1
2
3
4
5
6

Fig.34. Surface current direction as a criterion of monsoonal influence. The hatched area indicates a change of more than 90° in mean surface current direction between January and July. Duing (1970); The areas marked are for which the seasonal variations are studied.

interactions and feed back effects on a grand scale, between the ocean and atmosphere which have profound effects on the properties of the south-west monsoon circulation, are identified in the above chapters. The contrasts in the heat budget between the waters of the eastern and western parts of the ocean leading to the modification of the atmospheric circulation and the water masses are also suggested by the heat budget climatic models presented above.

A quantitative assessment of zonal differences in the heat budget is attempted based on climatic data here. The effect of the zonal differences of the components on the circulation pattern of the Arabian sea in a manner, which may effect the distribution of rainfall along the west coast of India and the repurcussions of the feed back mechanisms are discussed in detail.

Fig 2A gives the picture of monsoonal influence, taking surface current reversal as criterion (Düing, 1970). The influence of monsoon is found to prevail in the northern Indian Ocean north of 10°S. Six areas for detailed studies are fixed, which fall between 10°N and 10°S. (Fig 2B). Areas representing the western Arabian sea, eastern Arabian sea, Bay of Bengal and south China Sea, the south equatorial waters are studied. The monthly fluxes of energy exchange parameters, related parameters and their annual courses of variations are studied, to determine which variables

Table 8

Percentage frequences of Precipitation (U.S. Navy Marine Climatic Atlas of the World Vol.III Indian Ocean Revised 1976)

	Western Indian Ocean		Eastern Indian Ocean	
Months/Areas	(1)	(2)	(3)	(4)
January	03	03	11	08
February	01	01	07	05
March	01	02	07	03
April	01	02	09	03
May	03	08	13	07
June	02	17	08	10
July	00	15	08	10
August	00	10	10	09
September	02	10	12	10
October	05	13	18	13
November	07	07	15	12
December	04	04	14	12

Table.9

Latitudinal North Indian Ocean annual and seasonal means of heat budget components

N. Indian Ocean (1)	N. Indian Ocean (2)	N. Indian Ocean (3)	N. Indian Ocean (4)	N. Indian Ocean (1)	N. Indian Ocean (2)	N. Indian Ocean (3)	N. Indian Ocean (4)	N. Indian Ocean (1)	N. Indian Ocean (2)	N. Indian Ocean (3)	N. Indian Ocean (4)
Net Incoming radiation gm Cal cm^{-2} day^{-1}				**Effective back radiation** gm Cal cm^{-2} day^{-1}				**Net Radiation balance** gm Cal cm^{-2} day^{-1}			
418	413	361	348	111	113	102	91	307	300	258	254
490	454	420	431	105	104	94	93	385	351	326	339
469	387	366	380	94	84	77	87	374	303	289	293
459	403	348	372	102	96	90	91	357	307	277	282
459	414	379	382	103	99	91	90	356	315	288	292
Latent heat flux gm Cal cm^{-2} day^{-1}				**Sensible heat flux** gm Cal cm^{-2} day^{-1}				**Net heat balance** gm Cal cm^{-2} day^{-1}			
220	210	174	169	-02	01	06	-03	79	90	78	66
186	123	134	108	-01	02	03	01	228	227	189	230
262	164	232	161	-40	-03	-04	05	153	142	60	128
128	107	135	139	-09	01	05	06	239	199	117	136
194	151	174	144	-12	0.5	03	02	175	164	111	146

Regs	N. Indian Ocean (1)	(2)	E. Indian Ocean (3)	(4)	N. Indian Ocean (1)	(2)	E. Indian Ocean (3)	(4)	N. Indian Ocean (1)	(2)	E. Indian Ocean (3)	(4)
	Sea surface temperature °C				Air temperature °C				Dew point temperature °C			
	24.13	27.72	27.66	26.11	26.22	27.53	27.27	26.25	21.79	22.50	23.33	23.28
	28.26	28.96	28.86	28.36	28.08	28.71	28.54	28.25	23.94	23.86	24.75	24.64
	25.19	27.75	28.03	28.63	25.95	27.91	28.18	28.33	23.05	24.47	25.08	24.88
	26.18	27.73	27.94	28.09	26.41	27.56	27.52	27.66	23.12	23.87	23.88	24.48
	26.44	28.04	28.12	27.80	26.67	27.93	27.87	27.62	22.98	23.68	24.39	24.32
	Total cloud amount in tenths				Sea level pressure mb				Wind speed m/sec			
	0.43	0.40	0.54	0.58	1013	1011	1010	1011	6.79	3.54	5.42	7.37
	0.38	0.46	0.54	0.51	1011	1010	1019	1010	5.05	3.72	4.54	4.28
	0.40	0.60	0.65	0.61	1009	1009	1008	1008	12.49	6.21	8.36	5.45
	0.40	0.54	0.62	0.62	1011	1011	1010	1009	6.38	4.21	5.68	5.16
	0.40	0.50	0.59	0.58	1012	1010	1009	1009	7.68	4.42	6.35	5.57
	Drag coefficient 10^{-3}				Vapour pressure gradient between sea and air.				Temperature gradient between sea and air °C			
	0.13	0.09	0.12	0.14	7.10	9.20	7.66	4.58	-0.09	0.19	0.39	-0.14
	0.11	0.10	0.10	0.10	7.87	9.56	7.72	6.85	-0.18	0.28	0.32	0.12
	0.18	0.12	0.14	0.12	3.23	5.81	5.28	6.97	-0.76	-0.16	-0.14	0.30
	0.82	0.10	0.12	0.11	5.05	9.86	6.39	6.54	-0.23	0.17	0.42	0.43
	0.14	0.10	0.12	0.12	5.81	7.86	6.76	6.23	-0.23	0.11	0.34	0.36

TABLE 11.

Equatorial South Indian Ocean - Annual and Seasonal means of heat budget components.

Period/ Area	W.Indian Ocean (5)	E.Indian Ocean (6)	W.Indian Ocean (5)	E.Indian Ocean (6)	W.Indian Ocean (5)	E.Indian Ocean (6)
Parameters	Net incoming radiation		Effective back radiation		Net radiation balance	
	gm cal cm^{-2} day^{-1}		gm cal cm^{-2} day^{-1}		gm cal cm^{-2} day^{-1}	
Dec-Feb	425	398	103	109	322	289
Mar-May	448	392	104	95	344	298
June-Aug	373	351	99	102	274	256
Sep-Nov	456	381	102	97	353	283
Annual	426	380	102	101	323	282
Parameters	Latent heat flux		Sensible heat flux		Net heat balance	
	gm cal cm^{-2} day^{-1}		gm cal cm^{-2} day^{-1}		gm cal cm^{-2} day^{-1}	
Dec-Feb	131	151	05	02	186	136
Mar-May	110	100	02	01	232	197
June-Aug	161	141	02	04	111	111
Sep-Nov	94	128	01	04	259	151
Annual	126	130	02	03	197	169

Table.12

Equatorial South Indian Ocean-Annual and seasonal means of related climatic parameters

Periods/ areas	W.Indian Ocean (5)	E.Indian Ocean (6)	W.Indian Ocean (5)	E.Indian Ocean (6)	W.Indian Ocean (5)	E.Indian Ocean (6)
Parameters	Sea surface temperature °C		Air temperature °C		Dew point temperature °C	
Dec-Feb	27.76	28.19	27.36	27.95	23.59	21.68
Mar-May	28.75	28.72	28.47	28.62	24.01	23.97
June-Aug	26.22	28.21	26.12	27.81	22.97	22.99
Sep-Nov	27.08	27.71	26.96	27.34	23.50	23.15
Annual	27.45	28.21	27.22	27.93	23.52	22.95
Parameters	Total cloud amount in tenths		Sea level pressure mb		Wind speed m/sec	
Dec-Feb	0.51	0.58	1011	1010	4.54	3.74
Mar-May	0.42	0.57	1010	1009	3.54	3.37
June-Aug	0.55	0.60	1012	1010	6.51	4.08
Sep-Nov	0.46	0.63	1011	1010	4.22	4.24
Annual	0.48	0.60	1011	1010	4.70	3.86
Parameters	Drag coefficient 10^{-3}		Vapour pressure gradient between sea and air mb		Temperature gradient between sea and air °c	
Dec-Feb	0.11	0.10	7.43	11.51	0.40	0.24
Mar-May	0.09	0.09	8.84	8.82	0.28	0.10
June-Aug	0.13	0.10	5.33	9.41	0.10	0.40
Sep-Nov	0.10	0.10	6.17	8.08	0.12	0.37
Annual	0.11	0.10	6.94	9.45	0.23	0.28

cause a particular metmorological and oceanographical process to dominate the energy exchange picture.

In the earlier chapters the spatial annual and seasonal variations are studied. The zonal variations in the equatorial region of the long term means of the fundamental parametres like cloud amount, sea surface temperature and the sea level pressure values are noted, and their impact on the air-sea interaction system are discussed in the light of theories postulated by Saha (1970).

Seasonal and annual averages of heat budget components and the related variables of the six areas under concern are given in the tables (8-12). The Arabian sea areas (1 & 2) represent the Somali current region and the area near the south west coast of India respectively. Eastern Indian Ocean areas (3 & 4) represent South Bay of Bengal and South china sea respectively. Areas (5 & 6) of south equatorial waters represent the western and eastern south equatorial regions for comparison and studies of zonal differences. On the whole, there are three areas in the western, and three in the eastern region of the ocean.

The tables (8 - 12) give an appraisal of the zonal differences observed. Sea surface temperature increases towards

the east. During winter and summer transitions, the south China sea shows minimum values compared to East Arabian sea and Bay of Bengal. The Somali coast values are still lesser. Other seasons exhibit an increase of temperature towards the east. During the south-west monsoon season, the gradient is maximum due to the cool upwelled waters present along Somali coast. During winter transition the same conditions of sea surface temperature prevail. With the advent of winter, the temperature maximum is found in the eastern Arabian sea and the Bay of Bengal regions. The impact of winter is more prominent in the other two areas. The advection of cold dry continental air over the ocean, results in higher evaporative cooling in the western Arabian sea, due to very high speed winds observed here, inspite of the low temperature values. The annual values of fluxes of latent heat show a maximum in the Western Arabian sea and lesser value in the Eastern Arabian Sea. The eastern Indian Ocean values are also quite high. Bay of Bengal shows higher values than East Arabian sea and south China sea in the summer monsoon season. During winter, Bay of Bengal values are lesser than the East Arabian sea values. In the western Indian Ocean the air temperature is always greater than the sea surface temperature. Hence, the sensible heat flux is always directed towards sea, which makes the air stable, preventing convective processes. The pressure as a result is always greater, with a decreasing trend towards the east. Cloud amount shows increase towards east through out all seasons. The eastern Indian Ocean

values show no difference in the distribution of cloud amount, where as in the Arabian sea the eastern and western parts show different conditions which gives light to the convective activities in the western and eastern boundaries of the sea. Due to high cloudiness towards the east, the net incoming radiation shows a decrease towards the east. So is the effective back radiation, though an increase is expected of this component, due to warmer waters in the east. Net radiation again, shows a decrease towards east. The wind speed values show high values for Bay of Bengal and western Arabian sea, which conforms with the high evaporative cooling in these regions. The roughness as a consequence, is more in the western Arabian sea and Bay of Bengal. Eastern Arabian sea winds are lighter. South China sea has no summer monsoon maximum. Here the north east monsoon winds show more influence. But since the higher temperatures are observed in the summer monsoon season, the evaporation has two maxima. The Vapour pressure difference between sea and air is more in the eastern Arabian Sea. But the wind speed values are too low, to favour high evaporation. The temperature gradient between sea and air also is much less here. Hence the fluxes of sensible heat are less. During south-west monsoon the sea-air temperature values show negative values and hence downward flow of sensible heat. Same conditions are observed in Bay of Bengal also. The magnitude of air-sea temperature differences and wind speed values are high here. As a result of this, considerable sensible heat flux values

are noted. Hence on the whole, the western Arabian sea and Bay of Bengal give off more heat to the atmosphere.

The south equatorial Indian Ocean waters (Tables 10 & 11) show a similar contrast between the western and eastern parts of the equatorial south Indian Ocean, the sea surface temperature, total cloud amount are higher in the eastern side. The sea level pressure values are lower in the eastern side and are constant through out all seasons. This coincides with the quasi-permanent position of ITCZ (Saha, 1973). Unlike northern Indian Ocean, the dew point temperature decreases towards the east. In the eastern region, the cold air mass which invades the waters in winter, causes the dew point temperature to drop to a minimum. Hence, relatively high latent heat flux values are observed, though the wind speed values are not remarkably high. The south west monsoon impact is more on the western side. No wind speed maximum is observed for the eastern side region.

Table 8 which gives the percentage frequency distribution of precipitation of the four areas of the north equatorial Indian Ocean waters is given, for a clear understanding of the zonal distribution of precipitation over the north equatorial Indian Ocean and their seasonal march.

Seasonal march

The annual variation of the major heat budget components

Area-1
Area-2
Area-3
Area-4
Rn
Qe
Qh
Qst
Heat exchange gm cal cm⁻² day⁻¹
Temperature °C
Total cloud amount in tenths
Wind speed m/sec.
W
C
Ts , Ta , Td
D J F M A M J J A S O N D

Fig.25. Annual cycles of fluxes and variables in different locations in the northern Indian Ocean lying in the same latitude range.

and the related parameters is in Fig 25 displayed for the representative sea areas of the north equatorial Indian ocean, identifi in Fig.28.

Somali current region

This cold current, which is a strong north eastward flow parallel to the coast of eastern Africa, is of variable nature. The Somali Current is considerably stronger during summer monsoon than during winter months. In autumn, in response to the return of north-easterly winds over the northern Indian Ocean, the current reverses and thenceforth flow south westward. Between July and September surface flows of more than 3.5 m/sec have been observed off the Horn of Africa, south of Socotra and during this period, surface speeds exceeding 20 m/sec seem to be usual from near the equator to beyond Socotra (Swallow and Bruce 1966). In the western Arabian sea situations are made unique by the enormous upwelling caused by the north eastward flow parallel to the coast which maintains a cold ocean surface in the western Indian Ocean especially in the western Arabian sea west of about 65°E. The realm of cold surface is characterised by reduced cloud cover and increased net radiation. Downward flow of sensible heat, reduces rates of evaporative surface cooling than that is expected for a near-surface flow of very great speed during south west monsoons. Findlater (1969a) has reported wind speed maximum, reaching up to the range of 25.45 m Sec^{-1} from this region. It is

not clearly understood whether the Somali Current is caused by the effects of local winds (Leetma, 1972) or in response to the winds over the Indian ocean (Lighthill, 1969). However, temperatures as low as 16°C are reported (Stommel and Webster, 1963). An analysis of the wind speed over the Arabian sea, using Monex (1973) data, Jambunathan and Ramamurthy (1976) have also observed high wind speeds.

The variation of heat balance shows two equal maxima in April and October (about 300 gm cal cm^{-2} day^{-1}). Accordingly values of radiative heat balance reach maximum in the same months. Through out all seasons the net radiative heat balance values are of considerable magnitude. It shows a small decrease in winter. Rates of evaporation are larger in winter because dry north-easterly winds are present and they are large during summer monsoon months, on account of the strength of the south westerly monsoon winds. Latent heat flux is the key component in the variations of the heat-budget values. Sensible heat is considerably low. It shows strong negative values through out the monsoon season. Summer monsoon period, on account of strong upwelling shows minimum values of temperature (sea, air and dew point). The effective back radiation is reduced due to the low sea surface temperature, though the atmosphere is almost cloud free. Though the sea surface temperature is much lower than winter values, the evaporational cooling is much high due to the high speed winds

observed here. An annual mean value of heat balance of 175 gm cal cm^{-2} day^{-1} is observed.

The Eastern Arabian Sea

The eastern Arabian Sea shows a peak of heat balance in the summer transition month of March and a minimum during winter. By June the sea surface temperature and the air temperature start showing a decrease due to upwelling, which reach maximum during southwest monsoon. The minimum values, however is maintained till February. During winter and summer transitions the differences, in vapour pressure between sea and air is more, due to fall in dew point temperature. The highest value of evaporation is observed in June. Though the vapour pressure gradient is not conducive for evaporation, the wind speed soars up to the highest seasonal value and hence high evaporation. The net radiation does not show much variations. It exhibits a minimum during southwest monsoon, due to the heavy cloud coverage near the southwest coast of India. The air temperature shows greater values than sea surface temperature during July, August and almost equal in September. The negative gradient of temperature causes downward fluxes of sensible heat. The sea surface temperature is not as low as the Somali coast value. The period of upwelling as well as the intensity is less here. This is an extension of upwelling of the southwest coast of India, since the incursion of cool

upwelled waters of Somali coast, is observed to be restricted upto 70°E (Saha 1978). Though the wind speed maximum observed is lower, evaporation is found to be greater, since the warmer seas favour evaporation though the sea surface temperature values are lesser than the winter values. Winter peak of evaporation is not prominent. An annual residual heat export of 164 gm cal cm^{-2} day^{-1} is observed.

Bay of Bengal

The trend of seasonal variation of the heat balance is almost the same as that of eastern Arabian sea. The pattern of variation of net radiation also follow that of eastern Arabian sea. But the magnitude shows lesser values, due to more cloudiness which is attributed to higher temperature observed. The values of sea surface temperature are lesser than the air temperature. The sea surface is warmer than the western parts. The cooling could be mainly due to evaporation, besides upwelling. The south west monsoon peak is greater than the winter monsoon peak. Though the drop in dew point temperature with respect to sea surface temperatu is favourable, the sea is cooler and the wind speed values are lesser for a higher peak. Annual mean value of the residual heat export is much less compared to that observed in Arabian Sea (111 gm cal/cm^2/day).

South China sea

The Indonesian region of the south China sea lies in the same latitudinal band. This region has a pronounced bimodal distribution of net monthly heat divergence values. The summer transition peak is more prominent than the winter transition peak. They are separated by a minimum during summer monsoon. Though the wind speed values do not favour evaporation, the temperatures are reasonably high and the evaporation is considerable. Winter values also are quite high due to high speed winds observed. The summer transition values are much higher due to higher net radiation balance, which is an outcome of lesser cloudiness during this period, compared to other months. The heat gain is observed in this region during the transition periods. The annual heat balance value is 146 gm cal cm^{-2} day^{-1}.

Large residual is left for heat export and for storage within the oceanic water body in all regions, with largest values in the summer transition period, due to large values of net radiational balance and smallest seasonal values of latent heat flux. Zonal differences in net heat balance is observed for the eastern and western parts of Indian Ocean, both north and south sides of equatorial waters. The eastern side shows lesser heat balance.

The heat budget is basic to the climatic asymmetry between the western and eastern portions of the low-latitude oceans. In contrast to their relative constancy near the equator, energy fluxes associated with the monsoonal climate of the Arabian Sea and Bay of Bengal vary markedly during the year. To quote Budyko (1956) who studied annual march of energy-budget components of Arabian Sea, great quantities of heat are transmitted from the ocean surface to deeper layers and eventually transported in horizontal directions into other areas of the World's Ocean. The energy-budget of Arabian Sea, has also been investigated thoroughly by Colon (1964). He has suggested that energy exchanges between the Arabian Sea and the monsoon air have considerable influence on the monsoon flow Sumner (1965) has found greater heat accumulation in the western Arabian sea than eastern part and attributed this to greater intake from the western part due to cooler and drier air prevailing. Generally, non-adiabatic heating or cooling of the atmosphere through the air-sea exchanges will affect the temperature, pressure, humidity and the vertical stability of the lower atmosphere. The equation of continuity for water vapour demands that flux divergence should balance the difference between the rates of evaporation and precipitation in any volume of air. The excess of evaporation over precipitation discussed in the previous chapter, pin points western Arabian sea and the subtropical areas of southern hemisphere as major source areas. The precipitation frequency distribution (Fig 22)

presented in chapter 4, reveals that high precipitation occurs along the south west coast of India and the North Bay of Bengal and the west coast of Malaya. The spatial distribution of fluxes of latent heat for the south-west-monsoon months presented in the previous chapter shows marked difference in the equatorial trade wind zone. The distribution of cloud amount agree well with that of precipitation.

Bunker (1965) traced a low level jet off somalia and thence across the central parts of the Arabian Sea to the coast of India, decreasing in speed progressively to east. A maximum speed of about 50 kt is attained at the top of a 1000 metre thick layer of air, cooled by contact with cold upwelling water which may have as low a temperature as 14°C. The jet is a result of the strong pressure gradient at right angle to the somalia coast between the air over the heated land and cold off-shore waters. The upwelling and very low sea surface temperatures are due to the strong wind transporting large quantities of surface water eastwards. According to Ramage (1965) this summer regime over the Arabian sea is a strange one whose character seems basically determined by the heat low developed over the vast desert area extending from northeast Africa to northwest India and by coast-line orientation and the effect of the Arabian and somali troughs, is to elongate the circulation toward the southwest. The heat low is maintained and protected by its offspring-upwelling along

the west coast and subtropical cyclones in the northeast. The net result is the most intense monsoon system on earth gale force southwesterlies overlain by jet strength easterlies. The jet crossing equator pointed out by Findlater (1969, 1974). Dunbar's jet off somalia and the low level jet over the peninsula brought out by Joseph and Raman (1966) may all be different segments of the same feature. As the colder air is warmed during its further passage over the Arabian sea, the horizontal temperature gradient decreases and the jet's maximum value decreases progressively to east, dropping to less than 30 kt near India. According to Dunbar, in the west half of the Arabian sea, the jet winds are accelerating and there appears to be widespread subsidence. In the eastern half the jet is decreasing in magnitude and there is small mean convergence which accounts for the difference in weather between the two parts, caused by the lifting of the conditionally unstable air. Since the air mass is conditionally unstable, shower activity is initiated east of 60°E. This shower activity carries water vapour to greater heights in the atmosphere and produces the many layers of clouds that are characteristic of the monsoon sky.

The feed back mechanisms of the air-sea interaction in this region also are noted. The negative heat fluxes over the western Indian Ocean exerts a stabilising influence on the lower troposphere and the air originally lifted in Asian monsoon cloud systems subsides in the middle and upper troposphere over south-

west Asia (Ramage, 1966; Walker, 1975). The low level subsidence inversion, prevents the air mass from ascending sufficiently far for condensation to take place. The distribution of the base of inversion over the Arabian sea during summer monsoon as reported in the literature by Ramage (1966) and Colon (1964) show that the inversion is quite low over the western Arabian sea and rises towards the coast of India, but it is not present near the coast itself. This causes scanty cloud distribution in the western side and enormous amount of convective clouds in the eastern side. The areas of condensation and precipitation experience atmospheric heating due to the release of latent heat of condensation. Cooling of the atmosphere in areas of high evaporation and downward sensible heat flux leads to raising of pressure and continued non-adiabatic heating of the atmosphere in areas of condensation and upward sensible heat flux leads to lowering of pressure, creates an eastward pressure gradient in the equatorial region.

Thus the zonal anomalies of climatic parameters and the energy budget components present a complex picture of air-sea interactions and their feed backs, which is a viscious circle of interactions, influencing one another.

From the above discussions it is seen that the strong upwelling of the Somali coast plays a very important role in the monsoon circulation. The interactions of the cold sea surface

of the western Arabian sea and the atmosphere above, not only accounts for the clear cut differences in the climatic conditions over the two parts of the North Indian Ocean, but also has great significance in the context of the monsoon circulation and rainfall over India.

Chapter 6

Year-to-year changes of the heat balance in the Northern Indian Ocean

Problems of long-term changes of the heat balance in the Indian Ocean have hardly been investigated. Some attempts of such an investigation (decade to-decade changes) were made by Jagannathan and Ramasastry (1964). But only evaporation among the heat balance components was investigated. Here emphasis was given to the changes in sea-surface temperature and the superincumbent air over the Arabian Sea and Bay of Bengal from decade to decade. Marked variations are observed for evaporation and the related climatic elements like sea surface temperature, air-temperature, sea level pressure and relative humidity values. Like the spatial variations as observed by previous studies, temporal variations of the seasonal and annual heat balance components also could be observed in the same manner, as the temperature and other climatic variables change in time and in space.

Investigations of the inter-annual changes of the heat balance and its components are attempted. The heat balance of the sea surface for each location understudy for each year is computed using the formulae employed for making climatic models, and then averaged for the entire period of study from 1948 through

1972. The annual and long term course of the heat balance graphs were constructed based on the results. The monthly variations of each component understudy, for heat balance were depicted in graphs separately for the period 1948-59 and 1960-72. No Ocean weather station data are available from Indian Ocean, which could be safely applied for the calculation of the heat balance for individual years. The raw data compiled for specified areas (Fig.2) without regard to the suspected biases or inconsistancies, is made use of in the studies here. The processing procedure of this data which forms a part of the tape file TDF 11 which was made available by National climatic centre, Carolina NOAA is given in detail in the chapter 2. The monthly averages of each related climatic parameter for the years 1948 through 1972 for each area under study were found. These averages are made use of in the yearly variations computations.

It should be noted that neither all years nor all regions of the ocean are covered equally (Table.13). Greatest number of observations were collected in the regions 1, 2, 4 and 5 fewer observations were found in the region 3 and very few in the region 6. In addition to this, the most reliable data were obtained for the years (1951-56) and (1965-67) and less dependable for the years (1960-72). The number of observations for each year and for each area used for the computation of heat balance components is given in the Table.13, inorder to indicate the

Table. 13

Square	1	2	3	4	5	6
Coordinates 0°	10-12N 55-60E	16-19N 63-68E	12-15N 84-87E	07-10N 70-75E	2-7N 87-90E	1°S - 3°N 79-82°E
1948	0684	0180	0168	1008	0336	048
1949	1128	0204	0168	1272	0780	084
1950	0780	0144	0144	1164	0768	108
1951	1152	0228	0144	1284	0828	084
1952	1200	0264	0132	0912	0624	084
1953	1296	0276	0204	1500	1092	084
1954	1272	0300	0120	1368	1020	132
1955	1200	0228	0084	0828	0636	072
1956	0144	0144	0036	0168	0348	024
1957	0168	0240	0072	0240	0516	024
1958	0180	0396	0060	0252	0804	024
1959	0156	0396	0036	0240	0780	048
1960	0180	0324	0036	0120	0684	048
1961	0180	0228	0048	0168	0384	036
1962	0132	0180	0036	0192	0264	072
1963	0108	0240	0048	0192	0300	048
1964	0828	0336	0120	0840	0732	060
1965	1584	0828	0469	1908	1692	192
1966	2268	0876	0564	2544	2304	216
1967	1392	0792	0468	1380	1728	252
1968	0228	0300	0120	0204	0420	096
1969	0120	0240	0120	0072	0348	048
1970	0072	0096	0048	0060	0132	024
1971	0048	0108	0060	0084	0168	024
1972	0048	0168	0036	0072	6264	012
Total for 25 years	16,476	7,896	3,540	18,072	18,012	1,944

degree of reliance that could be assigned to conclusions drawn. Wind speed observations were the most frequent and observations of air temperature were almost as numerous. Sea surface temperature and cloud amount observations were less than the above two parameters. Observations of pressure were few, and observations of dew point temperature were much fewer.

The hourly distribution of the observations were very uneven, a number of hours in the different years having no observations to their credit. As such the classification according to time of the day had to be given up and the observations had to be grouped without regard to time.

Characteristic features of the hydrometeorological regimes of the regions for which inter-annual variations of heat balance components are made

In order to evaluate more objectively characteristic features in the distribution and the cause of the variability of the heat balance and its components in individual years in the northern Indian Ocean, it is necessary to consider the characteristic features of the hydrometeorological regimes of the areas in which detailed analysis is done (Fig. 2 and Table 13). Area number one is situated in the western Arabian Sea which is situated near the Somali Current region. Seasonal variations

of the circulation is observed maximum in this region. The characteristic features of this area is given again and again in this work.

Area 1 is located in the west-central portion of the sea along the strongest part of the south-west Monsoon Current, but away from the centre of upwelling. Despite of low temperatures observed during south west monsoon, strong winds cause very high evaporation. Water motions forced by the wind-stress which lead to advection of cold waters, increase in heat flux from sea surface to the atmosphere and increased net radiation input due to lack of clouds contributes to early, summer cooling. The range of annual variation of sea surface temperature reaches almost 5°C. Wind speed values more than 15m Sec^{-1} is observed in this region. During south-west monsoon months the combination of moist south-west current in the surface layers and a dry warm air mass above flows eastward from Africa and Arabia produces a characteristic thermal inversion which prevents the formation of convective clouds and hence precipitation. Surface wind vergence charts gives divergent area around this location. (Hantel, 1971). It has been pointed out that (Flohn, 1968). this region is characterised by large-scale subsidence and minimum precipitation and is identical with the lowest position of the inversion base level. In particular, it is related to Findlater's (1970) low-level jet over the western

Indian Ocean in the northern hemisphere summer. During winter the Asia high pressure system pump cold dry continental air over the warm waters of western Arabian Sea.

Considerable difference is noted between areas 1 and 2. This could be attributed to the seasonal distribution of cloud and sea surface temperature. During the summer monsoon there is an increase in cloud amount from 1 to 2. The average annual range for the period under investigations is 3.4 for the area 01 and 6.5 for area 02. The sea surface temperature annual range is 4.88 in area 1 and 4.38 in area 2.

The minimum temperature due to the south west monsoon season is observed in August in area 1 and in September in area 2. Due to heavy cloud activity during south west monsoon the net radiation input is less. The annual pressure range is 8.98 and 12.72 in area 1 and 2 respectively. Area 4 is situated in the down stream of the monsoon current which reaches the southwest coast of India. The monsoon air suffers considerable modification. Increased cloudiness and precipitation is observed. Pick up of sensible heat and moisture from the sea surface enhances the convective processes downstream. The tendency for lifting of the airmass and weakening or absence of inversion favours the possibilities of convective cloudiness and precipitati

Another feature to be considered in the East Arabian Sea is the orographic effects caused by Western Ghats. The coastal upwelling has its influence on the sea surface temperature, though the intensity is much less. The annual range of sea surface temperature is 2.5°C. The wind speed values are much less, compared to western Indian Ocean. Sea level pressure annual variation range is 4.27 mb for the period of study. Arabian Sea is under the influence of anticyclonic flow during the northern hemisphere summer. This vanishes with the advent of winter transition. Cyclonic activities are more during post monsoon and premonsoon seasons. During winter and south west monsoon season, cyclogenesis is almost absent. Heavy rainfall is observed near the south west coast of India during south west monsoon.

The Bay of Bengal areas (3 & 5) are much cloudier and warmer. Evaporational cooling is much higher. Variations of atmospheric and oceanic circulation is felt here too. The impact of north east monsoon is much pronounced. Wind speed in this region is higher than that of Eastern Arabian Sea. The annual range of cloud cover in the southern Bay of Bengal is 2.76 oktas and that of sea surface temperature and air pressure are 2.16°C and 1.7 mb respectively. The central Bay of Bengal area (3) has annual cloud cover range of 1.74 oktas and that of sea level pressure and sea surface temperature are 10.86°C

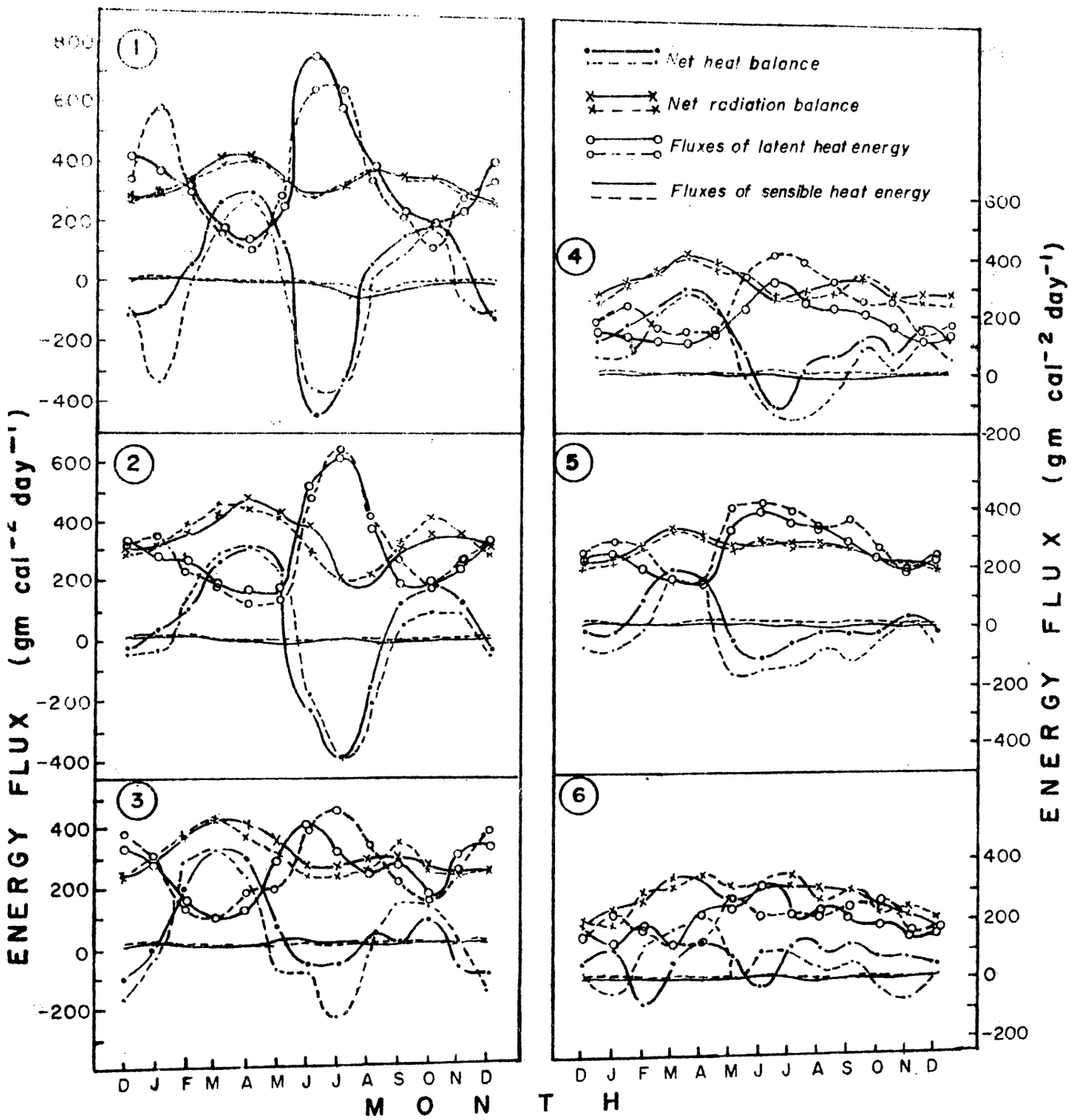
Net heat balance
Net radiation balance
Fluxes of latent heat energy
Fluxes of sensible heat energy
ENERGY FLUX (gm cal⁻² day⁻¹)
ENERGY FLUX (gm cal⁻² day⁻¹)
MONTH
D J F M A M J J A S O N D
1
2
3
4
5
6

Fig.26. Seasonal march of heat balance and its components for different areas in the northern Indian Ocean.

area 1 10–15°N 55–60°E

area 2 16–19°N 63–68°E

area 3 12–15°N 84–87°E

area 4 07–10°N 70–75°E

area 5 02–07°N 87–90°E

area 6 1°S–3°N 79–82°E

and 3.85 mb respectively. The influence of cyclones is much more in this area except during winter months. The equatorial area (no.6) is characterised by high annual pressure with less annual variations. The weak high pressure through out south-west monsoon is observed near this area (Varpeleigh, 1968). According to him the areas (1-5) are categorised as monsoon type, characterised by a secondary minimum in summer. The area no.6 is classified under maritime equatorial type, characterised by a maximum sea surface temperature in April and little variation during the rest of the year. This is reflected in the annual variations of sea surface parameters. The annual ranges of sea surface temperature, sealevel pressure and cloud amount are 2.8°C, 2.71 mb and 3.5 octas respectively.

Seasonal march of heat balance components

The seasonal march of heat balance components for the six areas are depicted in Fig.26. The heat balance components for the years 1948-59 and for 1960-72 are shown separately. The curves joined by full lines represent the former period, where as the curves joined by dotted lines are for the latter period. The curves show marked variations, though the trend is almost the same. The latter period shows more heat loss. The evaporational cooling is more during the same period. This pinpoints changes in climatic features. A pronounced maximum of evaporation is observed during the same season invariably

in all areas of Arabian Sea, the maximum values being observed in Western Arabian Sea. During individual years, the values reach staggering dimensions.

The west Arabian Sea area (area 01) shows heat losses to the sea during south west monsoon and northeast monsoon seasons. During transitions heat gain is observed. The net radiative heat balance does not show much of a variation except for a small maximum during summer transition. The radiation values are high throughout on account of less cloudiness. A pronounced maximum of latent heat exchange is observed in June; Though the values of sea surface temperatures are low, since the core of highest wind speed is observed in this area, the evaporation is much enormous. ($\gtrsim$ 700 gm cal/cm^2/day). As the summer monsoon progresses and the advected water from the region of Somalia reaches and minimum value is reached for the sea surface temperature in July and August Evaporation values show decreasing trend. The maximum heat gain is observed in April. This coincides with the summer maximum of radiative heat input. Due to the prevailing light winds the evaporation is at its minimum. During south-west monsoon season till December, since sea surface temperature is much less than that of air temperature the atmosphe loses heat to sea. Area no 2 which lies in the down stream of monsoon current, shows highest heat loss in July. The movement of cold water as shown by Saha (1970)[a] indicates that it reaches

Table.14

Heat balance components 1948-72 (K cal/cm²/Year)

Areas					
1	2	3*	4	5	6*
Net Radiation					
Long term averages					
125	127	116	114	95	107
Maximum by years					
137 (1971)	135 (1950)	125 (1972)	128 (1971)	105 (1948)	135 (1972)
Minimum by years					
116 (1970)	119 (1948)	86 (1959)	103 (1961)	88 (1970)	83 (1948)
Total heat exchange					
Long term averages					
126	111	100	81	90	65
Maximum by years					
176 (1971)	143 (1971)	147 (1970)	149 (1971)	106 (1951)	88 (1966)
Minimum by years					
92 (1958)	96 (1957)	103 (1971)	58 (1951)	76 (1968)	70 (1967)
Net heat balance					
Long term averages					
-02	14	-07	33	19	31
Maximum by years					
36 (1958)	31 (1957)	22 (1948)	58 (1948)	32 (1968)	36 (1967)
Minimum by years					
-62 (1970)	-14 (1971)	-54 (1970)	-37 (1971)	-40 (1951)	25 (1966)

*Total heat exchange and hence heat balance data available for areas 3 is only for years (1948, 1949, 1951, 1952, 1953, 1954 and 1964-69) and for areas 06 only for years (1965-67) respectively.

70°E longitude only by August. Hence till July it is not too low to inhibit evaporation. Due to heavy convective action of clouds, the values of radiative heat energy shows a pronounced downfall. Areas no.4 and 5 (of E.Arabian Sea and Bay of Bengal) also exhibit the above mentioned feature. The heat loss is not much pronounced as that of western Arabian Sea. The peak of highest evaporation in the area 4 is observed in June. Bay of Bengal shows longer duration of heat loss extending from south-west monsoon season to winter transition. Northern part of Bay of Bengal shows high heat gain during summer transition. The autumn peak is of lesser magnitude. This season is marked by cyclonic activity which causes much heat loss. The impact of north east monsoon is more in Bay of Bengal. The winter months experience heat loss. The variations in the equatorial region is not systematic and again the magnitude of radiative heat input (due to heavy cloud cover) and latent heat flux (due to light winds) are less, though sea surface temperature favours heat exchange).

<u>Heat balance of the sea surface and its components and its long-term variations.</u>

The long term annual averages of heat balance and its components (Q_{net} and $Q_a = Q_e + Q_h$) are presented in the Table 14. The deviations (maximum and minimum) by year are also given.

Heat radiation Fund

The mean annual net radiation is maximum in the western Arabian Sea areas and minimum in Bay of Bengal and equatorial area. This in general is governed by the annual average cloud cover. All areas show maximum in March and April. But since western Arabian Sea shows less clouds during monsoons, the amount of radiative heat input is much high, throughout. Since Bay of Bengal area shows maximum cloudiness during monsoons the radiative heat input is much less, which is reflected in the annual averages. Early 70Se show maximum radiation values. This is observed only for areas nearer to equator. Maximum variations are found in Bay of Bengal and equatorial area. Equatorial areas are always marked by heavy cloudiness. During, most of the seasons, ITCZ is located here.

Total heat exchange shows maximum values in the western Arabian Sea. Minimum evaporation is observed in eastern Arabian Sea and equatorial waters. Maximum variations are found in western and eastern Arabian Seas. Maximum heat exchange is found in 70-71 in Arabian Sea and Bay of Bengal. Maximum variations are found in western Arabian Sea (+50 to -36 k cal/ cm^2/year) and eastern Arabian Sea (+68 to -23 k cal/cm^2/year). Maximum heat loss is observed in Bay of Bengal, due to low incoming radiation energy and high evaporation. Western Arabian Sea also show net annual heat loss. Considerable heat gain is

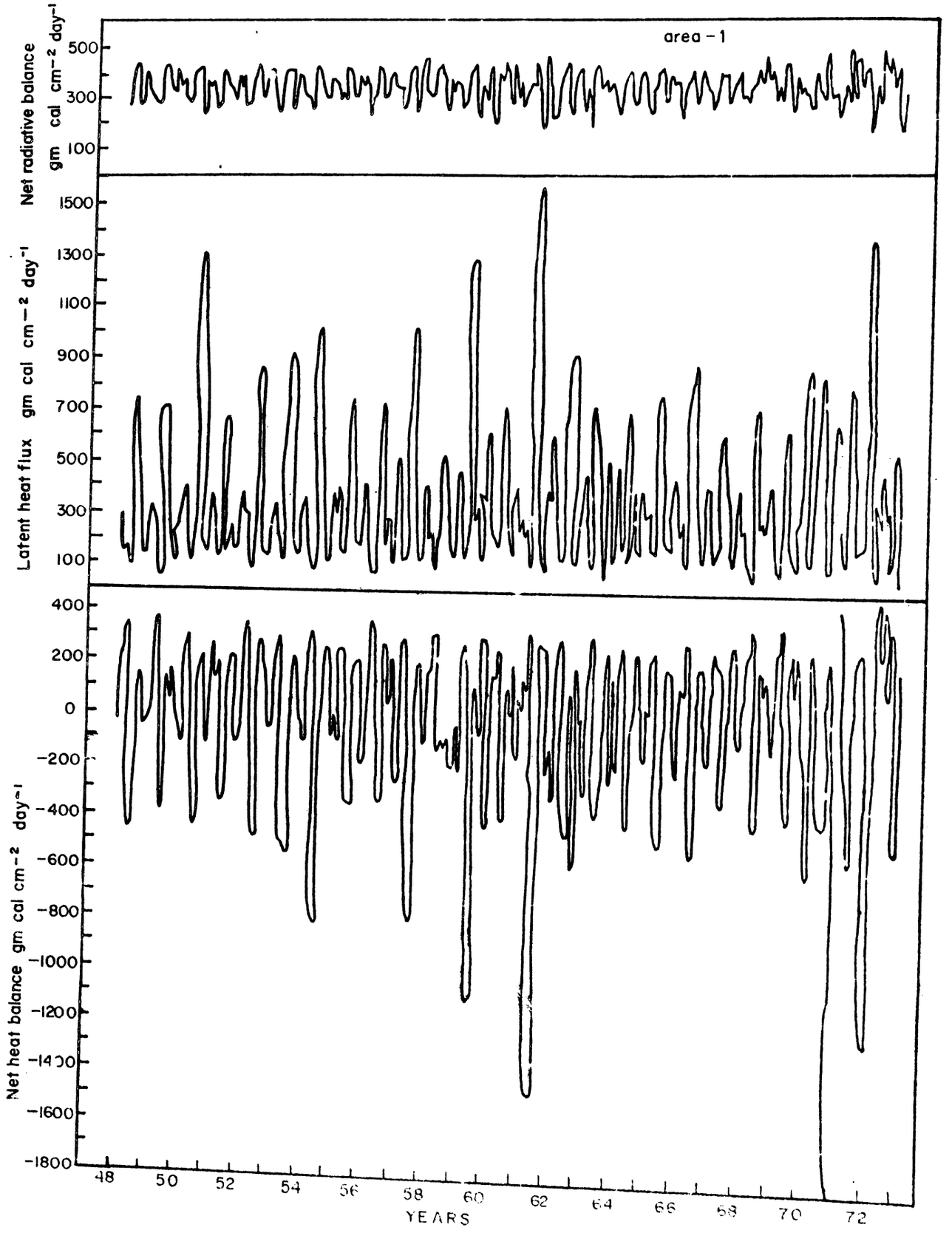
area – 1
Net radiative balance gm cal cm⁻² day⁻¹
500
300
100
Latent heat flux gm cal cm⁻² day⁻¹
1500
1300
1100
900
700
500
300
100
Net heat balance gm cal cm⁻² day⁻¹
400
200
0
-200
-400
-600
-800
-1000
-1200
-1400
-1600
-1800
48
50
52
54
56
58
60
62
64
66
68
70
72
YEARS

Fig.27. Long term variations of the heat balance and its components for area 01 (Western Arabian Sea).

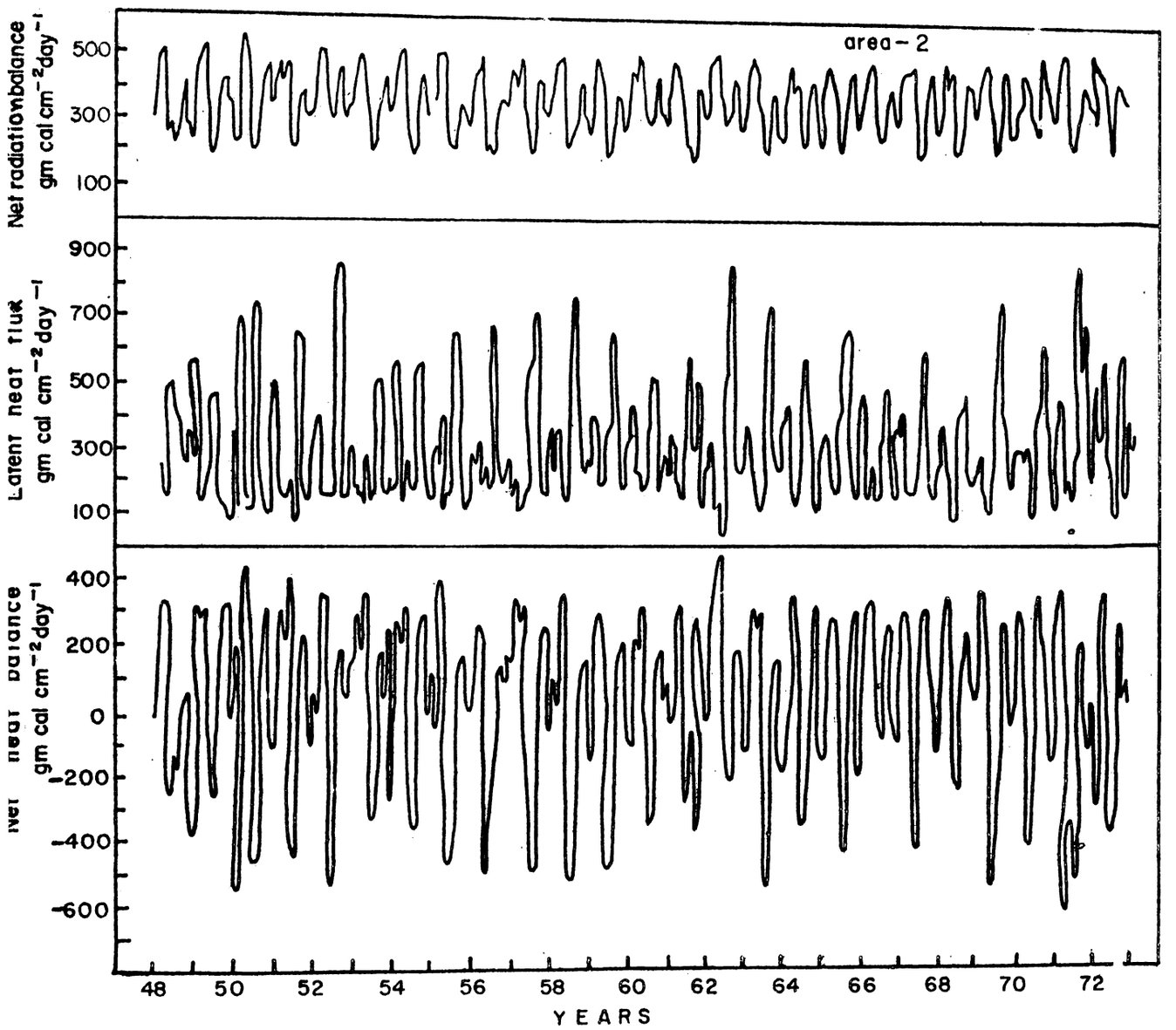
area – 2
Net radiation balance
gm cal cm⁻² day⁻¹
500
300
100
Latent heat flux
gm cal cm⁻² day⁻¹
900
700
500
300
100
Net heat balance
gm cal cm⁻² day⁻¹
400
200
0
-200
-400
-600
48
50
52
54
56
58
60
62
64
66
68
70
72
YEARS

Fig.3B. Long term variations of the heat balance and its components for area 02 (Central Arabian Sea).

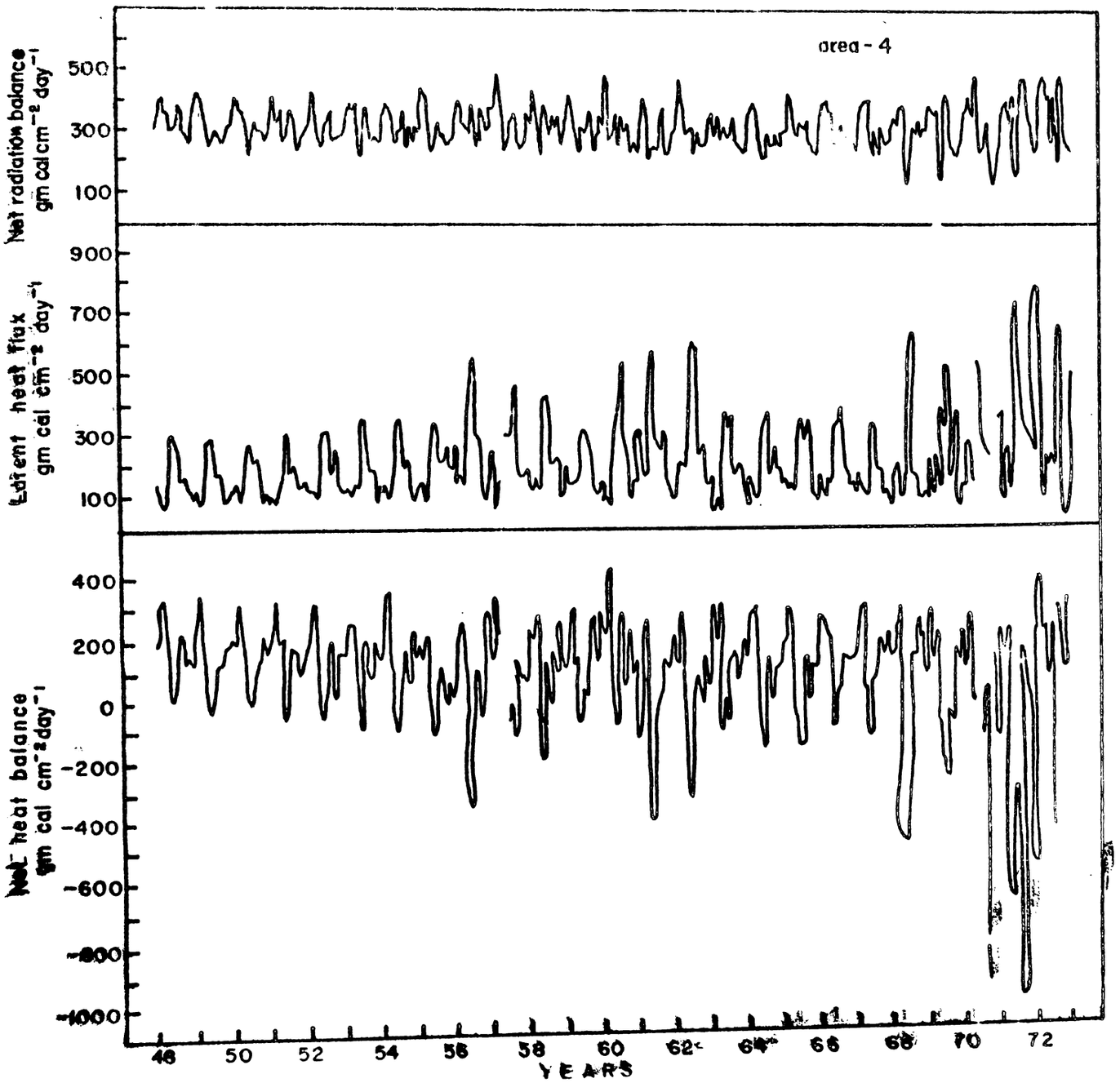
area - 4
Net radiation balance
gm cal cm⁻² day⁻¹
500
300
100
Latent heat flux
gm cal cm⁻² day⁻¹
900
700
500
300
100
Net heat balance
gm cal cm⁻² day⁻¹
400
200
0
-200
-400
-600
-800
-1000
46
50
52
54
56
58
60
62
64
66
68
70
72
YEARS

Fig.29 Long term variations of the heat balance and its components for area 06 (Eastern Arabian Sea).

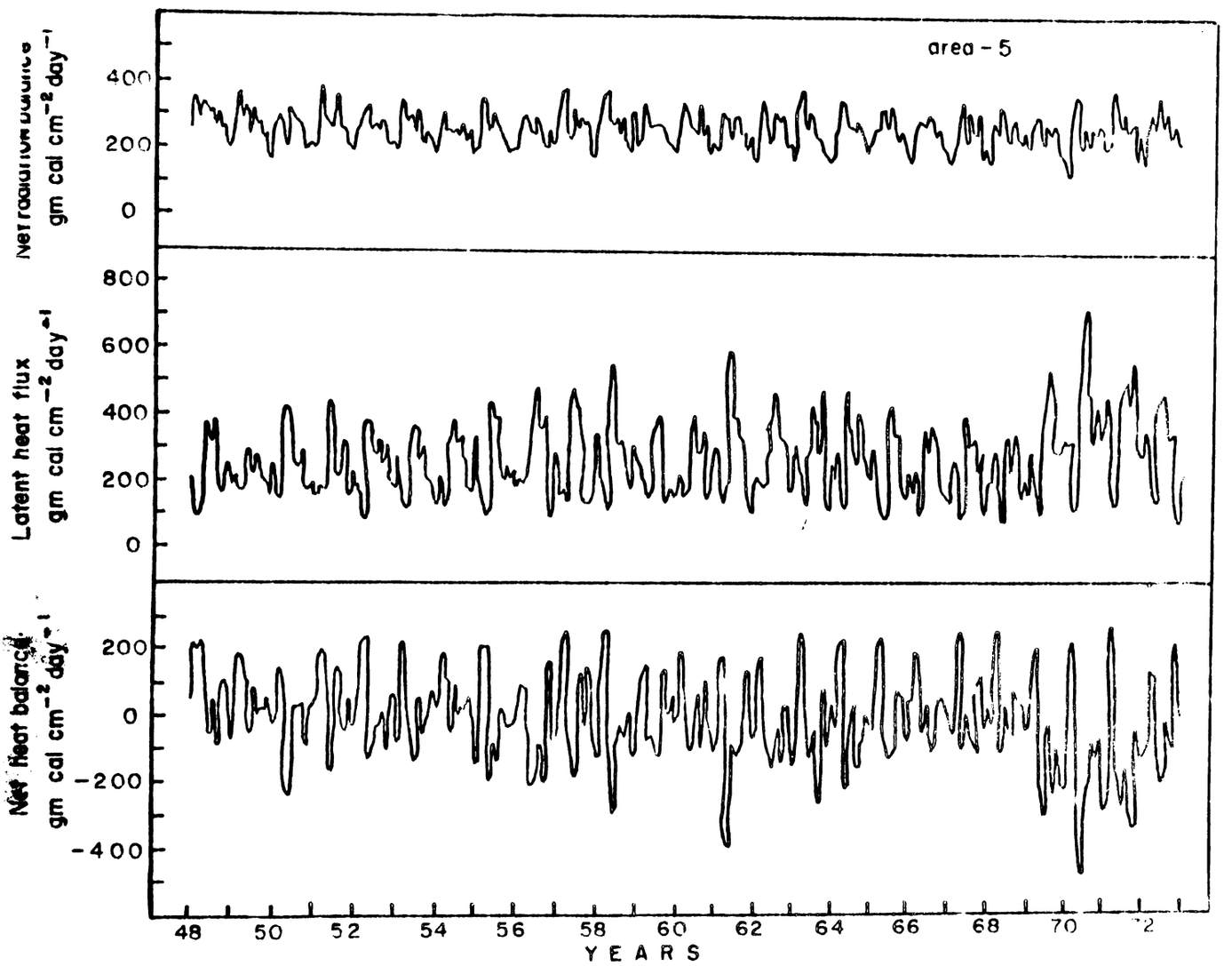
area - 5
Net radiation balance
gm cal cm⁻² day⁻¹
400
200
0
Latent heat flux
gm cal cm⁻² day⁻¹
800
600
400
200
0
Net heat balance
gm cal cm⁻² day⁻¹
200
0
-200
-400
48
50
52
54
56
58
60
62
64
66
68
70
72
YEARS

Fig.30 Long term variations of the heat balance and its components for area 06 (Bay of Bengal).

observed in eastern Arabian Sea. Much variations are observed throughout all stations, except the equatorial region. Maximum heat loss is observed during 1970-71.

Graphs depicting annual course of heat balance components and heat balance is presented (Figs.27-30). The annual course of the heat balance is disrupted during individual years and months chiefly as a result of a sharp increase or decrease of evaporatio especially in those regions where evaporation is high in general. Time series graphs of related climatic parameters are also presented. (Figs.31-33) for the appraisal of the trend of the climati variables with respect to heat balance components. The areas (01, 04 and 05) show great variations of heat balance values and the latent heat exchange values. Variations are stable throughout in the central Arabian Sea (02). Variations are enormous in the western Arabian Sea. It is all the more greater, during the last part of period under investigation. The impact is seen more in eastern Arabian Sea than Bay of Bengal. Radiativ heat values also exhibit variations though in lesser magnitudes. Similar variations are found in related climatic parameters (sea surface temperature, cloud amount and sea level pressure). From 1952 onward till 1964 the variations are stable. A sudden drop in temperature in 1969 and its repercussions are noted.

The long-term variations of the heat balance for the four

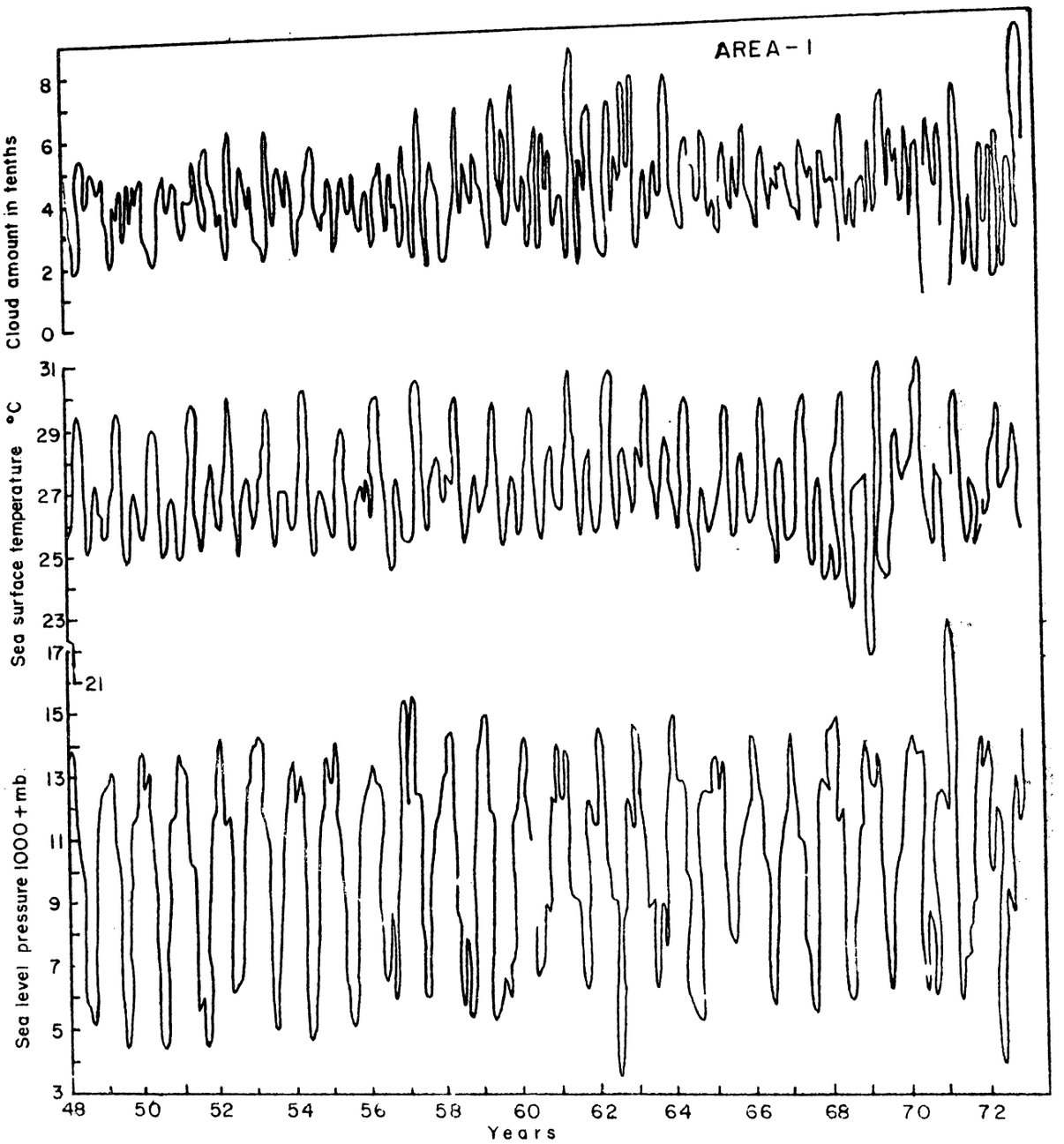
AREA - I
Cloud amount in tenths
0
2
4
6
8
Sea surface temperature °C
23
25
27
29
31
Sea level pressure 1000 + mb
3
5
7
9
11
13
15
17
21
48
50
52
54
56
58
60
62
64
66
68
70
72
Years

Fig.31. Long term variations of cloud amount, sea surface temperature and sea level pressure for area 01 (Western Arabian Sea).

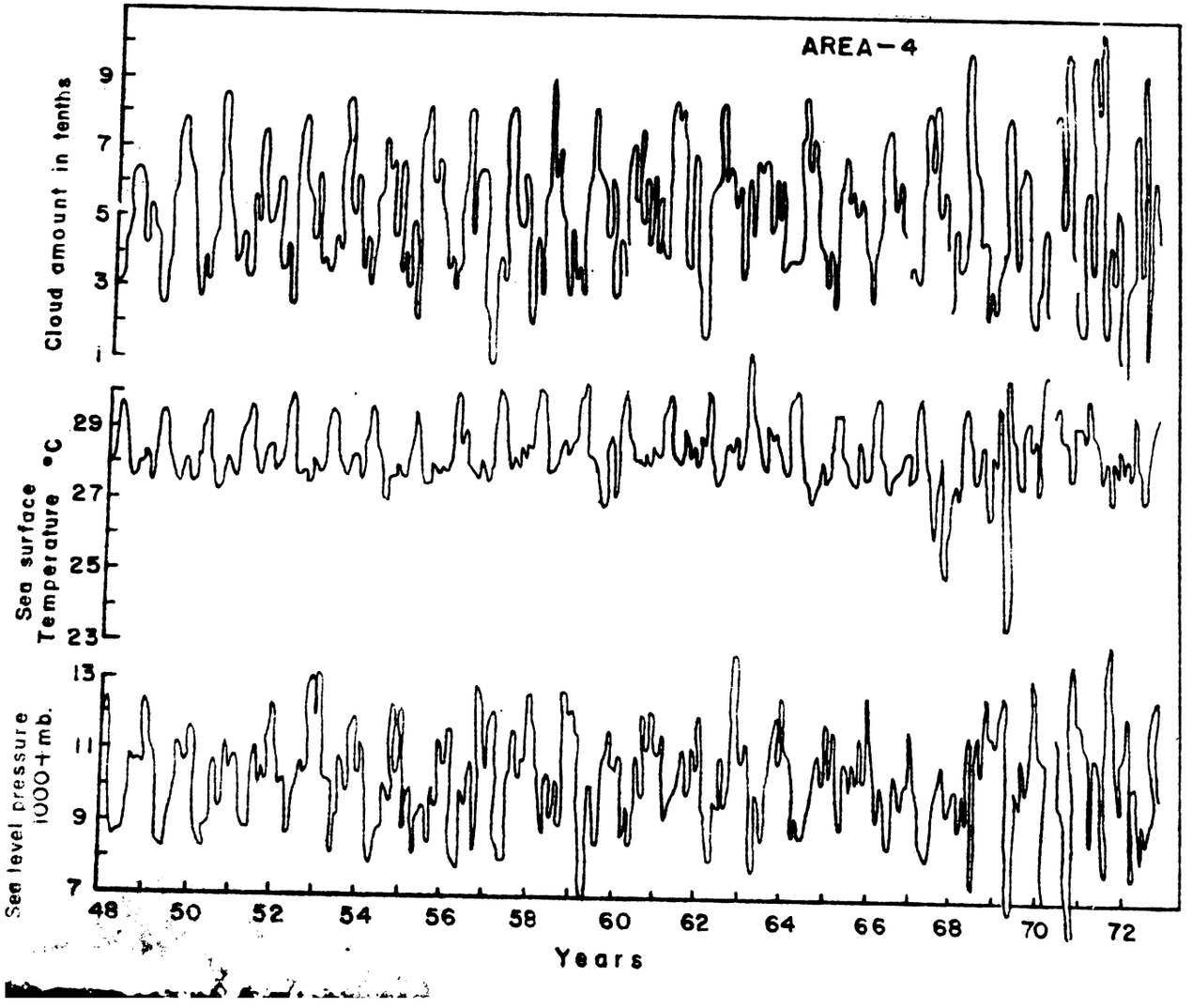
AREA—4
Cloud amount in tenths
9
7
5
3
1
Sea surface Temperature °C
29
27
25
23
Sea level pressure 1000+mb.
13
11
9
7
48
50
52
54
56
58
60
62
64
66
68
70
72
Years

Fig.32. Long term variations of cloud amount, sea surface temperature and sea level pressure for area 04 (Eastern Arabian Sea).

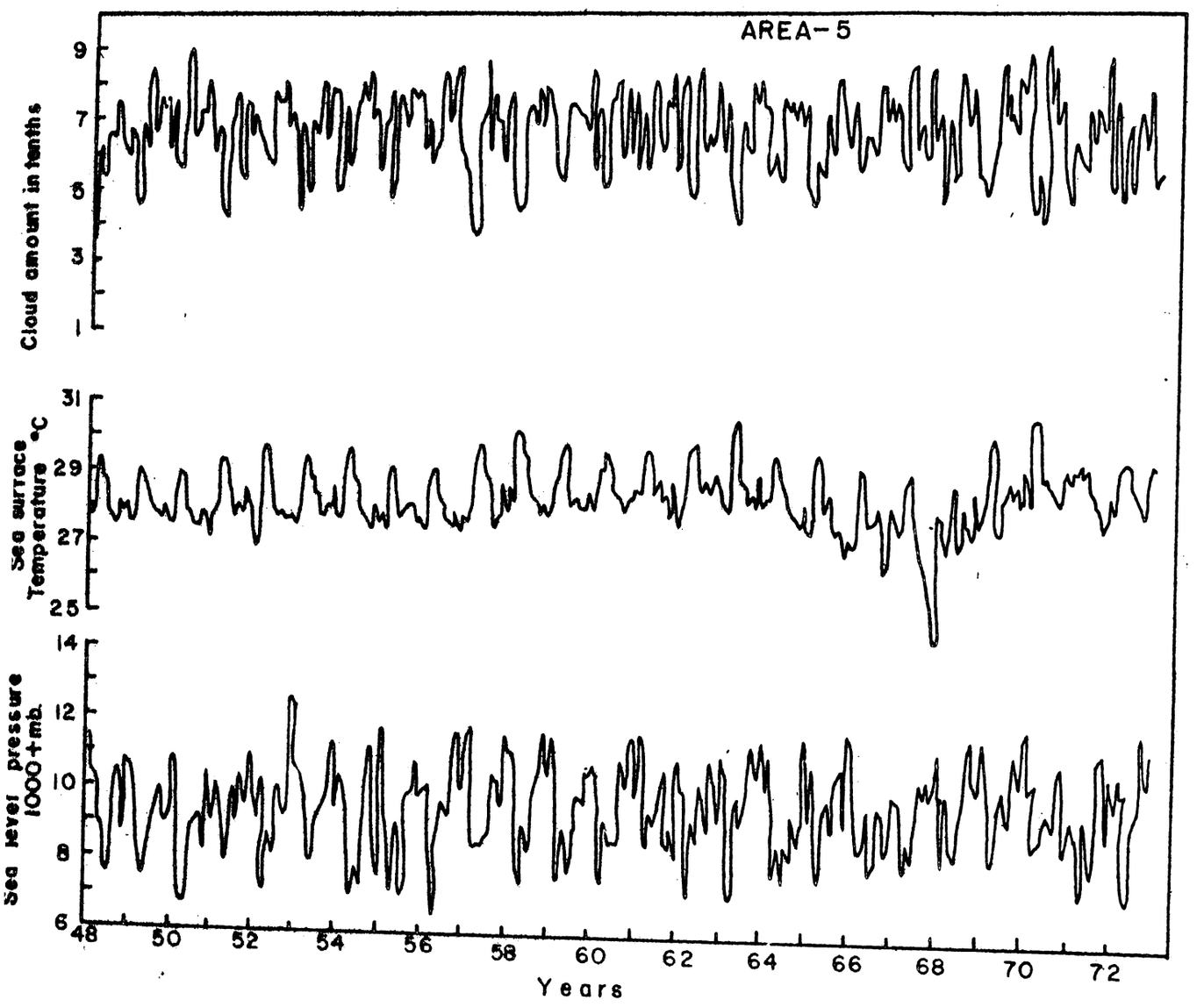
AREA-5
Cloud amount in tenths
9
7
5
3
1
Sea surface Temperature °C
31
29
27
25
Sea level pressure 1000+mb.
14
12
10
8
6
48
50
52
54
56
58
60
62
64
66
68
70
72
Years

Fig.33 Long term variations of cloud amount, sea surface temperature and sea level pressure for area 05 (Bay of Bengal).

Table.16

Monthly heat balance Values (in K Cal cm^{-2} $year^{-1}$) for area 92 (Central Arabian Sea)

February	March	April	May	June	July	August	September	October	November	December
31.0	62.1	122.3	48.2	-91.6	-53.7	-64.2	-17.2	5.5	19.7	-8.0
113.5	107.7	110.2	47.8	-40.5	-94.5	-36.1	62.8	108.4	117.5	-5.8
201.1	73.0	157.3	130.3	41.2	-166.1	-53.3	77.4	111.3	43.1	-65.0
57.3	109.9	78.1	141.6	-155.9	-165.0	-76.3	80.7	34.5	-2.9	-40.5
35.8	126.3	124.8	85.4	-141.6	-196.0	-17.5	67.5	16.1	43.4	51.1
103.7	68.6	127.8	101.8	-4.4	-122.3	-84.3	63.5	50.7	86.9	-100.4
96.0	76.7	112.8	108.8	-96.0	-125.6	-132.1	21.2	100.7	46.7	-4.7
-21.5	140.5	124.1	103.3	-104.0	-169.4	-84.5	48.2	88.8	27.0	-2.6
40.2	89.8	88.7	73.4	-181.8	-91.6	-23.0	40.9	48.5	32.9	59.5
121.5	102.6	114.2	87.2	-97.1	-181.0	-13.5	84.0	91.6	36.9	-23.4
7.7	97.8	125.9	34.1	-162.1	-191.6	-89.9	2.9	39.8	55.1	18.6
89.9	104.0	90.2	50.7	4.4	-178.9	-79.6	30.7	74.5	42.3	-29.2
74.8	67.5	114.2	84.9	-18.6	-125.9	-119.7	52.9	63.5	17.2	25.9
22.3	102.2	115.0	28.1	-104.8	-96.4	-24.1	-134.7	98.9	85.4	23.0
109.9	131.4	170.8	55.8	-89.8	-288.1	-77.7	32.9	65.0	35.8	-43.4
80.3	109.1	93.6	104.0	-72.3	-195.3	-64.6	30.1	53.7	-44.9	-64.2
27.0	122.6	89.1	34.7	-127.4	-100.4	-89.1	60.2	112.1	29.9	-53.7
69.0	101.8	100.0	69.0	-25.2	-160.2	-8.4	65.3	106.9	14.2	-74.1
90.9	71.9	119.4	73.9	-5.1	-94.7	-34.1	56.2	89.4	-7.7	-24.1
92.7	104.8	105.5	92.0	-48.9	-156.6	-40.2	48.2	109.1	76.3	6.9
5.8	95.3	123.7	75.6	-43.4	-83.6	-86.5	44.0	82.5	71.2	28.8
85.4	132.1	102.2	60.2	-88.0	-200.0	-59.9	-47.1	98.6	39.1	-18.6
5.5	108.0	96.7	14.2	-33.9	-152.6	-132.1	-35.0	130.3	71.5	1.8
83.6	107.7	132.9	67.9	-228.6	-123.1	-192.0	-11.3	72.3	23.4	7.7
104.4	79.9	129.2	69.7	-10.6	-140.5	-56.9	93.8	16.8	28.6	9.9

areas (01, 02, 04 and 05) are given in Tables 15-18. In order to follow more closely the variations of heat balance the monthly heat balance variations from the long term averages for the six areas are also given in Table.19.

Maximum variations are found in the area 01 (western Arabian Sea) for southwest monsoon seasons. This is reflected in other areas also. Variations in the central Arabian Sea (areas 02) is comparatively lesser. Excessive heat loss observed in 1971 & 1972 especially in western Arabian Sea is seen throughout in eastern Arabian Sea and Bay of Bengal. The enormous heat exchange and heat balance in 1971-72 January is seen in Arabian Sea and Bay of Bengal with maximum values in western Arabian Sea. The cause of such an anomaly is not readily seen here.

Conclusions

The above studies strengthen the emphasis given to the importance of southwest monsoons in controlling the overall climatic conditions of the North Indian Ocean. The pulsation of heat exchange in the Somali Current region and its repurcussions on the other areas are found to be important. The intensity of heat emissions and its periodic variations throughout the North Indian Ocean and its relation to the gigantic event of south-west monsoon are brought out here. The period of great variations as observed in the analysis coincides

with that of erratic variation in the rainfall activity of the summer monsoon over India as given by Joseph (1978). The earlier period of stable variations fall with in the period of good rainfall (1930-60). A sudden drop of sea surface temperature after 1964 signifies bad monsoon period and it coincides with the failure of monsoons for the years 1965 & 1966. The fall in sea surface temperature values is observed till 1970. Though the drop in temperature is observed through out all areas, the western Arabian Sea shows marked decrease. The evaporation rate is also minimum throughout. This supports Shukla's (1975) suggestion that colder SST anomalies over the western Arabian Sea could cause reduction in monsoon rainfall over India and adjoining seas. Higher pressure values are observed in western Arabian Sea. The overall cloud amount is more in eastern Arabian Sea and Bay of Bengal during this period. The Bay of Bengal latent heat exchange values show lesser magnitudes, inspite of high cyclogenesis duringythese years as presented by Ahmad (1978). The year to year variations of the sea surface temperature and the intensity of monsoons is studied in detail in the next chapter.

Chapter. 7

The annual and inter annual variations of the sea surface temperature over the Indian Ocean and its impact on the south west monsoon

****

The climatic influence of the oceans upon the atmosphere depends largely on the heat and moisture flux across the ocean-atmosphere interface. The monitoring of the ocean surface temperature, in its annual and inter-annual cycles, has therefore become important in climatology.

Some of the most important work on very large-scale, almost global, air-sea inter action has been carried out by Jacob Bjerknes, who has found a link between equatorial sea-surface temperature values in the central and eastern Pacific Ocean, the extent and intensity of subtropical anticyclones and the extra tropical westerlies. He has used time-series of surface winds and sea surface temperature values at Canton island (3^{0}S 172^{0}W) to show that major temperature changes in this part of Pacific are caused by varying strengths of the easterly winds which prevail there. When these are weak, as happened in late 1957 and early 1958 (Bjerknes, 1966), upwelling in the Ocean is eliminated and sea surface temperature values rise above normal, while in the overlying atmosphere convection is stimulated and rainfall amount increased. On the other hand, the records from midlatitude open ocean areas, with no appreciable

upwelling effects, do show, of course the dominant radiation produced seasonal cycle of sea surface temperature. In the year to year changes of ocean-surface temperature, the response both to inter annual anomalies of radiation flux and to anomalies of water advection can be seen.

The large-scale climatic effect of changing equatorial ocean surface temperature was suggested by Bjerknes (1969) to be identical with those already described under the concept of southern oscillation by Sir Gilbert Walker (1930, 1939) which is termed as 'Walker circulation' by Bjerknes, which derives its propulsion from the longitudinal temperature contrast. According to Bjerknes, the great inter-annual variations of tropical pricipitation involved in the shifts of phase of the southern oscillation, provides an inter-annually varying source of energy for the Hadely circulation of both hemispheres, which can be seen in the corresponding variations of strength and position of the upper-tropospheric westerly jet stream. Namias (1969) demonstrated how also middle latitude sea surface temperature anomalies can survive in the Pacific through several months in succession and during such periods of large-scale flow extending down wind to, and across, the north American continent.

Indian Ocean, which shows semi-annual variations of circulation with the advent of south-west monsoon season, with a modified Hadely cell noted for the westerlies in the lower level

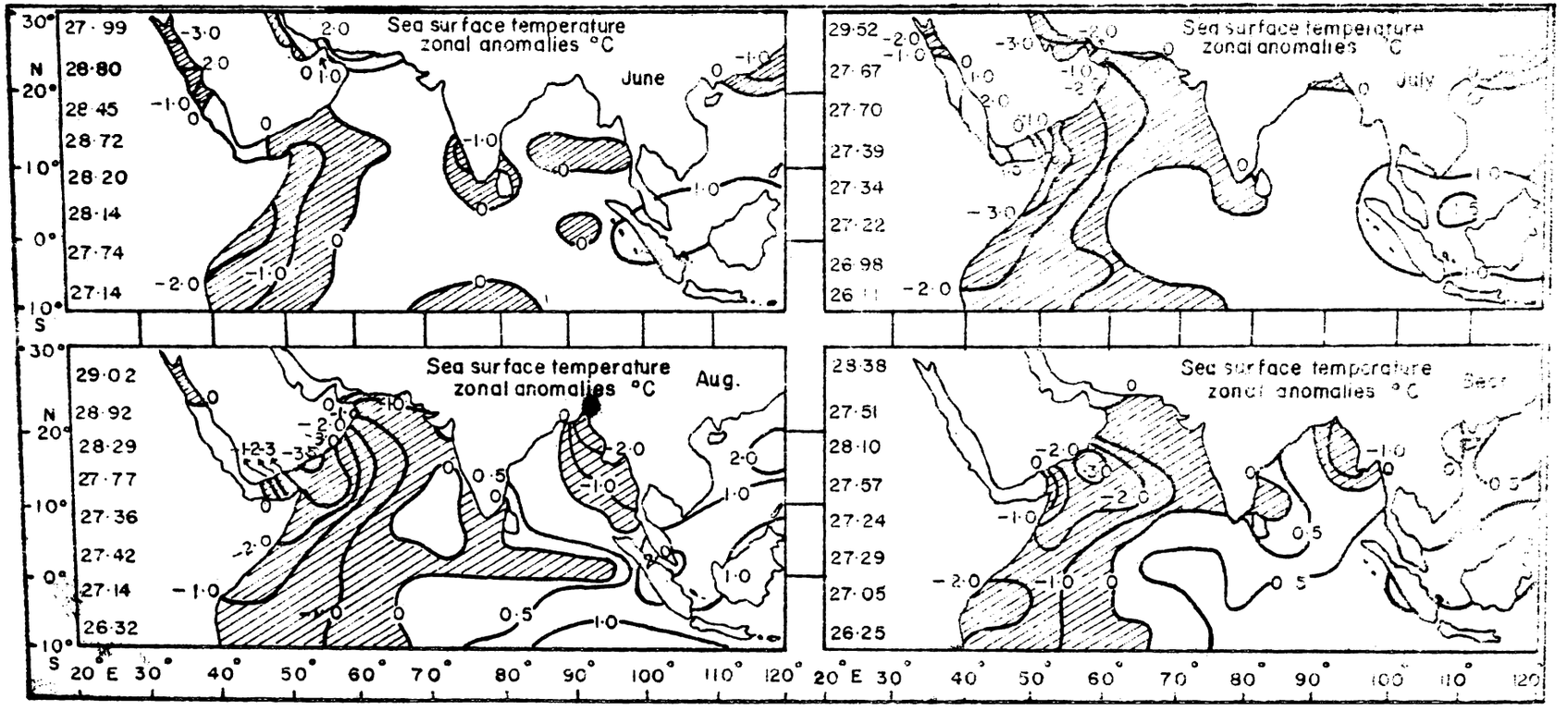
Sea surface temperature zonal anomalies °C
June
27·99
28·80
28·45
28·72
28·20
28·14
27·74
27·14
Sea surface temperature zonal anomalies °C
July
29·52
27·67
27·70
27·39
27·34
27·22
26·98
26·11
Sea surface temperature zonal anomalies °C
Aug.
29·02
28·92
28·29
27·77
27·36
27·42
27·14
26·32
Sea surface temperature zonal anomalies °C
Sept.
28·38
27·51
28·10
27·57
27·24
27·29
27·05
26·25
30° N
20° N
10° N
0°
10° S
20° E 30° 40° 50° 60° 70° 80° 90° 100° 110° 120°

Fig.34. Distribution of zonal anomaly of sea surface temperature in (°C) expressed as deviations from the latitudinal average. Zonal mean sea surface temperature is given on the ordinate at 5-degree latitude intervals in (°C).

and easterlies in the upper level, also provides another place where the sea surface temperature anomalies caused by the intense equatorial upwelling which could influence the precipitation patterns of southern Asia.

The time and space variations of the water temperature over the Arabian Sea previous to and during the south west monsoon season suggests the presence of important interactions and feed back effects on grand scale between the ocean and atmosphere which have profound effect on the properties of the south west monsoon circulation. Arabian Sea isotherms show values of high sea surface temperature ($> 29^{o}C$) in May before the advent of south west monsoon, which is the highest temperature anywhere in the ocean (Colon, 1964). A decrease in temperature is observed after May. The monal anomalies for the south-west monsoon period as illustrated in fig 34 depicts the summer cooling as a result of the establishment of the south west monsoon circulation. This cooling which makes the seasonal variation of sea surface temperature of the North Indian Ocean differ from the usual trend observe over most of the tropical oceans, which exhibits a late summer maximum and a late winter minimum.

Annual variations of the sea surface temperature, air temperature and the sea level pressure variations are studied by means of harmonic analysis for the period 1968-72.

The distribution and variations of the sea surface temperature enlighten the large-scale effects of an atmospheric system over a large oceanic body. On the contrary, the studies have revealed that the sea surface temperature anomalies and its consequent effects on the oceanic properties have a good bearing on the atmospheric circulation. Manabe etal.(1974) using the global general circulation model of Geophysical Fluid Dynamic Laboratory has found that, the locations of rainbelts and accompanying tropical disturbances are determined primarily by distributions of SST. This being so, Manabe et al felt that relationships between SST anomalies and tropical precipitation patterns should be investigated numerically. Shukla (1975) has responded to this suggestion and demonstrated with the Geophysical Fluid Dynamic Laboratory model that colder SST anomalies over the western Arabian Sea and Somali coast may cause reduction in the monsoon rainfall over India and adjoining areas. The features associated with the cold SST anomaly seem to be an increase in the surface pressure, a decrease in the rate of evaporation, and a reduction in the cross-equatorial wind and hence a reduction in the cross-equatorial moisture flux over the anomaly region and adjoining areas.

The trend of annual SST values for nearly a decade (1877-1972) is studied for the western Arabian Sea, eastern Arabian Sea and southern Bay of Bengal. Relation between sea surface

temperature values over the western Arabian Sea and rainfall at the west coast of India during summer monsoon months is studied.

The annual variations of sea surface temperature

The annual variations of the sea surface temperature and the superincumbent air and the sea level pressure over the Arabian Sea and the Bay of Bengal have been studied for the six areas (Fig 2., chapter 2) for which time series analysis were made, and depicted in the previous chapter. The annual variations of the above mentioned parameters are resolved into two harmonic components, one with a period of a year and the other with a period of six months. The parameter at any time t of the year is represented by the relationship,

$$P_t = (P) + a_1 \sin\left(\frac{1}{6}\pi t + \phi_1\right) + a_2 \sin\left(\frac{1}{3}\pi t + \phi_2\right)$$

where (P) is the mean annual value of the parameter, a_1 and a_2 are the amplitudes of the annual and semi-annual waves, and ϕ_1 and ϕ_2 are the respective phase angles and t refers to time in months of the year. The different constants (P), a_1, a_2, ϕ_1 and ϕ_2 which represent the seasonal variation of temperature during the different years (1948-82) have been determined in the usual manner. (Conrad and Pollark, 1950) assuming that the mean monthly temperature refers to the middle of each of the months

Table 20

Annual variations of sea surface temperature, air temperature and sea level pressure for the different areas in the North Indian Ocean.

Areas	Mean temperature °C	Annual Range °C	Std. Deviation °C	Harmonic constants Annual wave a°_1C	Date of maximum	Semiannual wave a°_2C	Date of maximum
Sea surface temperature °C							
1	26.21	4.68	1.38	0.97	May 5	1.84	May 10
2	27.25	4.28	1.25	0.30	July 2	1.10	June 29
3	28.29	3.85	1.16	1.26	July 17	0.76	May 2
4	28.43	2.73	0.79	0.79	April 24	0.60	May 2
5	28.31	2.14	0.64	0.64	May 5	0.38	May 1
6	28.12	3.30	0.58	0.58	May 23	0.35	March 8
Air Temperature °C							
1	26.72	4.44	1.28	1.03	May 29	1.32	May 16
2	26.84	5.32	1.58	1.8	July 8	1.26	May 14
3	27.84	4.20	1.30	1.52	July 2	6.79	May 4
4	28.13	2.58	0.76	0.72	June 1	0.49	May 2
5	27.82	2.18	0.60	0.67	May 18	0.25	April 14
6	27.54	3.29	0.52	0.71	June 4	0.44	April 21

Areas	Mean Pressure mb	Annual Range mb	Std. Deviation mb	Harmonic constants Annual wave a°_1 mb	Date of maximum	Semiannual wave a°_2 mb	Date of maximum
Sea level Pressure mb							
1	1010.33	8.58	2.74	3.80	Jan 14	0.86	April 17
2	1010.24	12.72	4.23	5.50	Jan 5	1.40	May 4
3	1008.27	10.86	3.47	4.61	Oct 6	0.78	Feb 16
4	1020.29	4.27	1.22	1.35	Dec 23	0.52	March 13
5	1009.56	3.70	1.02	1.11	Dec 30	0.48	March 8
6	1010.15	2.71	0.86	0.58	Oct 25	0.39	April 1

and that the months are all of equal length.

The mean values of annual mean, amplitudes and phase angles (date of maximum) of annual and semi-annual waves are calculated for the entire period of study using that for individual years. for sea surface temperature, air temperature and sea level pressure values are given in the Table 20. The number of years available for the study is different for different areas, as given in chapter 6, especially for the areas 03 and 06 (representing Central Bay of Bengal and Equatorial Waters).

Jagannathan (1957) has shown that the annual and semi-annual waves account for over 90 percent of annual variations of air temperature over the Indian area represented by 12 monthly values. Verploegh (1960) has shown that the annual pressure variation could, almost entirely, be represented by means of its first two harmonics components, viz. the annual and semi-annual pressure oscillation.

The relation between amplitude and phase (month of maximum) for the annual and semi-annual waves and its variations from station to station is depicted in harmonic dials for each parameter (Fig 35).

The annual means of sea surface temperature is always greater than that of air temperature. Eastern Arabian Sea and Bay of Bengal show greater temperature values (both air and sea)

Relation Between Amplitude And Phase (month of maximum)

from area to area

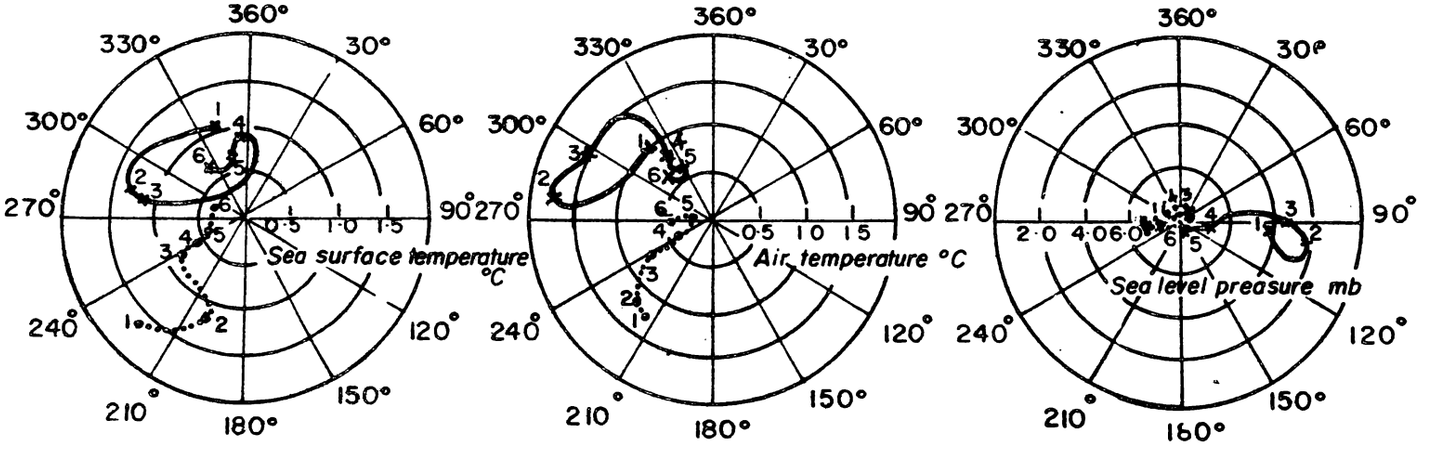

Annual Wave

Semi annual Wave

Fig. 35 Harmonic dials representing the relationship between amplitude and phase angle (date of maximum) and its variations from area to area for first and second harmonic constants, for sea surface temperature, air temperature and sea level pressure.

even greater than equatorial waters. The annual range of temperature is determined as the difference between the mean temperature of the hottest and coldest months. The ranges of air temperature values are greater than sea surface temperature, except for areas near Somali coast and south-east coast of India, where horizontal advection is marked. Standard deviations are higher for higher latitudes. The region near the upwelling area of Somali coast shows a maximum value for sea surface temperature. According to Sverdrup (1960) the standard deviation of the monthly mean values generally exhibits an annual variation, which is partly due to meteorological effects and partly to a seasonal-shift of the shipping routes. However, he suggests that it will be sufficient here to take into account only an annual mean value of it. The amplitude values of annual waves are generally higher for air temperature than for sea surface temperature. Amplitudes of semi-annual waves are comparatively smaller except for the western Arabian Sea area where the semi-annual variations of general circulation is at the maximum. The phase angles or the dates of maximum show a latitude dependance, higher latitudes showing delayed maxima. The areas of cold advection does not strictly stick to the usual picture. Though areas 01 and 03 (Fig 2) are along the same latitudes, the dates of maximum temperature are different.

The annual oscillations of sea level pressure appear to be correlated with that of air temperature. The semi-annual

oscillations are small compared to the annual oscillations. Apart from the latitudinal variations ranging from high values of oscillations in the subtropics to small values near the equator it could be observed that the ranges generally are higher over the western border of the ocean. The area near the Somali coast shows the maximum oscillations especially that of sea surface temperature.

The phase lag between times of occurance of maxima of air and sea surface temperatures can be related to the time required for the adjustment of the oceanic circulation to corresponding changes in air circulations and vice versa, though the response time of one medium to the other must represent a highly complex problem, since the time constant in the ocean is much larger than in the atmosphere. In general, areas marked for cold advection, shows considerable lag for air temperature maxima in western Arabian Sea, eastern Arabian Sea and southern Bay of Bengal.

The year-to-year variations of sea surface temperature is given for Western Arabian Sea, eastern Arabian Sea and Bay of Bengal (Tables 24-28). The annual values show a general tendency to increase in magnitude, in all three areas. A general tendency for advance of dates of maximum is observed in Arabian Sea areas till 1965. This is not much perceptible in the Bay of Bengal. The amplitude of semi-annual wave is practically of the same order for Arabian Sea. The area near Somali current region (western

Arabian Sea) shows a temperature maximum for the annual wave in the first week of May or the last week of April and a semi annual maximum in the second week of May. The eastern Arabian Sea area (near the south-west coast of India) shows a temperature maximum for the annual wave most frequently in the third week of April and a semi-annual wave with maximum in the third week of April or first week of May. The dates of maximum of Bay of Bengal almost coincides with that of eastern Arabian Sea.

The general pattern of date of occurance of temperature maximum almost coincides with the pattern of the onset of monsoon, which shows a delay in the northerly areas. It is of particular interest to note that, the early occurance of annual maximum coincides with the good monsoon years as given by Joseph (1976), according to whom the good monsoons are characterised by early onset and advance of monsoon. This again highlights the strong influence of general circulation over the sea surface temperature distribution or vice versa, though cause and effect relationship is not clear.

Inter-annual variations of sea surface temperature

It has been observed from the previous works and confirmed by the present analysis that unlike other oceanic areas, North Indian Ocean shows a summer maximum and a rapid cooling of waters in the early summer. The maximum temperature values are observed

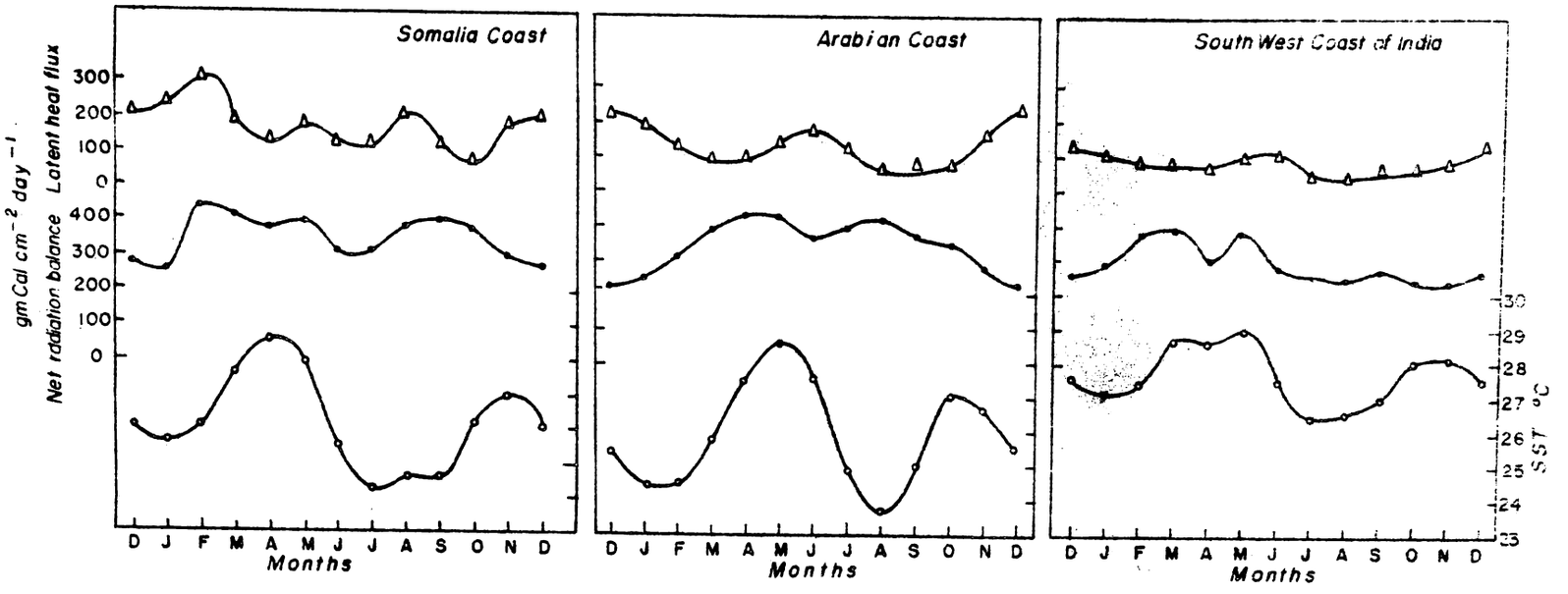
Somalia Coast
Arabian Coast
South West Coast of India
gm Cal cm⁻² day⁻¹
Net radiation balance Latent heat flux
300
200
100
0
400
300
200
100
0
30
29
28
27
26
25
24
23
SST °C
D J F M A M J J A S O N D
Months

Fig.36. Annual variations in sea surface temperature (^{o}C), net radiation balance and latent heat flux (gm Cal Cm^{-2} day^{-1}).

usually around May whence from the southwest monsoon current sets in. Fig 34 shows that the cooling starts in the western Arabian Sea and its spreading to other areas of Indian Ocean during main monsoon months and the ocean regaining its original picture, by the end of withdrawal of south-west monsoon current. The sea surface temperature values are given in the form of zonal anomalies. Three main areas of rapid cooling are identified; 1) Somali coast 2) Arabian coast 3) Southwest coast of India Western Arabian Sea areas are well known, upwelling areas. The intensity is much less in south-west coast of India compared to other two areas. It could be inferred that during south-west monsoon since the flow of currents is clockwise (Fig 7 a., chapter 3) horizontal advection of cold water could be expected. By July and August during peak months of monsoonal flow, the entire Arabian Sea is under the influence of this eastward moving upwelled cold water. By September, the summer circulation starts regaining its original state.

The areas of maximum upwelling is studied in detail. In order, to understand the role of heat flux in the water cooling, components of energy exchanges are presented in Fig 36.

Along the Somali coast, the summer maximum of temperature is observed in April. The cooling starts from May and remains till July, August and September. A secondary maximum for the month of November is observed. The coast of Arabia shows a maximum

temperature in May. The months of June and July shows a decreasin trend and an August minimum is observed. A secondary maximum in October is noted. South west coast of India shows maximum in March, April and May and minimum in July and August. The maximum and minimum temperatures are higher here. The coasts of Somalia and Arabia experience comparatively higher net radiative input. Along the south west coast of India the radiative heat input is much less, due to heavy cloudiness. Evaporational cooling is considerably less in all three regions, of which the Somali coast is comparatively higher due to strong winds. With the establishme of summer monsoon current, conditions are favourable for strong vertical and subsequent horizontal advection of cold water. Unlike the central west Arabian Sea, these coastal areas do not experience high amount of evaporational cooling. For the coasts of Arabia and Somalia, the net radiative heat input on account of cloudlessness is considerable. Inspite of that considerable cooling is observed. This points out the importance of upwelling process experienced in the western Arabian Sea, which is seen as a key factor in determining the weather of South-east Asia and the fluctuations of monsoons. This holds good only along the coast lines, where the advection of cold water and the effect of upwelli is maximum. Evaporational cooling plays a crucial part in the areas towards the east of this region. Previous chapters reveal that th influence of upwelled waters are felt towards the east also. Saha (1970) has shown the progressive eastward movement of cold water brought to surface by upwelling. The sea surface temperatur

anomaly charts presented here, also confirm this eastward movement of cold advected waters. It agrees well with Saha's observations of cold water enclosing the whole of western Arabian Sea during the peak monsoon months and confirmed by the studies of Bruce (1968) and Nimbus 2 observations of 1966. During July and August west of 60°E is marked by negative temperature anomalies. According to Saha (1970a) the ridge of high barometric pressure that develops over the Arabian Sea off the coast of Somalia during June and progressively shifts eastwards as coldwater advances towards India during July and August appears to bring about a profound change in the low-level air circulation over the Arabian Sea. In June, when the ridge lies near the coast of Somalia the winds over practically the whole Arabian Sea blow from a direction between west and southwest as observed by Saha. The deep and intense flow could be presumed to be reaching the southern part of the west coast of India. The Arabian coast, seasonal changes of temperature, indicates drop in temperature and hence, upwelling with a time lag compared to Somali coast. Duration of upwelling is also observed to be greater along the coast of Somalia. The progressive movement of cold water from Somalia coast (along 10-15°N) as observed by Saha (1970a) and observed in the present analysis also and the presence of upwelled waters along the coast of Arabia is presumed to be creating an extension of low pressure area and hence extension of the deep and intense current towards northward. This could mean a qualitative explanation for the delayed onset of south west monsoon in the northern part of west coast of India. Once the circulation starts changing the

movement of cold water from Somali coast reduces. The upwelling along the coast of Arabia is of less duration. By September, it could be observed from the Fig (34) that the extension of cold wat and hence low pressure area, recedes back and hence changes in the intensity of circulation. September marks the withdrawal of monsoon from the northern most parts of Indian sub-continent. This indicates

Occurance of Warm water zones off Cochin and Bombay during May and June 1977 fr the infrared thermal Scanning flight data just before the onset of monsoons these Stations were reported by Pisharoty (1981). He inferred that these temp ature anomalies caused the low pressure troughs along the West Coast of India which deepens the monsoon currents to 4 to 5 kms just before it strikes the c

It is seen from the previous chapters that the onset and existence of monsoon is due to a series of land-sea air interactio processes as explained by Bunker (1965). But the fluctuations and variability of the monsoon activity may depend to a large extent, on the air-sea interaction which takes place during the travel of the monsoon current over the oceans. Since sea surface temperatur and wind speed determine the air-sea interaction processes taking plac over the ocean surface, one of the factors could be taken as an indicator parameter. As has been postulated by earlier studies (viz. Saha, 1970, 1974; Ellis, 1952) and confirmed by the present analysis that sea surface temperature over the Arabian Sea has profound influence over the monsoon flow and associated rainfall. Ellis (1952) compared the observed SST over the North Indian Ocean during June 1929 and June 1933. In 1929 most of India experienced drought and in 1933 many Indian provinces had floods. His conclusion was that during the flood year (ie. 1933) the SST over the North Indian Ocean was generally warmer than that during the droug

year (1920). Shukla (1975) using the global general circulation model of the Geophysical Fluid Dynamic Laboratory had established that the colder SST anomalies over the western Arabian Sea and Somali coast may cause reduction in the monsoon rainfall over India and adjoining areas.

An attempt is made to examine the relationship between the yearly fluctuations of rainfall at the west coast of India and the south west monsoon season sea surface temperature from region bounded by latitude 10-23°N and longitude 55-60°E which is situate in the eastern side of Somali current region and coincides with the wind maximum during the summer monsoon period. The period of analysis is from 1951-66. Three year moving averages are computed of the yearly values for smoothening the fluctuations in the trend Because of the orographical influences upon rainfall, Hurty and Edelman (1970) have suggested the pressure gradients at the surfac during monsoon as one of the best and simplest expressions of the intensities of the monsoons in different years. Ramamurthi (1972) has suggested a method of identifying the effects of perturbations of active as well as weak Arabian Sea monsoons. This brought out that active Arabian Sea monsoon is associated with two cyclonic vortices, which in the mean are located over the Gulf of Cambay (Gujarat low) and the northern parts of east coast. Means of the pressure (0830 IST) reduced to sealevel were worked out in respect

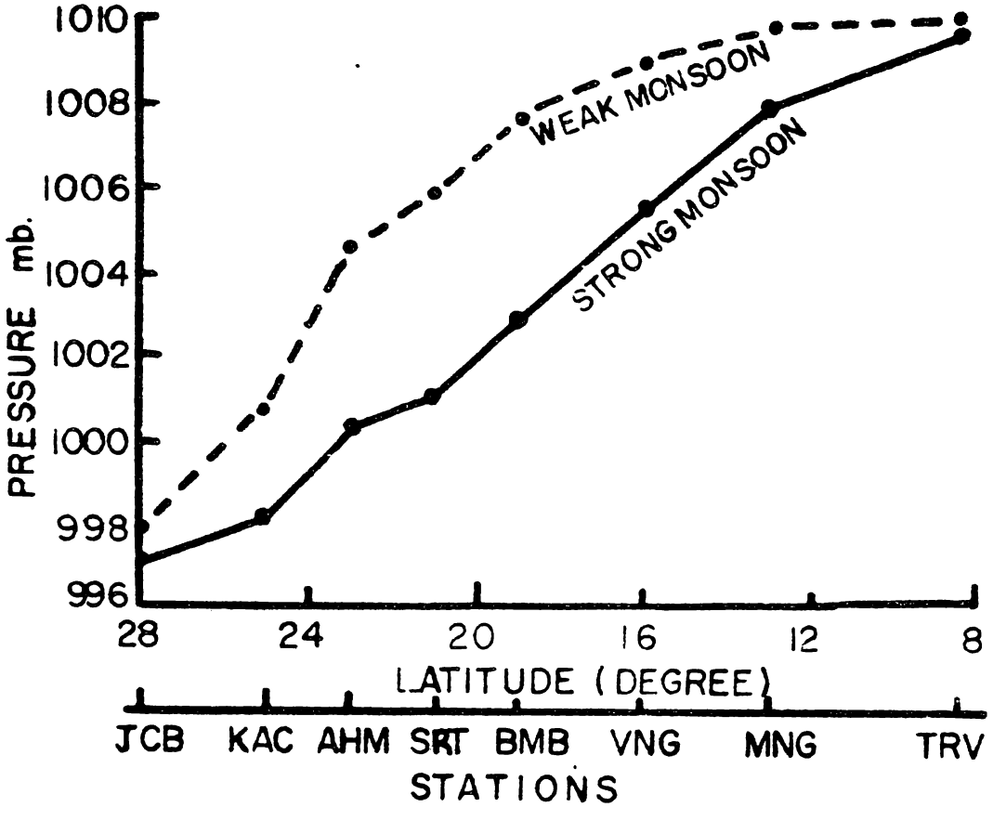
1010
1008
1006
1004
1002
1000
998
996
PRESSURE mb.
WEAK MONSOON
STRONG MONSOON
28
24
20
16
12
8
LATITUDE (DEGREE)
JCB
KAC
AHM
SRT
BMB
VNG
MNG
TRV
STATIONS

Fig.37. Mean pressure during spells of weak and strong Arabian Sea monsoons Ramamurthi (1972).

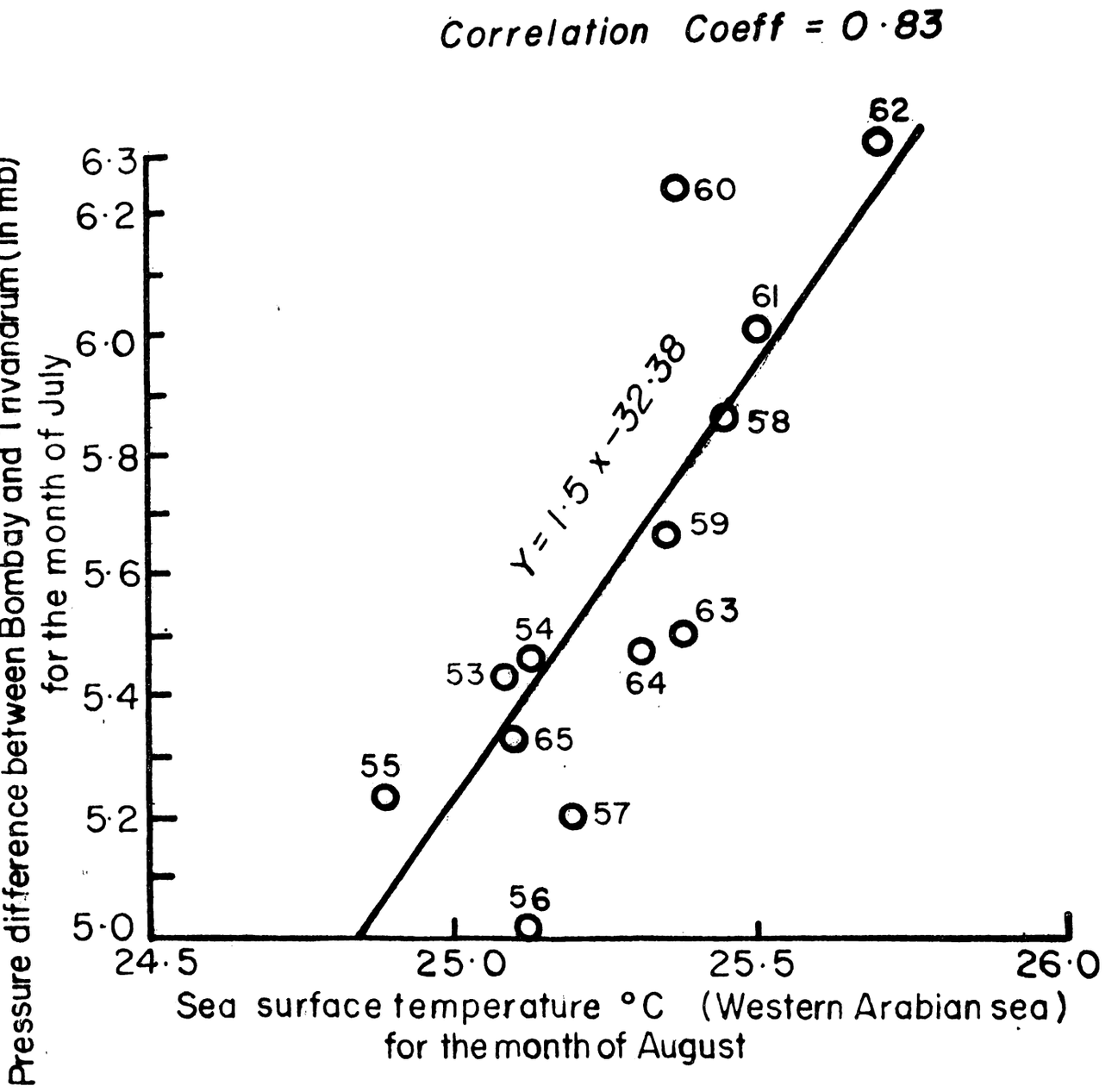
Correlation Coeff = 0·83
Y=1·5 x-32·38
62
60
61
58
59
63
54
53
64
65
55
57
56
6·3
6·2
6·0
5·8
5·6
5·4
5·2
5·0
24·5
25·0
25·5
26·0
Pressure difference between Bombay and Trivandrum (in mb) for the month of July
Sea surface temperature °C (Western Arabian sea) for the month of August

Fig.38. Relation between the sea surface temperature (°C) values of western Arabian Sea and the intensity of monsoon, when expressed as the pressure difference (mb) between Bombay and Trivandrum for the month of July. The sea surface temperature values (°C) and the pressure difference values (mb) are smoothened by 3-yr moving averages.

of selected stations adjoining the heat low and also stations along the west coast for strong and weak spell of the monsoons (Fig 37). During strong monsoon the pressure gradient between Bombay and Trivandrum is more than double that of weak monsoon, indicating that the monsoon perturbations themselves by producing large pressure defect over North Konkan and Gujarat deepens the pressure gradient south of Konkan and directly influence the low level monsoon flow also. Monthly mean values of sea level pressure for 0830 IST for the coastal stations of Bombay and Trivandrum for the month of July, have been obtained from the records of the India Meteorological Department. The pressure difference between Trivandrum and Bombay is a close representation of the pressure gradient vector over the Arabian Sea area adjacent to the western edge of the Peninsula. The values of the pressure differences during the individual years between Trivandrum and Bombay and the sea surface temperature from the western Arabian Sea are subjected to moving averages, taking three successive values into consideration at a time and representing the moving average value in the position of the middle term. Relation between the trend of pressure difference between Bombay and Trivandrum and the sea surface temperature values for July is given in Fig 38, when intensity of monsoon is expressed by the pressure difference between Bombay and Trivandrum. The correlation between the sea surface temperature and the intensity of monsoon at the west coast of India is generally good (0.88).

According to the eastern spreading of the upwelled waters of Somali coast observed by Saha (1970 a) and in the present studies, it could be assumed that the August sea surface temperature values are representative of that observed along Somali Coast during intense upwelling (July). Bruce (1968) has reported the existence of a large-scale anti-cyclonic gyre on the eastern flank of Somali current which may cause translatory motions of cold water over distances upto approximately 800 km. These results agree with Shukla (1975) that colder SST values over the western Arabian Sea and Somalia coast may cause reduction in the monsoon rainfall over India and adjoining areas. The features associated with the colder SST seem to bring an increase in the Somali coast surface pressure, a decrease in rate of evaporation and a reduction in cross equatorial wind and hence a reduction in the cross-equatorial moisture flux. The warmer the temperature, the lower the pressure observed in that particular area which would cause stronger cross equatorial winds causing higher evaporation and more cross-equatorial moisture flux making the monsoon currents more moist and unstable. But warmer temperature values over the west Arabian Sea adjacent to Somalia will reduce the land-sea contrast of pressure which would tend to reduce the intensity of lower troposphere westerlies consequently meaning a reduction in the evaporation over the Arabian Sea. It is observed that in the western Arabian Sea, windspeed values play a dominant role, over compensating the fall in temperature. Hence when conditions are favourable for cross equatorial moisture flux, less of evaporation over Arabian Sea could be expected. The GFDL simulation experiment

ment results by Shukla (1975) showed that when the cross-equatorial flux decreased considerably (due to negative sea surface temperature anomaly and higher pressure over the Arabian Sea, reducing, south-north pressure gradient and hence also the intensity of the meridional wind component across the equator), it has given rise to flux convergence south of the anomaly region and hence enhancement of rainfall there. Since the results reveal that for particular years when the temperature values are lesser, the rainfall amount is also lesser. This would mean that lesser the cross equatorial flux, lesser the precipitation experienced along the westcoast. The correlation between the latent heat exchange and the intensity of rainfall is worked out. The intensity of rainfall is represented by the pressure difference between Bombay and Trivandrum for the month of July. The latent heat exchange values from the same area from where sea surface temperature is taken, doesnot shows good correlation. The correlation coefficient for the evaporation values of the month of June is 0.42 and that for the total evaporation for the months June and July is 0.50. The previous chapters reveal that this area under study represents the area of highest evaporation and is identified as a major water vapour source region. Bhamralkar (1975), while examining the relationship between fluctuations of rainfall at the west coast of India, south of 20°N, and the synoptic-scale latent-heat exchanges over the Arabian Sea, following the trajectory of a parcel, found that the correlation is negligible when

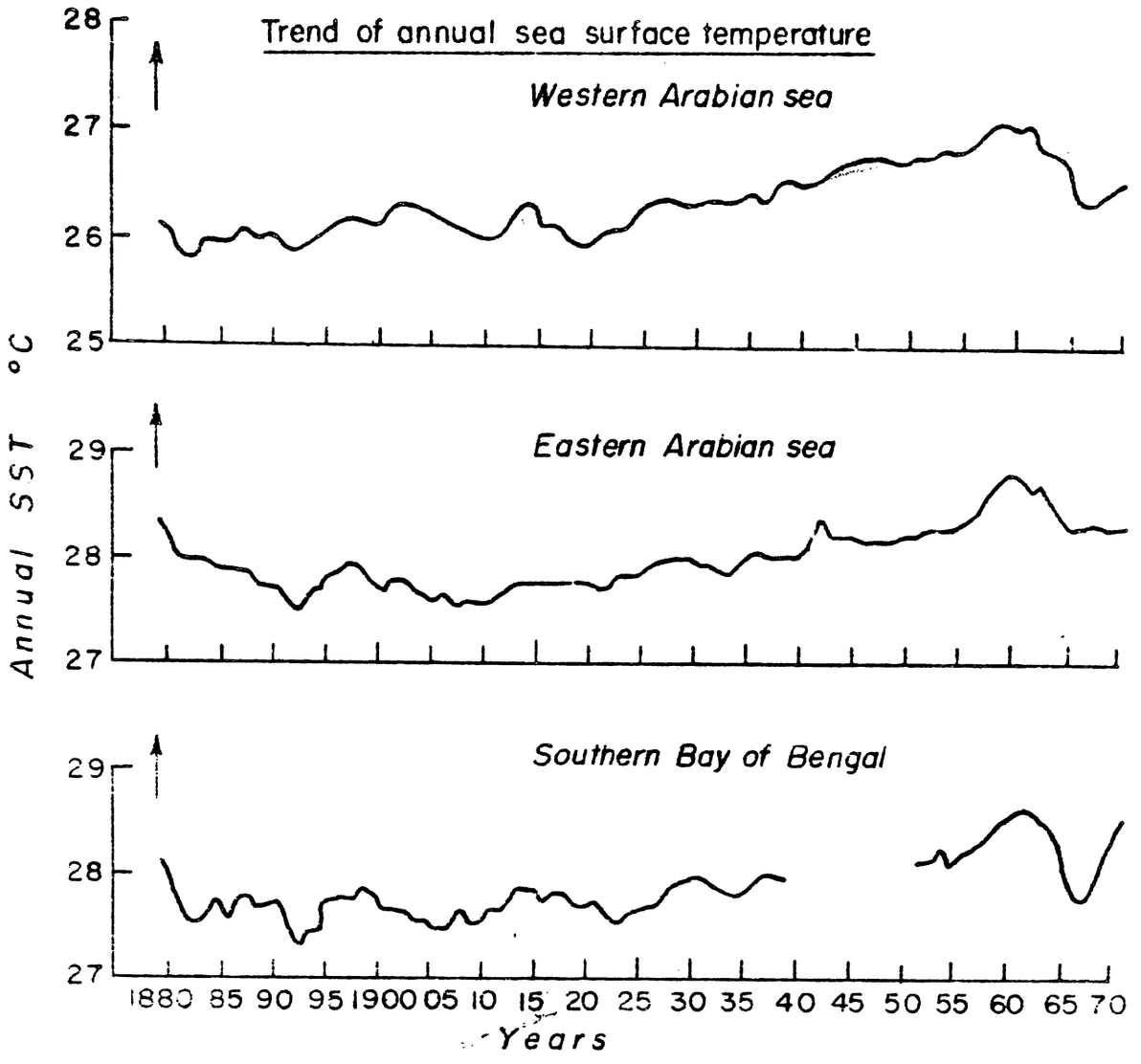
Trend of annual sea surface temperature
Western Arabian sea
Eastern Arabian sea
Southern Bay of Bengal
Annual SST °C
28
27
26
25
29
28
27
29
28
27
1880 85 90 95 1900 05 10 15 20 25 30 35 40 45 50 55 60 65 70
Years

Fig.39. Long term trends of annual sea surface temperature values (in ^{o}C) for North Indian Ocean areas - a) Western Arabian Sea b) Eastern Arabian Sea c) Bay of Bengal. The trend is smoothened by 5 Yr - moving averages.

the parcel is west of 60°E and is remarkable when the parcel is east of 60°E, for quasi-synoptic daily analysis. But it is found that evaporation from the eastern Arabian Sea is comparatively lesser, compared to that of western Arabian Sea. In the light of the present investigations it could be stated that, evaporation from the Arabian Sea contributes significantly for the rainfall over the west coast of India, though all water vapour flux across the west coast of India, need not be due to evaporation over the Arabian Sea. This again gives an emphasis on the importance of cross-equatorial flux of water vapour. ~~This again gives an empha-sis on the importance of cross-equatorial flux of water vapour.~~

The long term changes of the annual sea surface temperature values are given in the Fig 39. The trends of annual values of sea surface temperature are smoothened using 5-Yr moving averages. The general trend shows an overall increase in magnitude. The period 1890-1920 shows low values of sea surface annual temperature with an increasing tendency from 1920 to 1962. The occurance of low values of temperature for the period 1890-1920 coincides with large-scale monsoon failures occured during the 30-Yr period 1891-1920 and the high values of temperature for the period 1920-62 coincides with the period 1931-1964 which generally had good monsoon rainfall. Areas in Eastern Arabian Sea and Bay of Bengal also show similar trends. The values of Eastern Arabian Sea and Bay of Bengal show considerable correlation with that of Western Arabian Sea (Correlation coefficient = 0.89 and Correlation coefficient = 0.80 respectively). The western Arabian Sea surface

temperature values during peak summer monsoon months (July and August) show good correlation with the surface temperature values of summer monsoon months (July and August) of eastern Arabian Sea and Bay of Bengal. This shows that the variations in the general circulation created by that of oceanic circulation, have large-scale repurcussions. The present studies have shown that maximum variations are observed in the western Arabian Sea, especially in the summer monsoon months.

Conclusions

It could be concluded that the temperature variations are mainly caused by the upwelling and it can be inferred that the effects of upwelling over-compensates that of varying insolation. The cold water over the western Arabian Sea, during the summer monsoon months not only accounts for the marked differences in the weather and climatic conditions over the two parts of the North Indian Ocean but also has great significance in the context of the monsoon circulation and rainfall over India.

Chapter 8

S u m m a r y

An attempt is made to assess the large space-scale and time history of the energy flux fields, over the Indian Ocean north of 40°S latitude and its adjacent seas. Energy fluxes through the surface have been calculated using bulk aerodynamic equations with exchange coefficients which vary with windspeed and radiation equations based on Budyko. Long term ship observations that have recently become available provided an adequate data base for this purpose. Annual and seasonal models of net heat gain by the ocean, latent, sensible and radiational heat exchange, sea surface temperature and meteorological variables are presented. Averages for each month from 1948 through 1972 were computed for six specific areas in the North Indian Ocean to study the year-to-year variations and anomalies of the fluxes meteorological variables and sea surface temperature. The inter annual variations of sea surface temperature are studied and the annual variations of the sea surface temperature, air temperature and sea level pressure are studied using harmonic analysis.

The climatic models of, large-scale seasonal and annual distribution of heat balance and its components and the related climatic parameters show that the variations are conspicuous in the northern hemisphere, paralleling the

changes in climatic variables which result from the alternation between winter and summer monsoon circulations. During warming season of the year, the North Indian Ocean gains more heat than that gained by southern Indian Ocean, during the warming season of the respective hemispheres, Since enormous amount of radiative heat input for the northern Indian Ocean is experienced. Throughout all seasons, especially in the higher latitudes, the surface air is warmed in the southern hemisphere the maximum being in winter. Except for winter, warming of the air above is not prominent in northern hemisphere; 10-20°S latitude belt is seen as a semi-permanent source of water vapour. Unlike North Atlantic and Pacific, the North Indian Ocean shows highest values of evaporation during summer. The occurance of southern hemisphere maxima latent heat, in the subtropical anticyclonic region between east coast of Madagascar and southern Indonesia of 10-20°S and Aghulhas current region, also coincides with the same period. Northern Indian Ocean shows unique behaviour in its distribution of marine meteorological parameters and subsequent interaction with the atmosphere. The southern Indian Ocean conforms with the general pattern. The latent heat exchange is found to be the major component of the heat balance picture. Sensible heat exchange is found to be contributing less. The influences of monsoons and ocean currents are obvious from the

climatic models of northern Indian Ocean.

The Indian Ocean could be divided into three regions as far as the air-sea interaction processes are concerned.

1) Region of westerlies beyond 30°S
2) Southeast trade wind region
3) Region of monsoons.

The region of westerlies is marked by low values of radiative heat input, moderate evaporative cooling and high values of the fluxes of sensible heat. Very high values of latent and sensible heat fluxes are observed in the warm Agulhas Current region. Since the radiative heat input is low, maximum negative heat balance values are observed.

In the southern trade wind zone considerable heat loss is observed towards the east, in the region of subtropical anticyclone which is an area of intense evaporation. The western and eastern peripheries show contrast in the heat exchange processes.

The region of monsoons covers almost all the areas of northern Indian Ocean. Unlike other northern seas of the world, western part of the ocean is colder. The summer time cooling is another unique feature observed here. Inspite of this, intense evaporation is observed due to winds of very high speed.

The seasonal distribution of heat balance and its components presented here has enabled to study the seasonal variations of oceanic currents and water mass formation.

Large amounts of radiation energy are available in the western Arabian Sea for the genesis of the Indian monsoon and its movement. The same region shows the maximum advection of cold water, due to intense upwelling during Summer monsoon months. It is seen from the above studies that sea surface temperature values are governed by upwelling, net radiation and evaporational cooling. Along the Somali coast it is observed that the intense upwelling overcompensates the effect of enormous radiative input experienced. In this region, the net surface radiation is used for warming of the upwelled waters, evaporation is substantially reduced and due to the downward fluxes of sensible heat - large scale convection is supressed.

Zonal anomaly of sea surface temperature and other variables in equatorial North Indian Ocean is identified. A contrast between the heat budgets of Arabian Sea and Bay of Bengal is studied. During transitions, Bay of Bengal on account of warmer waters exhibit more evaporation, since the wind speed values are much low, where as during summer monsoon season, when the zonal anomalies are at the maximum, with very low values of cold upwelled waters in the western Arabian Sea, on

account of high speed winds of monsoonal current, western Arabian Sea exhibits more evaporation. The insolation maximum also is observed here. Eastern Arabian Sea and Bay of Bengal receive less of radiative input due to heavy convective clouds. Strong heating of the waters off the Somali and Arabian coasts is observed as a contrast to the moderate warming of the Eastern parts. The cold waters of Somalia lessens evaporation and reverses the direction of sensible heat exchange. The stability of air prevents the formation of many cumuleus clouds and hence insolation maximum in the western Arabian Sea. Strong negative sensible heat exchange results in sudden complete suppression of convection and shower activity. The strong horizontal variation of sensible heat is observed in the summer monsoon months. Upward heat fluxes or very small values of downward flux indicate occurance and high values of downward fluxes indicate non-occurance of convective activities respectively, and it could be inferred as triggering thermal circulation. This is obvious in the precipitation pattern of the North Indian Ocean. The quantitative assessment of zonal difference in the heat budget shows that the heat budget is basic to the climatic assymetry between western and eastern portions of the low-latitude oceans. Zonal anomalies of climatic parameters and the energy budget components present a complex picture of air-sea interactions and their feed backs which is a circle of interactions.

influencing one another. Cooling of the atmosphere in areas of high evaporation and downward sensible heat flux leads to raising of pressure and continuous non-adiabatic heating of the atmosphere in areas of condensation and upward sensible heat flux leading to lowering of pressure creates an eastward pressure gradient in the equatorial region.

Inter-annual and inter-decadal variations of the heat balance and its components are found to be much significant. Changes from 1948-59 to 1960-72 are considerable - much greater than that is expected. Anomalous behaviour of the heat balance values of 70s make the variability more prominent. Maximum variations are found in western Arabian Sea, during south-west monsoon season. These variations are reflected in the other areas also. Excessive heat loss is observed in 1971 & '72 throughout Arabian Sea and Bay of Bengal. The cause of the anomalous climatic behaviour could only be termed as abrupt breaks in climatic regimes as reported by Namias (1975), causing a different pattern of global climatic anomalies from those characterised in 1960s. Much interannual variations are observed throughout all stations, except the equatorial region. The pulsation of heat exchange in the Somali Current region and its repurcussions on the other areas are considerable. The time-series of heat balance and its components show that

the annual course of the heat balance is disrupted during individual years and months chiefly as a result of a sharp increase or decrease of evaporation. The intensity of heat emissions and its periodic variations throughout the North Indian Ocean and its relation to the gigantic event of monsoon is clearly seen. Maximum variations are found in the western Arabian Sea. The large variations of the western Arabian Sea is seen reflected in the other areas of North Indian Ocean. The period of great variations as observed in the analysis coincides with the erratic variations in the rainfall activity. The period of stable variations coincide with that of good rainfall (1930-60). When the variations are irregular the monsoon over the respective period is erratic.

The geographical extent of the equatorial cold water and its eastward spreading are found to have profound influence in the onset and maintenance of monsoon. The annual variations of sea surface temperature, air temperature and sea level pressure using harmonic analysis reveal a phase lag between times of occurance of maximum of air and sea temperatures, which could be attributed to the time lag in the coupling of air-sea systems. The general pattern of date of occurance of temperature maximum coincides with the pattern of the onset of monsoon, which shows a delay in the northerly areas. The influence of general circu

lation over the sea surface temperature or vice versa, where the cause and effect is difficult to be differentiated is obvious from the results. However, study of the major upwelling areas which reveal the areal extension of temperature anomalies indicates an important part played by it in the monsoonal circulation and a qualitative explanation for the delayed onset and early withdrawal of southwest monsoon in the northern part of west coast of India is inferred. The complete absence of cyclogenesis in the Arabian Sea during summer monsoon is attributed to this cold water advection and subsequent downward fluxes of sensible heat.

A significant positive correlation between simultaneous monthly water temperature during south-west monsoon from the western Arabian Sea and the intensity of monsoon is observed. Warm temperature in Western Arabian Sea is inferred to be favouring more rains in southeast Asia. Warmer temperature means reduction in land-sea contrast of pressure which subsequently reduces the intensity of lower troposphere westerlies. The colder Sea surface temperature values signify lesser rainfall and less cross-equatorial flux. Yearly latent heat values from the area of maximum evaporation showed no remarkable correlation with the yearly fluctuations of intensity of monsoons. Hence Arabian Sea evaporation cannot be considered

as the only source of water vapour, for the rainfall over southeast Asia.

South Indian Ocean semi-permanent area of maximum along 10-20°S in the eastern region is observed to be extending towards west for the period April-September (the period of Anti-Hadley Cell in the northern hemisphere asserted by Flohn Flohn (1975)) and almost merges with the area of intense evaporation in the western Arabian Sea. Other surface characteristics also indicate merging of southern Indian Ocean air and that of Arabian Sea, which could be due to cross-equatorial flow. (Le-Lp) values indicate deficiency of evaporation during summer monsoon season in the western Arabian Sea, excess of evaporation in the southern hemisphere, which indicate that the supply of moisture from the Arabian Sea alone is not sufficient to explain the profuse rainfall along the west coast. It could be inferred that through the evaporation over Arabian Sea is not the only source of water vapour for the monsoon rainfall, the contribution from the Arabian Sea especially the west and central Arabian Sea cannot be ruled out. Thus cold water over the western Arabian Sea during summer monsoon months not only accounts for the marked differences in the weather and climatic conditions over the two parts of the North Indian Ocean, but also has great significance in the context of the monsoon circulation and rainfall over India.

The long term changes of the annual sea surface temperature for the Arabian Sea and Bay of Bengal show an increasing trend. The period of low values of annual sea surface temperature are marked by large-scale monsoon failures for the years 1890-1920, and a period of warmer sea surface temperature coincides with the period of good monsoon rainfall 1921-54. The oscillations and persistence of the anomalies of SST are not studied. It is not known how long a large atmospheric adjustment must last before the new flow pattern destroys or makes a substantial change in SST pattern.

The harmonic analysis of sea surface temperature, air temperature and sea level pressure indicates latitude dependence with a tendency to show higher oscillations over the western side of Arabian Sea and Bay of Bengal.

The far-reaching sea surface temperature anomalies in the western Arabian Sea is quite astounding. It is clear that cold water anomalies along with the proximity of vast landmass creates the unique situation during northern summer. The intense upwelling influences profoundly the sea surface temperature and overcompensates the effect of profuse insolation experienced. The galeforce westerlies compensates the influence of low sea surface temperature and supplies considerable water vapour for the profuse rainfall encountered in the

Asian continent. The differentiation of cause and effect between SST and monsoon activity is not clear. Here most of the time the development of intense upwelling and cold water advection is arbitrarily chosen as starting point, which leads to a chain of events. However, it can be said that the monitoring of the largescale air-sea interactions as a consequence of sea surface temperature anomalies will have great impact on future attempts in climatic forecasting.

REFERENCES

Ahmad, M.N.	1978	Forecast five days ahead of the development of low pressure areas and depressions/storms over the northern part of the Bay of Bengal during the southwest monsoon season. Indian J. Meteorol. Geophys., 29(1 & 2) 419-424.
*Albrecht, F.H.M.	1949	Über die Wärme - und Wasserbil der Erde. Annalen Meteorol., 2: 139-143.
*Albrecht, F.H.M.	1950	Untersuchungenüber den Wärmeumsatz an der Meeresoberfläche und die Meeresströmungen im Indischen Ozean Gerlds. Beitr. Geophy., 28: 194-215.
*Anderson, J.C.	1954	Temperature measurement with thermistors, some practical instruments. Electronic Engineering., 26: 82-84.
*Angstrom, A.	1930	Applications of heat radiation measurements to the problems of the evaporation from lakes and heat conduction at their surfaces. Gerl. Beitr., 2: 237-252.
Ashbel, P.	1961	New World Maps of global solar radiation during IGY 1957-58 Hebrew University, Department of Climatology and Meteorology, Jerusalem, Israel.
Bathen, K.H.	1971	Heat storage and advection in the North Pacific Ocean. J. Geophys. Res., 76 (2):676-687.
*Baur, F., and H.Philipps.	1935	Warmeumsatz der Lufthulle der Nordhalbkugel im Januar und Juli und zur Zeit der Aquinoktien und Solstitien. Gerl. Beitr. Geophysik .. 44: 83-132.
Beard, J.T., and J.A.Wiebelt.	1966	Reflectance of a water wave surface as related to evaporation suppression J.Geophys.Res., 71: 3843-3847.

Bunton, C.S and 7 Co-authors.	1963	Interaction between the atmosphere and oceans. Bull. Amer. Met. Soc., 44: 4-17.
*Berliand, M.E and T.G. Berliand.	1952	Opredelenie effektivnove izlucheniia zemli s uchetom vliianiia oblachnost Isv. AN SSR, Seriia Geof. 9(1).
Berliand, T.G.	1960	Method of climatological estimation of global radiation. Meteor. Gidrol. 6: 9-12.
Bhamralkar, C.M.	1978	Relation between evaporation over t Arabian Sea and rainfall at the wes coast of India during summer monsoo Indian J. Met. Hydrol. Geophys. 29 (1 & 2): 155-161.
Bjerknes, J.	1966	A possible response of the atmosphe ric Hadley circulation to equatoria anomalies of ocean temperature. Tellus., 18: 820-829.
Bjerknes, J.	1969	Atmospheric teleconnections from the equatorial Pacific. Mon. Wea. Rev. 97: 163-172.
*Black, J.N.	1956	The distribution of solar radiation over the earth's surface. Arch. Met. Geophys., (B) 7: 165-189.
Bruce, J.G.	1968	Comparison of near surface dynamic topography during the two monsoons in the western Indian Ocean. Deep Sea Res., 15: 665-677.
Budyko, M.I. (editor)	1955	Atlas teplovo balansa. GUMZ, Leningrad 41 pp.
————	1956	Teplovoi balans zemnoi poverkhnosti. GUMZ, Leningrad. 256 pp.
————	1963	Atlas teplovogo balansa zemnogo shara., Akad. Nauk SSSR, Moscow.
Budyko, M.I.	1974	Climate and Life (English edn. Ed. D.H. Miller), Academic Press, 508 pp.

Bunker, A.F. 1965 Interaction of the Summer Monsoon air with the Arabian Sea. Proceedings of the symposium on meteorological results of the International Indian Ocean Expedition, Cochin, India., 16-21 July 1965., 1-11.

Bunker, A.F. 1976 Computations of Surface Energy Flux and Annual Air-Sea Interaction Cycles of North Atlantic Ocean. Mon.Wea.Rev. 104 (9): 1122-1140.

Burt, W.V. 1953 A note on the reflection of diffuse radiation by the sea surface. Trans. Amer.Geophys.Un., 34 (2): 329.

*Burdecki, Feliks 1956 Remarks on the distribution of solar radiation on the surface of the earth. Arch. Met.Geophys. (B) 8:326-336.

Cadet Daniel., Clery-Eagbe Paul and Demmerin Gilles. 1978 Lagrangian study of the low-level flow field over the Indian Ocean during the summer monsoon. Indian J.Met. Hydrol. Geophys. 29 (1 & 2):63-68.

Charnock, H. 1955 Wind stress on a water surface. Quarterly Journal of the Royal Met.Soc. 81: 639-640.

Colen, J.A. 1964 On interaction between the southwest Monsoon Current and the sea surface over the Arabian Sea. Indian J.Met. Geophys., 15: 183-200.

Conrad, V and L.W.Pollak 1950 Methods in climatology 2nd Ed., Harvard University Press, Cambridge, Massachusett.

*Crawford, A.B. 1969 Sea-surface temperature, some instruments methods and comparison W.M.O.Technical Note. No.103, 117-120.

*Cummings, N.W. 1939 Relation between evaporation and humidity as deduced quantitatively from rational equations based on thermodynamics and molecular theory. [illegible] 47-86.

*Dalton, J. 1802 Experimental essays on the constitution of mixed gases on the force of steam or vapour from water and other liquids in different temperatures, both in a torricellian vacuum and in air., on evaporation and on the expansion of gases by heat [illegible] of the Manchester Literary and [illegible] Society, England. 5: 535-602.

Deacon, E.L., P.A. Sheppard and E.K. Webb. 1956 Wind Profiles over the sea and the drag at the sea surface; Austral.J. Phys., 9: 511-541.

Deacon, E.L. and E.K.Webb. 1962 Small-scale interactions ... The Sea Vol.1 (Ed.M.N.Hill), Inter Science Publ. (Wiley), 43-87.

*Dogiyarev, G.M., A.A.Kevelin and Yu.A.Man'ko kov. 1964 Radiation reflected from the surface of the open sea, Translated by Stephen [illegible] Izv.Akad.Nauk.SSR., No.10, 961-966.

*Dietrich, G and K.Kalle. 1957 Allgemeine Meereskunde eine Einfuhrung in die Ozeanographie, Gebruder Borntraeger (Berlin), 492 pp.

Düing, W. 1970 The monsoon regime of the currents in the Indian Ocean, International Indian Ocean Expedition. Oceanographic Monograph No.1, East-West Centre Press (Honolulu), 68 pp.

Ellis, M.S. 1952 A preliminary study of a relation between surface temperature of the North Indian Ocean and precipitation over India. M.S. Thesis, Dep. of Met., Florida State University.

Eliassen, M.M. 1937 On some properties of the water vapour spectrum and their relation to atmospheric motion. Trans. Amer. Geophys. Un. 18 (9): 323-326.

Findlater, J. 1969 (a) A major low level air current over the Indian Ocean during the northern summer. Quart. J. R. Met. Soc., 95: 362-380.

1969 (b) Interhemispheric transport of air in the lower troposphere over the western Indian Ocean. Quart. J. R. Met. Soc. 95: 400-403.

Findlater, J. 1970 Discussion of papers on a major low level air Current. Ibid, 96: 557-

Findlater, J 1974 The low-level cross-equatorial air current of the western Indian Ocean during the northern summer weather., 30: 411-416.

Findlater, J. 1981 An experiment on monitoring cross-equator flow at low level over Kenya and rainfall over Western India during the northern summers Monsoon Dynamics (Lighthill & Pearce, eds.) Cambridge Univ. Press.

Flohn, H. 1968 Contributions to a meteorology of the Tibetan Highlands. Dept. Atmos. Sci., Colorado State Univ. Atm. Sci. Paper No. 130.

Flohn, H., and Fiser, H. 1975 Climatic Tele connections with the Equatorial Pacific and the Role of Ocean/Atmosphere coupling. Ninth Annual CMG Conference, Vancouver, B.C., 30th Nov 1975.

Fritz, S. 1949 The albedo of planet earth and of clouds. J. Meteor., 6 (4): 277-282.

*_____ 1950 Measurements of the albedo of clouds. Arch., 21: 25-37

_____ 1954 Scattering of solar energy by clouds of "large drops" J. Meteor., 11: 291-300.

Garratt, J.R. 1977 Review of Drag Coefficients over the Oceans and Continents. Mon.Wea. Rev., 105 (7):915-929.

Gerstang, H. 1967 Sensible and latent heat exchange in low latitude synoptic scale systems. Tellus., 19: 492-508.

Giblett, M.A. 1921 Some problems connected with evaporat on from large expanses of water. Proc. Roy.Soc.Lond. Ser.A., 99: 472-490.

Godbole, R.V. and Sh.V.Ramana Murty. 1970 The Indian Summer Monsoon as seen by Weather Satellite. Journ.of Met.Soc. of Japan., 48 (4):

Hantel, M., 1971 Monthly charts of surface wind vergenc over the tropical Indian Ocean. Bonner Meteorologischa Abhandlungen No.14

Helland-Hansen, B. and Nansen. 1920 Temperature variations in the North Atlantic Ocean and in the Atmosphere, Introductory studies on the causes of climatological variations. Miscellaneous collections., 70 (4) Smithsonian Institute, Washington, D.C. 408 pp.

Howson, E.W. 1943 The reflection, absorption and transmission of solar radiation by fog and cloud. Quart.J.Roy.Met.Soc., 69: 47-62.

Hicks, B.B. 1972 Some evaluations of drag and bulk transfer coefficients over water bodies of different sizes. Bound. Layer Meteor., 3: 201-213

Hidy, G.M. 1972 A view of recent air-sea interaction research. Bull. Amer.Meteor.Soc., 53: 1083-1107.

Holland, J.Z. 1972 Comparative evaluation of some BOMEX measurements of sea surface evaporation, energy flux and stress. J.Phys.Oceanography., 2:476-486.

India Meteorological Department 1979 Tracks of Storms and Depress in Bay of Bengal and Arabian S 1877 - 1970. IMD Publication.

Jacobs, W.C. 1942 On the energy exchange between sea and atmosphere. J.Mar.Res., 5(1):37-66.

——— 1951 (a) The energy exchange between the sea and atmosphere and some of its consequences. Pub. Scripps Instn. of Oceanography, Univ. of Calif., 6: 27-122.

——— 1951 (b) Large scale aspects of energy transformations over the Ocean. Compendium of Meteorology, Amer. Meteor.Soc., pp.1057-1070.

Jagannathan, P. 1957 Seasonal oscillation of air temperature in India and neighbourhoo Indian J.Meteorol.Geophys., 8(2). 115-122.

Jagannathan, P and A.A. Ananantry. 1964 Climatic changes in the Indian Seas Journ.Geophys.Res., 69 (2):215-221.

Janakumathan, P and K. Ananantry. 1973 Sea and air temperatures distribution over the Arabian Sea during south-west monsoon 1971. Indian J.Met. Geophys., 24(4):465-470.

*Jeffrys 1918 Some problems of evaporation. London; Phil.Mag. and Jour.Sci (Ser.6) 35: 270-280.

Joseph, I.V. 1970 Subtropical Westerlies in relation to large scale failure of Indian monsoon; Indian J.Met.Hydrol. Geophys., 21 (1 & 2): 413-418.

Joseph, P.V. and P.L. Simon. 1966 Existence of low level westerly Jet stream over Peninsular India. Indian J.Met. Geophys. 17: 407-410.

Kimball, H.H. 1928 Amount of solar radiation that reaches the surface of the earth on the land and the sea. [illegible], 24: 393-399.

Kitaigorodskii, S.A. 1970 The physics of the air-sea interaction. Gidrometeorologicheskoe Izdatel'stvo Leningrad (trans. from the Russian by A. Baruch) Israel program for Sci.Trans. (Jerusalem), 1973. 237 pp.

Kondratyev, K. Ya. 1969 Radiation in the atmosphere. Academi Press, 912 pp.

Kraus, E.B. 1969 The evaporation-precipitation cycle of the tradew. [illegible], 11(2): 168-187.

_____ 1969 What we do not know about the sea-surface wind stress. [illegible], 42 : 247-253.

_____ 1972 Atmosphere - Ocean Interaction Clarendon Press (Oxford) 275 pp.

Kusuda, T. 1969 Factors affecting the temperature of the surface layer of the sea. [illegible], 31:1-136.

*Landsberg, H.E., Lippmann, K.H.Paffen and C.Troll. 1963 Weltkarten zur Klimakunde .Springer Verlag, Berlin.

Leetma, Ants 1972 The response of the Somali Current to the southwest monsoon of 1970. [illegible]

Lighthill, M.J. 1969 Dynamic response of the Indian Ocean to onset of southwest monsoon. [illegible], 45-92.

Livingston, G.J.	1908 1909	An annotated Bibliography of Evaporation. Mon.Wea.Rev., Vol.36, p.161, 281, 375, & Vol.37 p.65, 102, 157, 193 and 240.
*London, J.	1957	Study of the atmospheric heat balance. Final Report. New York Univ. College of Engineering. Res.Div.
Malkus, J.S.	1962	Large-scale interactions. The Sea Vol.1, pp.88-294; Edited by M.N. Hill. Interscience, New York - London
Mani, A., O.Chacko, V.Krishnamurty and V.Desikan.	1965	Radiation Balance of the Indian Ocean Proceedings of the Symposium on Meteorological Results of the International Indian Ocean Expedition Bombay, India, 12-20 July 1965 - 168-177.
Mc Ewen, G.F.	1938	Some energy relations between the sea surface and atmosphere. J.Mar.Res., 1: 217-238.
Mc Donald, W.F.	1938	Atlas of climatic charts of the Oceans. U.S. Weather Bur., Washington D.C.
Miller, F.R., M.V.Siva Ramakrishnan and R.Sgryganaragana.	1963	Preliminary results and future plans of IIMM meteorology programmes - computer plans Proc.Seminar, jointly sponsored by NSF (USA) and Indmet. Dept. and U.S.I.S., 30-41.
Miller, F.R., and R.M.Keshavamurty.	1968	Structure of Arabian Sea summer monsoon system. Int.Indian.Ocean. Expedition.Meteorol.Monogr.1
Mishra, D.K. and M.S.Singh.	1968	The large scale cloud patterns over the Indian Ocean during June 1967. Mausam., 19 (3):403-408.
*Moller, F.	1943	Das Strahlungsdiagram. Wiss.Abh.D.R. Reich.Wetterd.

Montgomery, R.B. 1940 Observations of a vertical humidity distribution above the ocean surface and their relation to evaporation. Pap.Phys. Oceanog. Met., Mass.Inst.Tech and Woods Hole Oceanog.Inst., 7, 30 pp

*Mosby, H. 1936 Verdunstung and Strahlung and dem Meere. Ann.Hydrog.Marit. Met., 64: 281-286.

Murty, T.V.S. and M.S. Edelman. 1970 On the relation between the intensity of the southwest monsoon and the oil sardine fishery of India. The Indian Journal of Fisheries., 17 (1):142-150.

Namias, J. 1969 Seasonal interactions between the North Pacific Ocean and the atmosphere during the 1960's. Mon.Wea.Rev., 97:173-192.

Namias,J. 1974 Longevity of a coupled air-sea - continent system. Mon.Wea.Rev., 102: 638-648.

National Climatic Centre 1968 The Data Family - 11 Reference Mannual, Asheville.

Newell, R.E., D.G. Vincent., T.G.Dopplick., D.Ferruzza and J.W. Kidson. 1970 The energy balance of the global atmosphere in the Global circulation of the Atmosphere. (Ed.G.A.Corby) Royal Meteorological Society (London). 42-90.

Nimeroger, M. 1948 The reflection of diffuse radiation by the sea surface. Trans.Amer. Geophys. Un.29 (5). p.667.

Nieuwolt, S. 1977 Tropical climatology, John Wiley and sons (London), 207 pp.

Palmen, E., and H.Riehl. 1957 Budjet of angular momentum and energy in tropical cyclones. J.Meteor., 14:150-159.

Pant, M.C. 1977 Wind stress and fluxes of sensible and latent heat over the Arabian Sea during ISMEX - 1973. Indian J. Met.Hydrol.Geophys. 28 (2):189-196.

Pasquill 1949 A portable indicating apparatus for the study of temperature and humidity profiles near the ground. Quart.J. Met.Soc., 75: 239-248.

Phillips, O.M. 1966 The Dynamics of the Upper Ocean. Cambridge University Press. 261.pp.

Pisharoty, P.R. 1965 Evaporation from the Arabian Sea and the Indian SW monsoon. Proceedings of the symposium on Meteorological results of the International Indian Ocean Expedition, Bombay, India, 12-28 July 1965, 43-50.

_____ and E.N.Srinivasaiah. 1965 The Indian Ocean and its influence on the meteorology of the adjoining lands. Bull.Nat.Inst.Sci.India, 28 (Part II):1004-1010.

Pisharoty, P.R 1981 Sea Surface temperature and the Monsoon Dynamics. Cambridge Univ.

*Pivavarov, A.A., E.P.Aninimova and A.M.Erilova. 1965 Diurnal course of the albedo and of solar radiation penetrating the sea. Izv.Atmos.Ocean Physics, 1, 713-71

Pond, S.G.T. Phelps, J.E. Paquins, G.Mc Dean and R.W.Stewart. 1971 Measurement of the turbulent fluxes of momentum, moisture and sensible heat over the ocean. J.Atmos.Sci., 28: 901-914.

Portman, D.J., and S.Rymar. 1971 An investigation of heat exchange. Int. Indian Ocean Exped. Meteorol. Monog East-West Press (Honolulu), 78 pp.

Prandtl. 1932 Beitr.Phys.fr.Atmos.Vol.19.pp 188.

Priestley, C.H.B. 1959 Turbulent transfer in the lower atmosphere. University of Chicago Press, pp 130.

Privett, D.W. 1959 Monthly charts of evaporation from the N.Indian Ocean (including the Red Sea and the Persian Gulf). Quart.J.R.Met.Soc., 85: 424-428.

Quayle, R.G. 1974 A climatic comparison of ocean weather stations and transient ship records. Mariners Weather Log, 18: 307-311.

Quinn, W.H., and W.V.Burt. 1968 Incoming solar radiation over the tropical Pacific Nature, 217: 148-150.

Ramm 1960 An attempt to trace the monsoon flow using natural radon. Indian J.Met.Geophys, 19: 167-170.

Ramage, C.S. 1974 Monsoonal influences on the annual variation tropical cyclone development over the Indian and Pacific Oceans. Mon.Wea.Rev, 102: 741-753.

——————— 1966 The Summer atmospheric Circulation over the Arabian Sea. J.Atmos.Sci, 23: 744-750.

——————— F.R.Miller and C.Jefferies. 1972 Meteorological Atlas of IIOE. Part, University of Hawaii, Honolulu.

Ramamurty, K.M. 1972 On the activity of the Arabian Sea monsoon. Indian J.Met.Geophys. 23 (1): 1-14.

Ramana, C.R.V. 1970 Structure of the summer trough system over the northern Indian Ocean. International Indian Ocean Expedition, Meteorol.Monogr. 10.

Ramanadham, R.R. O.R.Lakshmana Rao and D.P.Rao. 1968 Seasonal variation in heat flux from the Sea surface over the Bay of Bengal. Bull.Nat.Inst.Sci.India Part II; 38: 1004-1016.

Rangarajan, C and S. Gopalakrishnan. 1975 Studies on the movement of radioactive debris across the equator. Indian J.Met.Hydrol.Geophys. 26 (3): 391-396.

Rangarajan, C., S. Gopalakrishnan and K. G. Vohra 1969 Transport and interhemispheric mixing of radioactive nuclear test debris. BARC, Bom Report No. 392

1970 T. Geophys. Res, 75: 1753-1

Rao Bankara N.S. N.N.Khambete and Joshi, K.S. 1972 Satellite clouding Associated with the Monsoon trough J.Met. Phil.Ass.India. 14 (2):785-794.

Rao Krishna, P. 1966 A study of the onset of the monsoon over India during 1962 using TIROS IV radiation data. Indian J.Meteor.Geophys. 17, 267-276.

Rao, R.K., S.V.S. Sommadhan and Syed Nizamuddin. 1978 Study on the influence of surface energy budget of North Indian Ocean on the behaviour of Indian summer monsoon. Indian J.Met. Hydrol.Geophys. 29 (1 & 2): 253-256.

Rao, Y.P. 1964 Inter hemispheric circulation. Quart.J.R.Met.Soc., 90, 196-194.

Rao, Y.P and B.N.Desai. 1972 Origin of the South-westerly Monsoon Current over the Arabian Sea. J.Mar.Phil.Ass.India., 14(2): 836-861.

Richardson, B. 1931 Evaporation as a function of insolation by means of a pan. Phil.Res.Council.Bul.68: 56-61.

Robinson, G.D. 1964 Surface measurements of solar and terrestrial radiation during the IGY and IGC. Annals of the IGY. Pergamon Press, 32: 17-61.

Roden, G.I. 1959 On the heat and salt balance of the California Current and region. J.Mar.Res., 18: 36-61.

———— 1974 Thermohaline structure, fronts, and air-sea energy exchange of the trade wind region east of Hawaii. J.Phys.Oceanogr., 4: 168-182.

Roll, H.U. 1965 Physics of the Marine Atmosphere Academic Press, 426 pp.

Rossby, C.G. 1936 On the frictional force between air and water and on the occurance of a laminar boundary layer next to the surface of the sea. Papers in Phys. Oceanogr. and Meteor., 5 (3) (Cambridge, Mass.)

...ousby, ...G. and ...B.Montgomery.	1935	The layer of frictional influence in wind and ocean currents. Papers in Phys.Oceanogr. and Meteor., 3(3):101 pp (Cambridge, Mass.)
Saha, K....	1970 (a)	Zonal anomaly of sea surface temperature in equatorial Indian Ocean and its possible effect upon monsoon circulation. ...., 22(6): 404-409.
_____	1970 (b)	Air and water vapour transport across the equator in western Indian Ocean during northern summer. Ibid., 22: 681-687.
_____	1969	Some flow features of the Indian Summer monsoon, deduced from Nimbus II radiation data ibid 21(6): 806-1
_____	1971 (a)	Mean cloud distribution over tropical Oceans. Ibid., 23: 183-194.
_____	1971 (b)	Cloud distributions over equatorial Indian Ocean as revealed by satellites ...., 23, 389-396.
_____	1972 (a)	Some aspects of air-sea interaction in the Indian Ocean deduced from satellite cloud photographs. ...., 14 (2):627-635.
_____and ...Suryanarayana.	1972 (b)	Mean monthly, vertical fluxes of sensible and latent heat from the surface of the Arabian Sea. Ibid., 14:663-670.
_____and S.N.Bavadekar.	1973	Water vapour budget and precipitation over the Arabian Sea during the northern summer. ...., 99: 273-278.
_____	1974	The Indian summer monsoon as seen by weather satellite ...., (6) (4).
*Sauberer, F and I.Dirmhirn.	1954	Über den strahlungs haushalt der oceane auf der Nordhalbkugel, ..., B.6: 113-127.
Saur, J.F.T.	1963	A study of the quality of sea-water temperature records in logs of ships' weather observations. ...., 2:417-421.

Schmidt	1936	Z.ges.Geophys., 336-339.
Sethuraman, S and G.S.Raynor.	1975	Surforce drag coefficient dependence on the aerodynamic roughness of the sea J.Geophys.Res., 80 (36): 4985-4988.
Sharma, G.S.	1976	Seasonal variation of some hydrographic properties of the shelf waters off the westcoast of India. Bull.natn.Inst.Sci.India., Part II 253-275.
Sheppard, P.A.	1958	Transfer across the earth's surface and through the air above. Quart.J. Roy.Meteor.Soc., 84: 205-224.
Shukla, J.	1975	Effect of Afabian Sea - surface temperature anomaly. On Indian summer monsoon; a numerical experiment with the GFDL model J.Atmos. Sci, 32, 503-511.
Simpson, G.C.	1928	Some studies in Terrestrial radiatic Memoirs of the Royal Met.Soc, Vol. II, Memoirs Nos.22, & 20. pp 70-95.
Smith, W.L.and E.G.Banke.	1975	Variation of the Sea-surface anomalies from satellite high resolution infrared window radiatio measurements. Mon.Wea.Rev., 99. 604-611.
Smithsonian Institution.	1939	Smithsonian Meteorological Tables. 5th Rev.Ed. Smithsonian Inst. Washington.
Stommel, H and W.S.Wooster.	1965	Reconnaissance of the Somali Current during the southwest monsoo Proc.Nat.Acad.Sci., 54:8-13.
Sundara Raman K.V, C.K.Balakrishnakurup and K.V.Sreerama Murty.	1968	Water masses of the Arabian Sea in the upper 500 metres. Bull.natn. Inst.of Sci. of India., No.38 Part, 240-253.
Suryanarayana,R and D.R, Sikka, D.V.	1965	Evaporation over the Indian Ocean during 1963. Proc.Sym.Met.Res., 110 E, Bombay, 68-69.
Sutton	1932	A theory of eddy diffusion in the atmospheric Proc. of the Royal Soc, London, (A) 135:143-165.
_____	1934	Wind structure and evaporation in a turbulent atmosphere.Proc. of the Royal.Soc.London. (A). 146:701 pp.

Sverdrup, H.U. 1937 On the process of upwelling. Jourl.of Mar.Res. 1 & 2 : 155-164.
1938

Sverdrup, H.U. 1951 Evaporation from the Oceans' in Compendium of Meteorology (Ed.T.F. Malone). Amer.Met.Soc., 1071-81.

Swallow, J.C. and J.G.Bruce. 1966 Current measurements off the Somali Coast during the southwest monsoon of 1964. Deep-Sea Res., 13: 861-888.

Tabata, S. 1964 A study of the main physical factors governing the oceanographic conditions of station P in the northeast Pacific Ocean. Transactions of the Royal Society of Canada, Vol.3(4):367-418.

*Taylor, G.I. 1915 Phil.Trans.Roy.Soc.A., 215, p.1.

Thornthwaite, C.W. and Holzman,B. 1939 The determination of evaporation from land and water surfaces.Mon. Wea.Rev., 67:4-11.

Ter-Markayantz, N.E. 1960 On the average daily values of the sea's albedo-Trans.(Trudy) Main Geophys.Observ., Issue 100.

U.S.Navy 1976 Marine climatic Atlas of the World U.S.Govt.Printing Office, Washington.

Venkateswaran, S.V. 1956 On evaporation from the Indian Ocean.Ind.J.met.Geophys.7: 255-264.

Verpeleqh, G. 1960 On the annual variation of climatic elements of the Indian Ocean.Koninklijk Nederlands Meteorologisch Instituut Mededelingen en Verhan-delingen, No.77.

Vonder Haar, T.H. and J.S.Ellis. 1974 Atlas of radiation budget measurement from satellites (1962-1970) Colorado State University, Atmospheric Science Paper No.221 - Fort Collins Colo.180 pp.

Vonder Haar, T.H., and Suomi.V.E. 1969 Satellite observations of earth's radiation budget. Science 163 (3868): 667-669.

——— 1971 Measurements of the earth's radiation budget from satellite during a five-year period Part I:Extended time and space means. J.Atm.Sci., 28:305-314.

Vonder Haar, T.H. and A.H.Oort. 1973 New estimate of annual pleward energy transport by northern hemisphere oceans.J.Phys.Oceanogr. 3:169-172.

——— 1976 On the observed Annual cycle in the Ocean-Atmosphere Heat Balance over the northern hemisphere J. Phy. Oceanogr.6(6):781-799.

*Vonkarman, Th 1935 Some aspects of the turbulence problem. 4th International Congress. Appl.Mech.Proc. 54-91.

Walker,G.T. and E.W.Bliss. 1930 Some applications to seasonal Forecasting Memoirs of the Royal Society 1 (26):81-95.

——— 1932 Ibid 4 (36): 53-84.

Walker, J.M. 1975 On summer atmospheric processes over southwest Asia Indian., 87:489-496.

Washington W.M., L.O.Chervin and G.V.Rao. 1977 Effects of a variety of Indian Ocean surface temperature anomaly patterns on the summer monsoon circulation Expts. with the NCAR general circulation models. Pure & Appl.Geophys., 115:1335-1356.

Nilson, B.N. 1960 Note on surface wind stress over water at low and high wind speeds. J.Geophys. Res. 65(10):3377-3382.

Winston, J.S. 1969 Global distribution of cloudiness and radiation as measured from weather satellites. in World Survey of Climatology, Vol.4 (Ed.D.F.Rex) Elsevier, 337-380.

Wu, J 1968 Froude number scaling of wind-stress coefficients - A correlation for wind-stress determined at all fetches. Tech.Rep. 221-23, Hydronautics, Inc., Laurel, Md., 38 pp.

Wu,J. 1969 Wind stress and surface roughness at air-sea interface J.Geophys. Res., 74 (2) 444-455.

*Wüst,G 1920 Die Verdunstung auf dem Meere. Veröff.Inst.F.Meereskunde,Univ.Berlin, N.F. Reihe A. No.6: 1-98.

Wüst, G. 1936 Oberflächensalzgehalt, Verdunstung und Niederschlag auf dem Weltmeere. Landeskundl.Forschung, Festschrift No. Krebs, 347-359.

Yamamoto 1950 On nocturnal radiation. Geophysical Mag.,Jp., 21:87-43.

Zilman, T.M and J.A.Bell. 1968 Sea-to-air heat fluxes in the southwest Indian Ocean in summer. J.Geophys.Res., 73 (22): 7057-7068.

* Not referred in original.

NOTE ADDED IN PROOF

While this Thesis was in final stages, Climatic Atlas of the Indian Ocean Part I (surface climate and Atmospheric circulation) and Part II (The Oceanic Heat Budget) by Stefan Hastenrath and Peter J.Lamb., The University of Wisconsin Press., 1979., has been published, where an updated surface circulation and heat budget climatology of the Indian Ocean are presented. In comparison with the present work the large-scale fields of annual and monthly values of heat budget components and their related parameters, in general shows similar trends, though the magnitudes of energy-exchange parameters show differences at certain places. The causes for the differences are mainly two, the differences in methods and differences in the method of presentation. In the Thesis variable exchange coefficients are used, where as in the Atlas constant values are used. In the Thesis, large-scale distribution of seasonal and annual values of heat budget components and related variables are presented, where as in the Atlas monthly and annual values of the same are given.